Institut für Erd- und Umweltwissenschaften
Mathematisch-Naturwissenschaftliche Fakultät
Universität Potsdam

Hydrology Across Scales

Sensitivity of East African Lakes to Climate Changes

Lydia Atieno Olaka

Cumulative dissertation submitted for the fulfilment of
Doctor of Natural Science (Dr. rer. nat) requirements,
at the Faculty of Mathematics and Natural Sciences
at Potsdam University

Potsdam, August 2011

Gedruckt mit Unterstützung des Deutschen Akademischen Austauschdienstes
Printing financed by the German Academic Exchange Services (DAAD)

Published online at the
Institutional Repository of the University of Potsdam:
URL http://opus.kobv.de/ubp/volltexte/2011/5502/
URN urn:nbn:de:kobv:517-opus-55029
http://nbn-resolving.de/urn:nbn:de:kobv:517-opus-55029

Hydrology Across Scales

Sensitivity of East African Lakes to Climate Changes

by

Lydia Atieno Olaka

Advisor

Apl Prof. Dr. Martin Trauth

ABSTRACT

The lakes of the East African Rift System (EARS) have been intensively studied to better understand the influence of climate change on hydrological systems. The exceptional sensitivity of these rift lakes, however, is both a challenge and an opportunity when trying to reconstruct past climate changes from changes in the hydrological budget of lake basins on timescales 10^0 to 10^4 years. On one hand, differences in basin geometrics (shape, area, volume, depth), catchment rainfall distributions and varying erosion-deposition rates complicate regional interpretation of paleoclimate information from lacustrine sediment proxies. On the other hand, the sensitivity of rift lakes often provides paleoclimate records of excellent quality characterized by a high signal-to-noise ratio. This study aims at better understanding of the climate-proxy generating process in rift lakes by parameterizing the geomorphological and hydroclimatic conditions of a particular site providing a step towards the establishment of regional calibrations of transfer functions for climate reconstructions. The knowledge of the sensitivity of a lake basin to climate change furthermore is crucial for a better assessment of the probability of catastrophic changes in the future, which bear risks for landscapes, ecosystems, and organisms of all sorts, including humans.

Part 1 of this thesis explores the effect of the morphology and the effective moisture of a lake catchment. The availability of digital elevation models (DEM) and gridded climate data sets facilitates the comparison of the morphological and hydroclimatic conditions of rift lakes. I used the hypsometric integral (HI) calculated from Shuttle Radar Topography Mission (SRTM) data to describe the morphology of ten lake basins in Kenya and Ethiopia. The aridity index (AI) describing the difference in the precipitation/evaporation balance within a catchment was used to compare the hydroclimatic of these basins. Correlating HI and AI with published Holocene lake-level variations revealed that lakes responding sensitively to relatively moderate climate change are typically graben shaped and characterized by a HI between 0.23-0.30, and relatively humid conditions with AI >1. These amplifier lakes, a term first introduced but not fully parameterized by Alayne Street-Perrott in the early 80s, are unexceptionally located in the crest of the Kenyan and Ethiopian domes. The non-amplifier lakes in the EARS either have lower HI 0.13-0.22 and higher AI (>1) or higher HI (0.31-0.37) and low AI (<1), reflecting pan-shaped morphologies with more arid hydroclimatic conditions.

Part 2 of this work addresses the third important factor to be considered when using lake-level and proxy records to unravel past climate changes in the EARS: interbasin connectivity and groundwater flow through faulted and porous subsurface lithologies in a rift setting. First, I have compiled the available hydrogeological data including lithology, resistivity

and water-well data for the adjacent Naivasha and Elmenteita-Nakuru basins in the Central Kenya Rift. Using this subsurface information and established records of lake-level decline at the last wet-dry climate transitions, i.e., the termination of the African Humid Period (AHP, 15 to 5 kyr BP), I used a linear decay model to estimate typical groundwater flow between the two basins. The results suggest a delayed response of the groundwater levels of ca. 5 kyrs if no recharge of groundwater occurs during the wet-dry transition, whereas the lag is 2-2.7 kyrs only using the modern recharge of ca. 0.52 m/yr. The estimated total groundwater flow from higher Lake Naivasha (1,880 m a.s.l. during the AHP) to Nakuru-Elmenteita (1,770 m) was 40 cubic kilometers. The unexpectedly large volume, more than half of the volume of the paleo-Lake Naivasha during the Early Holocene, emphasizes the importance of groundwater in hydrological modeling of paleo-lakes in rifts. Moreover, the subsurface connectivity of rift lakes also causes a significant lag time to the system introducing a nonlinear component to the system that has to be considered while interpreting paleo-lake records.

Part 3 of this thesis investigated the modern intraseasonal precipitation variability within eleven lake basins discussed in the first section of the study excluding Lake Victoria and including Lake Tana. Remotely sensed rainfall estimates (RFE) from FEWS NET for 1996-2010, are used for the, March April May (MAM) July August September (JAS), October November (ON) and December January February (DJF). The seasonal precipitation are averaged and correlated with the prevailing regional and local climatic mechanisms. Results show high variability with Biennial to Triennial precipitation patterns. The spatial distribution of precipitation in JAS are linked to the onset and strength of the Congo Air Boundary (CAB) and Indian Summer Monsoon (ISM) dynamics. while in ON they are related to the strength of Positive ENSO and IOD phases

This study describes the influence of graben morphologies, extreme climate constrasts within catchments and basins connectivity through faults and porous lithologies on rift lakes. Hence, it shows the importance of a careful characterization of a rift lake by these parameters prior to concluding from lake-level and proxy records to climate changes. Furthermore, this study highlights the exceptional sensitivity of rift lakes to relatively moderate climate change and its consequences for water availability to the biosphere including humans.

ZUSAMMENFASSUNG

Die Seen des Ostafrikanischen Riftsystems (EARS) wurden bereits intensiv untersucht, um den Einfluss des Klimawandels auf das hydrologische Systeme besser verstehen zu können. Dabei stellt die außergewöhnliche Sensitivität dieser Riftseen sowohl eine Herausforderung als auch eine Möglichkeit dar, um den historischen Klimawandel von dem hydrologischen Budget der Seebecken auf Zeitskalen von 10 bis 10000 Jahre abzuleiten. Auf der einen Seite verkomplizieren verschiedene Beckengeometrien (Form, Fläche, Volumen, Tiefe), unterschiedliche Niederschlagsverteilungen der einzelnen Zuflüsse und variierende Erosions- und Sedimentationsraten, die aus den Informationen von Seesedimenten generierten, regionalen Interpretationen des Paleoklimas. Andererseits ergibt sich aus der hohen Sensitivität der Riftseen eine exzellente Datenqualität, was sich in dem hohen Signal - Rausch-Verhältnis widerspiegelt. Das Ziel meiner Untersuchungen ist das verbesserte Verständlichkeit der Klimainformationen generierenden Prozesse in den Riftseen als Voraussetzung für weitere Klimarekonstruktion. Fortschritte gab es vor allem in der Entwicklung von regionalen Kalibrationen durch die Parametrisierung der geomorphologischen und hydroklimatischen Gegebenheiten einer wichtigen Lokalität, wodurch es jetzt möglich ist, von Sedimentfunden auf die Umgebungsbedingungen Rückschlüsse zu ziehen. Das Wissen um die Reaktion der Seebecken auf Klimaschwankungen ist unerlässlich für eine bessere Abschätzung der Wahrscheinlichkeit von katastrophalen Änderungen in der Zukunft:ein Szenario das sowohl für Umwelt, Ökosysteme und Organismen, einschließlich des Menschen, Risiken birgt.

Im ersten Teil meiner Doktorarbeit untersuche ich den Effekt der Morphologie und der effektiven Feuchtigkeit auf das Einzugsgebiet eines Sees. Die Verfügbarkeit von digitalen Höhenmodellen (DEM) und gerasterten Klimadatensätzen ermöglicht den Vergleich von morphologischen und hydroklimatischen Bedingungen der Riftseen. Ich nutzte das hypsometrische Integral (HI), berechnet aus Daten der “Shuttle Radar Topography Mission (SRTM)”, um die Morphologie von zehn Seebecken in Kenia und Äthopien zu beschreiben. Der Dürreindex (AI), der die Differenz von Niederschlag zu Verdunstung innerhalb eines Einzugsgebietes beschreibt, wurde benutzt, um das Hydroklima dieser Becken zu vergleichen. Die Korrelation von hypsometrischem Integral und Dürreindex mit publizierten holozänen Seespiegelschwankungen zeigte, dass vor allem Seen mit kleiner Oberfläche und großer Tiefe (Grabenform), charakterisiert durch ein HI von 0.23-0.30 und feuchte Bedingungen mit einem AI > 1, empfindlich auf relativ moderate Klimaänderungen reagieren. Diese “verstärkenden” Seen (amplifier lakes), ein Begriff der von Alayne Street-Perrott in den Achzigerjahren eingeführt wurde aber bis heute nicht völlig quantitativ definiert ist, sind ohne Ausnahme in

den tiefen Gräben der kenianischen und äthiopischen Dome zu finden. Seen innerhalb des EARS, die nicht derart empfindlich reagieren, haben entweder ein niedrigeres HI von 0.13-0.22 und einen höheren AI (>1) oder ein höherers HI (0.31-0.37) aber einen niedrigen AI (<1) und zeigen großflächige, flache Morphologien (Pfannenform) unter trockenen klimatischen Bedingungen.

Der zweite Teil der Arbeit beschäftigt sich mit einem weiteren wichtigen Faktor innerhalb der Klimarekonstruktion, wenn Seespiegelschwankungen und indirekte Messungen (Proxies) betrachtet werden:den störungsbezogenen und porösen Gesteinsschichten geschuldeten Grundwasserverbindungen zwischen den Becken. Als erstes habe ich die vorhandenen hydrogeologischen Daten bestehend aus den Gesteinsformationen, deren Widerstandsfähigkeit und den wasserbezogenen Bohrdaten für die Seen Naivasha und Elementaita-Nakuru zusammengestellt. Mit diesen bereits etablierten Untergrunddaten, z.B. zum Seespiegelrückgang am letzten Übergang von feuchtem zum trockeneren Klima am Ende der afrikanischen Feuchperiode (AHP) um 15000 bis 5000 Jahre vor heute, schätzte ich den typischen Grundwasserfluss zwischen den beiden benachbarten Becken mittels eines linearen Modells ab. Die Ergebnisse zeigen eine Zeitverzögerung der Grundwasserspiegelanpassung um ca. 5000 Jahre an, falls keine Auffüllung der Grundwasserzufuhr zum Ende der letzten Feuchtperiode eintrat. In heutiger Zeit, ist bedingt durch die Grundwassererzufuhr von ca. 0.52 m/Jahr, nur eine Zeitverzögerung um ca. 2000-2700 Jahre zu sehen. Der geschätzte totale Grundwasserfluss vom höher gelegenden Naivasha See (1880 m über dem Meeresspiegel zum Ende der AHP) zum Elementaita-Nakuru See (1770 m) betrug 40 km^3. Dieses unerwartet große Volumen, mehr als die Hälfte des Volumens vom Naivasha See während des frühen Holozäns, verdeutlicht, dass das Grundwasser für die hydrologische Modellierung von Paleoseen in Riftgebieten unbedingt mit einbezogen werden muss. Darüber hinaus führt die Grundwasserverbindung dieser Riftseen zu einer Zeitverzögerung in deren Reaktionen, was eine nichtlineare Komponente darstellt und bei jeder Interpretation von Paleoseespiegeldaten beachtet werden muss.

Der dritte Teil dieser Arbeit untersucht die intrasaisonale Niederschlagsvariabilität innerhalb von 11 Einzugsgebieten die im ersten Teil Arbeit vorgestellt wurden, mit Ausnahme des Viktoriasees, aber inklusive des Tanasees. Aus Satellitenbilddaten des FEWS NET der Jahre 1996-2010 wurden Niederschlagsabschätzungen für die Monatsreihen März-April-Mai (MAM), Juli-August-September (JAS), Oktober-November (ON) und Dezember-Januar-Februar (DJF) berechnet. Der jahreszeitliche Niederschlag wurde gemittelt und mit den dominierenden regionalen und lokalen Klimafaktoren korreliert. Die Ergebnisse zeigen eine deutliche zwei- bis dreijährige Niederschlagsvariabilität. Die räumliche Niederschlagsverteilung innerhalb des Ostafrikanische Rifts im JAS ist an die Ausbildung und Stärke der Kongoluftmassengrenze (CAB) und an die Dynamik des Indischen Sommermonsuns gekoppelt, während sie im ON an die Stärke der positiven ENSO und IOD Phasen gebunden ist.

Diese Doktorarbeit beschreibt den Einfluss von Grabenmorphologien, extremen Klimakontrasten innerhalb der Zuflussgebiete und die unterirdischen Beckenverbindung durch Störungszonen und poröse Gesteinsschichten zwischen den Riftseen. Damit zeigt sie die Unerlässlichkeit einer genauen Charakterisierung von Riftseen durch morphologische und klimatische Parameter, bevor von Seespiegelschwankungen und indirekten Datensätzen auf Klimaänderungen geschlossen werden kann. Desweiteren stellt diese Arbeit die hohe Empfindsamkeit dieser Seen gegenüber relativ moderaten Klimaänderungen und deren Konsequenzen für die insgesamte Wasserverfügbarkeit heraus.

CONTENTS

LIST OF FIGURES xiii

LIST OF TABLES xv

ACKNOWLEDGMENTS xvii

1. INTRODUCTION 1

2. THE CLIMATE SYSTEM 7
    2.1 Society under a varying climate 9

3. THE SENSITIVITY OF EAST AFRICAN RIFT LAKES TO CLIMATE FLUCTUATIONS 11
    3.1 Introduction 11
    3.2 Tectonic setting and climate 13
    3.4 Methods 18
    3.5 Results 20
    3.6 Discussion 24
    3.7 Conclusions 28

4. SIGNIFICANCE OF GROUNDWATER FLOW FOR THE HYDROLOGIC BUDGETS OF PALEO-LAKES IN EAST AFRICA: 29
    4.1 Introduction 29
    4.2 Setting 31
    4.3 Methodology 35
    4.4 Results 37
    4.5 Discussion 44
    4.6 Conclusion 47

5. CONTRIBUTIONS TO CLIMATE PROXY SITES OF EAST AFRICA: 49
    5.1 Introduction 49
    5.2 Setting 51
    5.3 Materials and Methods 55
    5.4 Results and Discussion 56
    5.5 Preliminary Conclusions 68

6. CONCLUSIONS AND GENERAL PERSPECTIVES 71

7. BIBLIOGRAPHY 75

8. APPENDIX.....87

9. ENVIRONMENTAL VARIABILITY IN LAKE NAIVASHA, KENYA, OVER THE LAST TWO CENTURIES.....89

A1.1 Introduction 89

A1.2 Study site 90

A1.3 Material and Methods 91

A1.4 Results.....95

A1.5 Discussion 100

A1.6 Summary and Conclusions.....103

10. SUPPLEMENTARY MATERIAL 109

LIST OF FIGURES

Figure 1.1 Schematic illustration of general and fundamental processes within lakes varying with lake basin slope.....2

Figure 1.2 Schematic diagram illustrating groundwater and lake water interaction for three lake types-recharge, thoroughflow and discharge. 3

Figure 2.1 Schematic diagram of the major components of the climate system.....8

Figure 2.2 IPCC's Regional climate change prediction for mean and extreme precipitation, drought, snow using AR4 AOGCM simulations (21 simulations) 9

Figure 3.1 Map of the eastern branch of the East African Rift System (EARS) showing the lake basins of the study and the main faults and volcanic centers defining them. 12

Figure 3.2 Morphometric characteristics of lake EARS lake basins from the SRTM dataset 21

Figure 3.3 Spatial distribution of aridity index values in the EARS.....22

Figure 3.4 Topographic cross-section through the lake basins from south to north and the corresponding Hypsometric integral (HI; circles) and aridity index (AI; triangles) values of lake basins 24

Figure 3.5 Hypsometric integral (HI) plotted against the aridity index (AI) of the basins of the EARS. 25

Figure 4.1 Regional map of the Central Kenya Rift (A) Geomorphology (B) Climate regions within the study area.....30

F**igure 4.2** The Geological map of the CKR and a E-W cross section through Eburru area, from the Mau Escarpment to Aberdares 30

Figure 4.3 The geological cross section of the Eburru and resistivity iso map from the Transient Electromagnetic Method (TEM), at three depths:- 2400 m asl, 2100 m asl and 1800 m asl. 36

Figure 4.4 Groundwater levels map with boreholes, overlaid on the fault lineament densities and NW-SE /W-E cross sections of the water levels between two wells ..37

Figure 4.5 Graphs showing the loss of water between upper and lower Gilgil gauge stations trough subsurface seepage in the lower section the river runs along a 20 km N-S striking fault. 38

Figure 4.6 S-N schematic topographic-hydrological section through the Central Kenya Rift lake catchments, showing groundwater head decay from the Early Holocene to present day.....40

Figure 4.7 Lineament density map of the Central Kenya Rift. 41

Figure 5.1 Location of lake basins and regional climate of East Africa. Cross-section of the eastern branch of the East African Rift System (EARS) showing the location of lake basins in relation to the geographical distribution of rainfall regimes across East Africa. 48

Figure 5.2 Synoptic climatology of tropical East Africa for four representative months of the seasons discussed in this study. 48

Figure 5.3 Topography and location map of catchments within the East African Plateau and the Ethiopian Plateau. Schematic illustration of general and fundamental processes within lakes varying with lake basin slope.....49

Figure 5.4 Distribution of ENSO and IOD events during one 11-year solar cycle between 1996-2009 in comparison to the Indian Monsoon strength.....52

Figure 5.5 Monthly overview of the development of (A) ENSO and (B) IOD events compared to solar irradiation changes (C) between 1996-2009.. 53

Figure 5.6 Seasonal averaged watershed mean and total rainfall for the 11 watersheds of East African lake basins within one 11-year solar cycle.....55

Figure 5.7 Topographic and precipitation swath profiles along the East African Rift System between 35-40° E.....56

Figure 5.8 Schematic diagram of moisture transport across the East African Plateau. The crosssection is from Mau Escarpment to the Aberdares over lakes Nakuru and Naivasha 60

Figure A1.1 Location map for Lake Naivasha within the highest basin of the Kenyan Rift System, together with the catchment area and sites discussed in the text.....85

Figure A1.2 Lithology, chronology, sampling slices and diatom-based zonation of NSA-3/4. Sediment chronology in years AD, based on seventeen 210Pb dates from NSA-4.....86

Figure A1.3 Radiometric chronology of Lake Naivasha sediment core NSA-4 87

Figure A1.4 Summary of the diatom assemblages from Lake Naivasha core NSA-3, PC1 scores, and diatom-based zonation 90

Figure A1.5 PCA biplot of species and sample data. Arrows represent species and circles represent samples. Ellipses indicate the diatom-inferred zones.....90

Figure A1.6 Down-core variations in diatom habitat preferences, diatom-based zonation, diatom-inferred conductivity and TP, SAR and geochemical variables 92

Figure A1.7 Compilation of diatom assemblage variations, sediment accumulation rate (SAR), total phosphorus (TP) and historical records of environmental and land use data.....95

Figure S1 Rainfall distribution for each season between 1996-2010 102

LIST OF TABLES

Table 3.1 East African rift lakes, their location and key characteristics 14

Table 5.1 Lake catchment characteristics 50

Table A1.1 210Pb chronology of the Lake Naivasha core NSA-4-2007.....88

Table A1.2 Fallout radionuclide concentrations in the Lake Naivasha core NSA-4-2007 91

Table A1.3 Stratigraphical zonation inferred by diatoms their dominant and subdominant diatom taxa and Performance of the conductivity and TP models used for diatom-inferred reconstructions 91

Table A1.4 Performance of the conductivity and TP models used for diatom-inferred reconstructions 91

ACKNOWLEDGMENTS

So many have contributed to the successful completion of my PhD at Potsdam University that it is impossible to thank everyone here, and I apologize for any oversights.

First, my heartfelt gratitude goes to my advisor Martin Trauth for the guidance and inspiration in shaping the basis of this thesis. His important support extended beyond academic to ensure that I had an easy stay. I owe most sincere gratitude to Manfred Strecker for his valuable advice and important support throughout this work. I thank my co-authors, Eric Odada and Dan Olago, Ulrich Kniess, Annette Junginger, Kathleen Stoof and anonymous reviewers for the comments, constructive criticism and suggestions they provided to improve the original Manuscripts. I also wish to thank Franziska Wilke, Jenipher Mwanza; René Dommain for translating the abstract to German

I am very grateful to the organisations that funded me through my PhD: The German Academic Exchange Service (DAAD), the German Research Foundation (DFG) through the DFG Graduate School GRK1364 and Manfred Strecker (through his Leibniz Prize), without you this work would not have been possible.

I also want to acknowledge Olkaria Geothermal Company, Naivasha (through Geofrey Muchemi of) and of the Water resources Management Authority in Naivasha for providing the geophysical data, borehole well logs, and water quality data sets.

Potsdam colleagues whom am indebted to are Yannick Garcin, for very insightful discussions, and Gerold Zeillinger for troubleshooting all the GIS-related hiccups I encountered. I am grateful to the GKR 1364 members for the times we shared together during the field schools in Kenya and India and the good discussions we had especially Kathleen and Annette whom we discussed our projects together and got to understand the ‘monsoon phenomenon’ in East Africa. Many thanks to my office mates Anke, Andres, Fred, Henry, Mauricio, Nico, Veronica and Yanqui for keeping the snack table full!

To my friends in Berlin; thanks to Jenny Radeisky who ensured that my transition to Berlin was smooth, many thanks to my Crossway church family Johanna, the Dyes and the Goods, Kristi, the ladies group for keeping me sane and encouraged during my stay.

I owe loving thanks to my family for their love and support in many ways that saw me through tough times.

CHAPTER 1

INTRODUCTION

Lakes can be extremely sensitive to changes in climate on a variety of temporal and spatial scales. Inevitably, they keep an archive of climate and environmental dynamics that can be used to understand dynamics of the global climate system and associated ripple effects on lake water quality and ecological success of species (Skinner, 2000; Smol, 1992). The seminal work by Street and Grove (1976) identified glacial-interglacial timescale variability in African lake levels and pioneered the usage of lake basins in the low latitudes for paleoclimate reconstruction. Consequently, the past three decades, has seen development of new and diverse proxy records, improved dating techniques and field sampling methods. These lacustrine sediment investigations have established patterns of global teleconnections in climate variability at orbital, glacial-interglacial, and shorter time scale but also reveal distinct tropical climate processes.

The reliability of paleoclimatic inferences from lake-sediment records rests on understanding the sensitivity of various sediment variables to climatic and environmental changes. Much progress has been made in recent years in understanding Quaternary climate, however important uncertainties and caveats still exist with regard to both empirical reconstructions and model estimates in resolving high frequency (decadal to century scale) variability over several millennia and resulting spatio-temporal heterogeneity (Verschuren, 2000; Gasse, 2000; Johnshon et al., 2002; Garcin, 2006; Fritz, 2008; Pienitz and Lotter, 2009). As biophysical systems, lakes act as hydroclimate filters incorporating all the physical, chemical and biological processes in them to transform input forcing variables into something other than a simple output recording (Cohen, 2003). This climate-proxy generating process in active rift settings is complex and has not yet been fully investigated.

A concept that has largely remained unexploited since its inception in the 80’s within climate reconstruction studies is the amplifier lake phenomenon. Street Perrott, (1985) established that closed lakes are sensitive to climate shifts. This implies that within the same regional setting, two lakes systems modulated by the same external forcing elements can differ in response. Although the concept is already known, it has remained largely unexploited in understanding and refining empirical climate-proxy relationships for spatial and temporal heterogeneities. The scope of challenges within paleoclimate reconstruction studies, along with the interdisciplinary nature of the problem, point to the need to develop and improve numerical foundations for quantitative paleolimnology to better constrain the ecological

indicator values for lacustrine biotic and abiotic proxies (Birks, 1998; Eggermont et al., 2006; Verschuren and Russell, 2009). Understanding basin/site specific responses and feedbacks to climate variability for example would aid calibration-in-space and calibration-in-time. In the East African Rift System (EARS) lake basins three physical aspects can be explored to this effect.

First, lakes basins in the eastern arm of the EARS have developed from tectonic processes associated with rifting and volcanism. Consequently they have highly contrasting geometries, character and hence erosion an depositional environments. Their geometries vary from graben-shaped to pan-shaped lakes, with implications on both rate of lake level response to regional climate (steep sided lakes respond faster) and initial deposition and potential reworking of lake floor sediments, with greater degree of reworking in very steep basins (Fig. 1.1). Studies in deep tectonic lakes such as Lake Tanganyika and Malawi on the western arm of the EARS have shown this downslope transport of sediment by creep, debris flows and turbidity currents (Johnson, 1996, Tiercelin, 1990; Soreghan et al., 1999). Lacustrine sedimentary sequences and shoreline proxies exposed in these basins would be constrained by such morphological differences thus creating disparity in space.

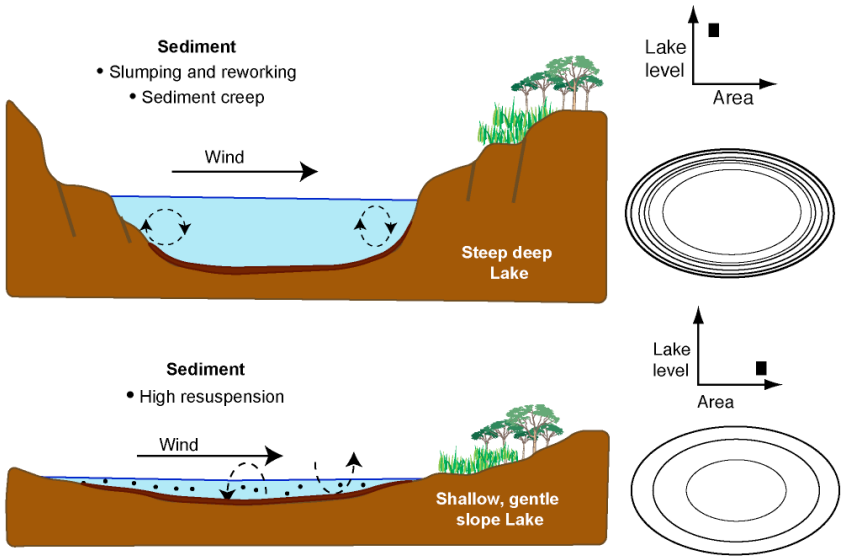

Figure 1.1 Schematic illustration of general and fundamental processes within lakes varying with lake basin slope.The steep and deep lake experiences high fluctuations in lake levels as less changes in aerial extent compared to the basin with gentle slopes. The sediments in steep sloped lakes are subject to slumping and reworking while in gently slopping basins, they are prone to high resuspension from wind

Second, rocks in the rift floor and margins are faulted and fractured by at least two generations of faults. This tectonic setting enhances secondary porosity and permeability of the volcanics. Moreover, due to the active extensional tectonics of the region, existence of hot and cold springs and surface-groundwater interaction, interbasin connectivity becomes important in estimating lake hydrological and solute budgets. Both Kenya and Ethiopian domes which are topographic highs within the rift create a hydrological gradient that facilitates local and regional groundwater flow thus effecting the hydrological and solute budgets of

affected lakes (Figure 1.2). For instance, during drier months recharge lakes will have no evaporites present whereas throughflow and discharge lakes can have evaporites sustained by the groundwater component. Because lakes exchange both solutes and water with groundwater, it is generally unjustified to regard lakes as simple “closed basins”, even for extremely saline cases (Sanford and Wood 1991, Donovan et al., 2002). The Central Kenyan rift lakes are suitable for hydrological interbasin connectivity investigations.

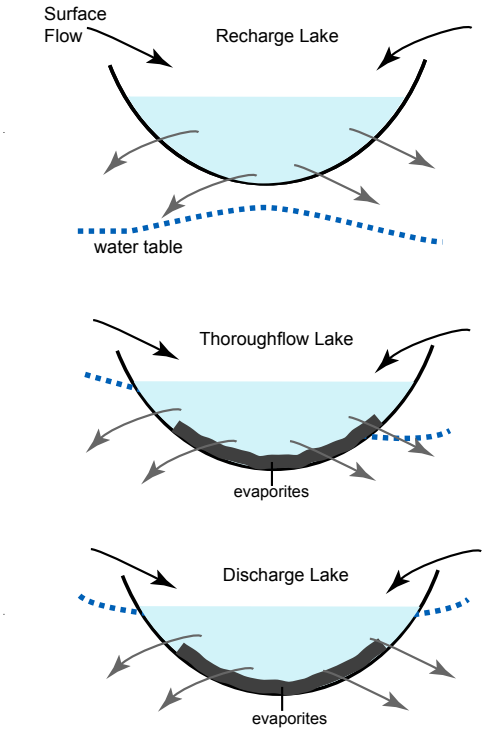

Figure 1.2 Schematic diagram illustrating groundwater and lake water interaction for three lake types-recharge, thoroughflow and discharge. Recharge lakes tend to be dilute which thoroughflow and discharge lakes can have evaporates (modified from Tweed, et al., 2010)

Third, within the rift system, lake catchments are encompassed by high relief escarpments and mountains that influence orographic rainfall distribution and exerting control on runoff routing and catchment sizes leading to large differences in the hydrological budgets from one lake to another despite their spatial proximity. On seasonal to decadal time scales the amount and spatial distribution of rainfall within the EARS is determined by climate mechanisms such as the location of the Intertropical Convergence Zone (ITCZ), the Congo Air boundary (CAB), and strength of El Niño Southern Oscillation (ENSO) and Indian Ocean Dipole (IOD). The hydrology of lake basins are governed by variability of these tropical climate phenomena.

My interest is to decipher EARS lake sensitivities to climate variability and advance quantitative parameters for the ‘amplifier lake phenomenon’. The study is carried out on two spatial and temporal scales; a regional scale with ten lakes within the EARS and a local scale in the central Kenya Rift with two lake systems that have good records of climate on short (annual) to medium (10^3) timescales. In this thesis, I use a multidisciplinary approach that integrates geomorphological statistics and digital terrain analysis, geologic and vegetation

mapping, remote sensing, time-series analysis, and hydrologic modelling of ten large lake basins in East Africa:Lakes Ziway-Shalla, Awassa, Turkana, Baringo-Bogoria, Nakuru-Elmenteita, Naivasha, Victoria, Magadi-Natron and Manyara. Subsequently, I investigate interbasin hydrological connectivity in the Central Kenya rift of the sensitive Naivasha and Nakuru-Elmenteita basins by carrying out detailed hydrogeological investigations and applying a hydraulic head decay model. The model uses a linear-reservoir depletion approach that allows us to estimate groundwater level modification in both basins following the decline of the African Humid Period (AHP). Finally I investigate the distribution of rainfall in 14 years (1996-2009) and explore the distribution of rainfall related to the forcing mechanisms of the IOD, ENSO, CAB using NOAA satellite. Understanding recent intraannual variability on different temporal and spatial domains is very important for a variety of applications related to physical and chemical and biological parameters of hydrological systems within east Africa.

Chapter 2 of this thesis introduces the Earth's climate system and its components. The emphasis is on the tropical equatorial climate of East Africa, its major wind systems, convergence zones and seasonal to interannual fluctuations. Furthermore, Chapter 2 gives an overview of climate change on recent time scales and the significance to societies.

In Chapter 3, an attempt to classify lake sensitivity to climate change is made to facilitate spatial and temporal variation calibrations in the East African Rift. I have used geomorphological ratios and indices, present climatic indices and published Early Holocene lake levels of ten lakes in the East African Rift; Ziway-Shalla, Awassa, Turkana, Suguta, Baringo-Bogoria, Nakuru-Elmenteita, Naivasha, Victoria, Magadi-Natron and Manyara. The lakes classified as sensitive to climate changes show major lake level fluctuation in response to moderate climatic changes, they are also referred to as amplifier lake systems and these lakes are potential sites for high resolution paleoclimatic studies. The chapter was published as an article in the Journal of Paleolimnology (Olaka, L.A., Odada, E.O., Trauth, M.H., Olago, D.O., 2010, The sensitivity of East African rift lakes to climate fluctuations. Journal of Paleolimnology, 44, 629–644).

Chapter 4 is a paper that seeks to understand the interbasin, hydological connectivity in the Central Kenya rift lakes Naivasha and Nakuru-Elmenteita in the course of climate change –a great unknown in lake-balance modeling so far. I make a detailed hydrogeological analysis of the region and mapped out groundwater flow paths and depressions from geological, geophysical and structural data. A linear decay model is used to estimate the duration of groundwater would take to lower to current level from the AHP level. The chapter has been submitted as a manuscript to the journal Global Planetary Change (Lydia Olaka; Ulrich Kniess; Dan O Olago; Eric O Odada; Martin H Trauth, submitted, The significance of groundwater flow for the hydrologic budgets of paleo-lakes in East Africa: how closed are closed-basin lakes in rifts? Global and Planetary Change).

Identifying lakes which can provide proper proxies for prevailing rainfall mechanisms in East Africa is pre-eminent to understanding paleo-proxies. In Chapter 5, Satellite, rainfall estimates from FEWSnet are used to investigate intraseasonal rainfall variability of eleven East African rift basins for the last 14 years (1996-2010). The aim is so to understand the

precipitation disparities induced by the terrain and water bodies on the prevailing regional climate at a seasonal scale. The strengths of climate mechanisms are investigated on seasonal precipitation of ITCZ, CAB, solar radiation and the influence of the El Niño/Southern Oscillation (ENSO) and the Indian Ocean Dipole (IOD). This work is the result of the collaboration with Annett Junginger, also member and doctoral student of the DFG Graduate School GRK1364 at the University of Potsdam. My contribution to the manuscript to mine the data whereas Annett Junginger contributed knowledge the correlation of rainfall mechanisms The chapter will be submitted to the journal Climate Dynamics after completion of this thesis.

Chapter 6 summarizes the findings of this study and a brief mention of the planned follow up study in the Central Kenya rift.

The appendix of this thesis contains a manuscript in collaboration with two other members of the DFG Graduate School GRK1364, Kathleen Stoof (Biology, Molecular Genetics) and Annett Junginger (Sedimentology, Paleoclimatology). With Kathleen Stoof as the lead author, Annett Junginger and I are listed as equal contributors on this manuscript. This study investigates the human vs climate changes in the last two centuries using a diatom record. Kathleen Stoof analyzed and interpreted the diatom assemblages, Annett Junginger performed the sedimentological analyses, and I contributed my knowledge in historical climatic and environmental change, the hydrological and anthropogenic implications of these changes in my home country Kenya. Kathleen Stoof drafted the first versions of the manuscripts, and Annett Junginger and I made text contributions and and jointly developed the main conclusions of the project.

CHAPTER 2

THE CLIMATE SYSTEM

The climate system is an interactive system composed of four subsystems- the atmosphere, cryosphere, biosphere, and hydrosphere, influenced by various external forcing mechanisms, such as solar radiation, tectonic motions of Earth's lithosphere driven by mantle convection and human activities (Figure 2.1). Many physical, chemical and biological interaction processes occur among the various components of the climate system on a wide range of space and time scales, making the system extremely complex. Although the components of the climate system are very different in their composition, physical and chemical properties, structure and behaviour, they are all linked by fluxes of mass, heat and momentum since all subsystems are open and interrelated. Moreover, each subsystem has characteristic physics and time scale of response. For example both the atmosphere and oceans are considered fluids on the rotating earth, but with different time scales of response (weeks to months for the atmosphere, years to centuries for the ocean). The biosphere processes (e.g. vegetation and soil moisture feedbacks) react on time scales similar to the atmosphere than to the ocean but the physics of the processes is completely different, similarly the cryosphere's fluctuations (except for sea ice) are generally on a much longer time scale than for the atmosphere and ocean (Crowley, and North 1991; Philander and Fedorov, 2003; Medina-Elizadle and Lea, 2005; IPCC, 2007).

Any change in the components of climate may result in climate variability, throughout its history the Earth's climate has shifted dramatically and frequently. It is established from climate proxies that climate variability and change occurs in cycles with characteristic periods, for example 200 million, 400,000, 100,000, 41,000, 22,000 or 4-9 years (Bjerknes, 1969; Berger et al., 1994; Berger and Lowre, 1997; Zachos et al., 1997; 2001; Chiang, 2009). Climate variability on time scales of 10^2-10^5 years is recorded as shifts between humid and arid phases in the low latitudes, while in high latitudes it manifests as shifts in cold and warm phases. These shifts can be responses to both low latitude insolation trends (e.g. Partridge et al., 1997) and high latitude forcing mechanisms (Scheufuß et al., 2005), occurring sometimes abruptly over time scales from 10^1-10^3 years.

External climate forcings can be spatially heterogeneous e.g. aerosols and land cover changes, such heterogeneous climate forcings could represent a more significant threat to our future climate systems. For example, as the Earth's average temperature has increased in the last 50 years, some weather phenomena have become more frequent and intense (e.g. heat

waves and heavy downpours), while others have become less frequent and intense (e.g. extreme cold events). However, the interplay of the components of the climate system and the associated feedbacks is still an area of investigation.

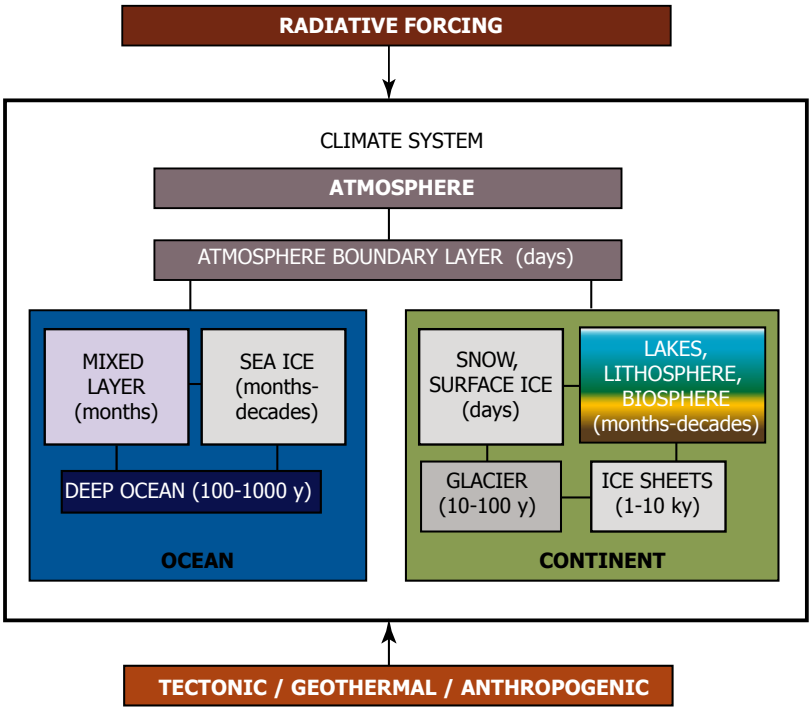

Figure 2.1 Schematic diagram of the major components of the climate system with estimated response times or adjustment (equilibration) times for different components of the climate system. Feedbacks between various components play an important role in climate variation (After Crowley 1991).

However, major uncertainties remain in our understanding of the interplay of the components of the climate system and how rapidly feedbacks perturb the climate systems. Climate records show that large widespread, abrupt climate changes have occurred repeatedly throughout the geological record, e.g., temp changes of 5°C over ice age cycles generally believed to have resulted from small, globally averaged net forcing (Alley et al., 2003). Though some of these mechanisms have been identified and their model simulations are also improving, the models that are currently being used to assess human impacts on climate do not yet simulate the past changes with great accuracy (Alley et al., 2003). High resolution reconstructions of past climate conditions make it possible to validate climate models with increasing level of detail and contribute to shaping our expectations of the climate system. Integration of various climate data such as instrumental, satellite and highly resolved proxies could help improve climate models and their reliability for future predictions (Stute et al., 2001; Donders et al., 2008). Currently climate predictions are on a seasonal and annual scale but little is know on the decade and centennial scales due to the complexities of response within the climate system.

2.1 Society under a varying climate

Climate change research on decadal and centennial levels seeks to answer some fundamental questions which are fundamental to ecological and societal survival such as: is the hydrological cycle changing? Is the planet getting warmer? Is climate becoming more extreme or variable?

Climate exerts a significant control on the day-to-day economic development of Africa, particularly for the agricultural and water-resources sectors, at regional, local and household scales (IPCC, 2007). Much research has been devoted to understanding the climate or at least to monitor it and abate the negative effects. Since 1960, warming trends have been observed ranging between 0.1 and 0.3°C in Africa (IPCC, 2007). While precipitation has shown great intrannual variability, decreasing by about 4% in central africa and upto 40% in western Africa, however an increase of 10 % has been observed in New Guinea coast (IPCC, 2007 and refs therein). The climate predictions show a grim picture and there is interest to slow the warming seen in the 21st century. In the IPCC report on regional average predictions for Africa based on 21 models show that East Africa will become wetter, South Africa and Sahara will become drier while the predictions are less clear for West Africa (Christensen et al., 2007; IPCC 2007 fig. 2.2).

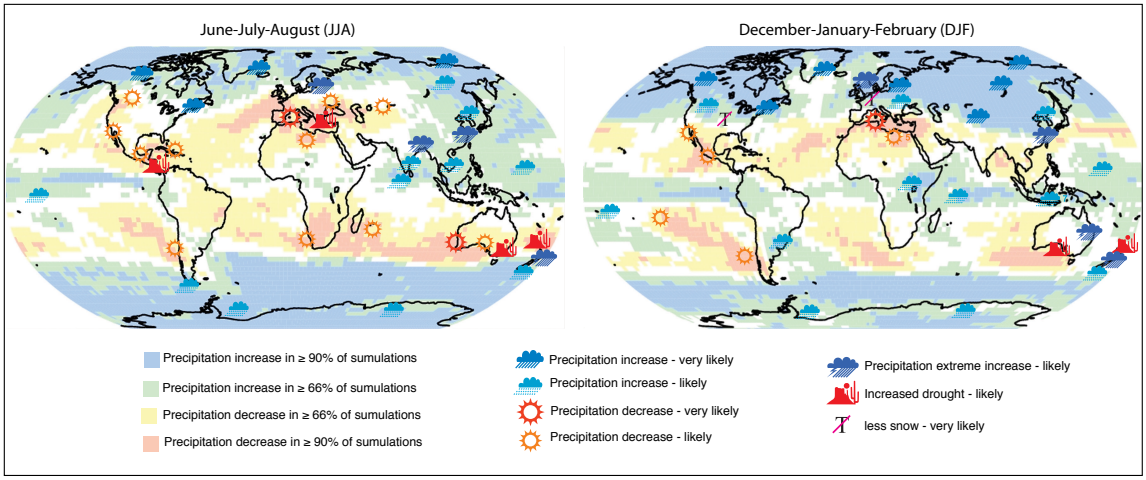

Figure 2.2 Regional climate change prediction for mean and extreme precipitation, drought, snow using AR4 AOGCM simulations (21 simulations used). Precipitation is projected to increase in the green and blue regions it project to decrease in the yellow and red regions by the end of the century (IPCC, 2007).

Studies have shown that human societies resilience is somewhat governed by climate - food production and water resources are dependent on the state of climate variables. Extremes of which lead to droughts, floods and destruction of environmental and economic systems. In historical times extended droughts have been linked to collapse of civilizations. Examples include the Maya (2000 B.C. to A.D. 1500), Khmer Empire, (Haug et al., 2003; Buckley et al., 2010) and 14th century southern migration of Bantus and Nilotes tribes from Central Africa driven by famine and wars. However, changes in those societies could have been instigated by a number of factors including, economic and political instability, diseases, cultural innovation and environmental degradation which may have been indirectly related to

climate changes. In recent times, studies interested in climate-environment-and society interactions have shown climate variability, especially changing water resources have led to changes within societies in affected regions (Verschuren et al., 2000; Holmgren and Öberg 2006). This highlights the need to improve understanding of short term climate variability on different scales especially in arid and semi arid areas of the world that lack a diversified economy and have a high dependence on seasonal rainfall for agriculture to ensure adaptation and mitigation.

An emerging issue linked with climate variability is the emergence and re-emergence of infectious diseases and epidemics. Systematic increases in mean temperature and precipitation, resulting in greater humidity and high water temperatures, has facilitated the spread of many vector borne infectious diseases such as malaria, dengue and encephalitis, cholera (Thomson et al., 2006; Bomblies et al., 2008; Hazishume et al., 2008; Paaijmans et al., 2010). When these communicable diseases spread to other continents and adapt to new environment, the impact resulting is equally disastrous (eg. the east coast fever for animals when British arrived in Africa).

Currently about 290 million people live in Eastern Africa. This region with mainly semi-arid to sub-humid climate is quite vulnerable to water stress. Thus proper water resource allocation is increasingly becoming important for the increasing population. Knowledge of sensitivity of the lake basins to different forcing factors is needed to ensure sustainability of the water resources and also alleviating waterborne disease vectors dependent on water temperatures (Paaijmans et al., 2010). Thus, integrating paleolimnological information of basins with information based on their distinct characteristics and forcing factors on different scale combined will undoubtedly contribute to effective management protocols can improve basin management systems (Smol, 1992).

CHAPTER 3

THE SENSITIVITY OF EAST AFRICAN RIFT LAKES TO CLIMATE FLUCTUATIONS

Abstract

Sequences of paleo-shorelines and the deposits of rift lakes are used to reconstruct past climate changes in East Africa. These recorders of hydrological changes in the Rift Valley indicate extreme lake level variations on the order of tens to hundreds of meters during the last 20,000 years. Lake-balance and climate modeling results, however, suggest relatively moderate changes in the precipitation-evaporation balance during that time interval. What is the reason for this difference? We introduce simple tools for morphometric analysis and hydrology to investigate this question. Ten lake basins:Ziway-Shalla, Awassa, Turkana, Suguta, Baringo-Bogoria, Nakuru-Elmenteita, Naivasha, Victoria, Magadi-Natron and Manyara in the eastern branch of the East African Rift System (EARS) are used for this study. Our classification of lake response to climate is based on empirical measures of topography (hypsometric integral) and climate (aridity index). With reference to early Holocene lake levels, we find lakes in the crest of the Ethiopian and Kenyan domes to be most sensitive to recording regional climatic shifts. Their hypsometric values are between 0.23-0.29, in a graben-shaped basin and their aridity index is above unity (humid). Of the ten lakes, three lakes in the EARS are sensitive lakes:Naivasha (HI=0.23, AI=1.20) in the Kenya Rift, Awassa (HI=0.23, AI=1.03) and Ziway-Shalla (HI=0.23, AI=1.33) in the Main Ethiopian Rift (Main Ethiopian Rift); two lakes have the graben shape, but lower aridity indices; Lakes Suguta (HI=0.29, AI=0.43) and Nakuru-Elmenteita (HI=0.30, AI=0.85) are most sensitive to local climate changes. Though relatively shallow and slightly alkaline today, they fluctuated by four to ten times the modern water depth during the last 20,000 years. Five of the study lakes are pan shaped. Knowledge of the sensitivity of these lakes is critical in establishing the timing or synchronicity of regional-scale events or trends and predicting future hydrological variations in the wake of global climate changes.

3.1 Introduction

The sedimentary sequences of equatorial African lakes have been used widely as archives of past climate changes in the low latitudes on diverse time scales (Verschuren et al., 2000; Gasse 2000; Barker and Gasse 2003; Trauth et al., 2005; Legesse et al., 2002). In these studies, biological and geochemical proxies, and sequences of paleoshorelines have been used to study past climate fluctuations (Gasse 2000; Barker and Gasse 2003). A crucial prerequisite for paleoclimate interpretation of lacustrine sedimentary sequence, however, is an understanding of the lake system under investigation, such as the: (a) response to changes in climate and catchment activities, (b) response of biological and physico-chemical properties to

moisture changes, and (c) site-specific processes governing the incorporation of environmental signals into the sediments (Street-Perrott and Harrison 1985; Legesse et al., 2002). Complexities, however, also arise in inferring climate from these records, especially in tectonically active settings, because responses of lakes to climate are also mediated by geomorphic and hydrologic setting of basins thus creating non-linearity and spatial heterogeneity in the pattern and timing of inferred change.

Large lakes in East Africa experienced large hydrologic fluctuations, driven by insolation changes, during the late Pleistocene and early Holocene (15-5 ka BP, Figure 3.1). Although the timing and magnitude of the hydrological shifts in the basins are known, the climate conditions at those times are not well defined. Lake water-balance modeling results for some East African lakes show only moderate changes in effective moisture (ca. 25% more rain) that cannot account for the high lake stands (Hastenrath and Kutzbach 1983; Bergner et al., 2004; Dühnforth et al., 2006). Street-Perrott and Harrison (1985) explained this response of East African Rift System (EARS) lakes to climate changes using a Precipitation-Evaporation balance in the catchment and introduced the term “amplifier lakes.” Their classification of lake sensitivity showed closed lakes are more sensitive ‘amplifiers’ than open lakes with large outflows. They suspected the graben morphologies of the EARS lakes had an influence on whether a basin was an “amplifier lake,” but did not pursue the idea. Another common ratio used in sensitivity studies has been catchment/lake area ratio. Basins with large catchment-to-lake-surface area ratios have demonstrated large amplification factors (Burrough and Thomas 2009).

Basic morphometric features such as volume, surface area, and mean depth, as well as information related to hypsographic curves, are increasingly being used to describe limnological changes that occur as lake volume changes (Johansson et al., 2007). In very flat basins, changes in lake volume cause horizontal oscillations rather than vertical changes in shoreline position, making lakes that are steep over a wide range of water depths more suitable for sensitivity studies. Morphometric variables in basins can be determined by hypsometric analysis of Digital Elevation Models (DEM). In the past, routine hypsometric analyses were limited by computer power. With advances in computing and GIS technology since 1952, hypsometry is being reinvestigated to improve understanding of geomorphologically controlled dynamics of sediment proxies. A combination of lake bathymetric maps and hypsometric curves can provide visual representation of 2D and 3D properties of a lake (Johansson et al., 2007). The integral of the curve provides a simple index of the depth distribution within the lake/area under consideration, which can be used to quantify the size and form of a lake.

This paper investigates the sensitivity of EARS lakes as climate recorders by incorporating variables that describe lake form and hydrology, and is a continuation of the work by Street-Perrott and Harrison (1985) who first introduced the term “amplifier lake.” We investigated nine closed-basin rift lakes between 5°S and 10°N latitude and 30°E and 40°E longitude, from Ethiopia through Kenya to Tanzania. The study included Lakes Ziway-Shalla, Awassa, Turkana, Suguta, Baringo-Bogoria, Nakuru-Elmenteita, Naivasha, Magadi-Natron, Manyara, and one open non-rift lake, Victoria, which is situated in the plateau region between the eastern (Gregory Rift) and the western arms (Albertine Rift) of the EARS. The latter basin

was included for comparison. Results from our analysis can be used to better constrain climate interpretations from lakes.

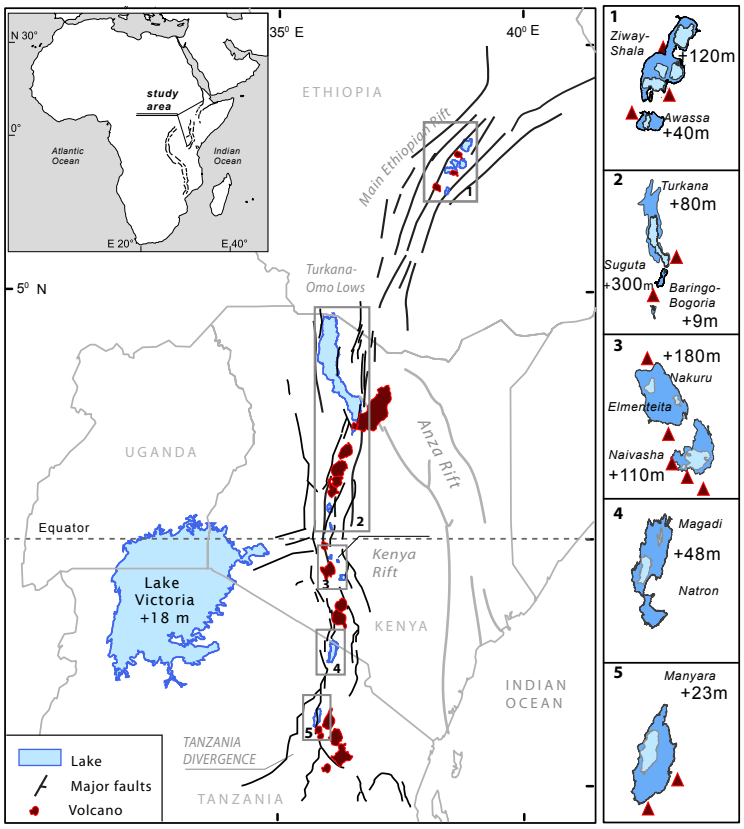

Figure 3.1 Map of the eastern branch of the East African Rift System (EARS) showing the lake basins of the study and the main faults and volcanic centers defining them. Inset 1-5 show the extent of the early Holocene lakes and their height above the modern lake (see Table 1 for references)

3.2 Tectonic setting and climate

The EARS has two main branches, the eastern and the western branches that crosscut Eastern and Central Africa, beginning at the triple junction of the Red Sea and Gulf of Aden oceanic ridges, and the Afar Rift at about 10°N latitude to more than 30°S latitude, terminating on land with the Lake Malawi basin. It is structurally and magmatically controlled, creating complex relief and drainage conditions that are highly variable through time, initiated about 45 Ma and continuing to present (Baker et al., 1972; Strecker et al., 1990; Ebinger et al., 2000; Chorowicz 2005). We study lakes in the Eastern branch, which extends over a distance of 2200 km, from the Afar triangle in the north, through the Main Ethiopian Rift (MER), the Turkana-Omo lows, the Kenyan (Gregory) rift, to the basins of the North-Tanzania divergence. The EARS is generally <100 km wide, with the exception of the region between southern Ethiopia and Northern Kenya, and the region in Northern Tanzania, where the Kenyan (Gregory) rift terminates. In these regions, the rift is more than 300 km wide (Chorowicz 2005).

The NE-striking MER (330 km long, 50 km wide) floor rises progressively from the northeast with elevations of 750-1700 m southwestwards, and finally downgrades to 1100 m in the south (Ayenew et al., 2007; Chorowicz 2005). The Kenyan (Gregory) rift region corresponds to the Kenyan dome. Elevations in this rift floor rise from about 1050 m in the north around the Baringo-Bogoria Basin to about 2000 m in the middle, and steps down progressively southwards to about 600 m asl in the Natron basin (Chorowicz 2005). The floor of the rift is highest in the central portion, between Lake Nakuru and Lake Naivasha, and decreases in altitude in both directions along the rift. The basins in the rift are generally bordered on both sides by high relief, comprising almost continuous parallel mountain lines and plateaus, and sometimes, volcanic massifs. Between these domes are the Turkana-Omo lows, with significantly lower (250 m asl) elevations than the dome regions. This low area has no pronounced rift shoulders, but there are several N- to NE-striking half-graben basins, e.g. Omo Valley, Lake Turkana and Chew Bahir.

Late Cenozoic tectonic activity in the EARS commenced with southward propagation of rifting and magmatic activity and progressive formation of faulted troughs throughout the length of the rift, in which lakes have formed (Tiercelin and Lezzar 2002; Trauth et al., 2007). These troughs are generally half-grabens bounded by major high-angle boundary faults on one side and a faulted flexural margin on the other, or less frequently, grabens bounded by two faults of similar importance. These lakes are typically elongate, following the dominant trend of the faults:NNE-SSW-trending lakes within the MER, NS-trending within the Turkana-Omo lows. Further south in the Kenyan rift they assume a NNW-SSE to NS trend and NS to NNW trend in Northern Tanzania, at the termination of the rift (Le Turdu et al., 1999). In contrast to the large (ca. 30,000 km^2) and deep (ca. 1,000 m) lakes of the western rift, the lakes in the eastern rift are small (about 100-200 km^2 surface area), shallow (<10 m deep) and mostly of the closed-basin type, with internal drainage (Ebinger et al., 1993; Singer and Stoffers 1980). Few of the lake basins in the EARS contain fresh water, and most are quite saline.

Rifting of the EARS was preceded by doming of the Ethiopian and the Kenyan domes. This morphotectonic evolution contributed significantly to creating important orographic barriers and environmental changes (Sepulchre et al., 2006; Spiegel et al., 2007). Modern climate is governed by the seasonal influence of several major air streams and convergence zones that interact with regional orography, large inland water bodies and sea-surface temperature fluctuations in the Indian and the Atlantic Oceans (Nicholson 1996). Meridional moisture transport shows the Ethiopian Highlands deflect the northeast monsoon flow southward along the Somalian coast during winter and the Kenyan highlands deflect the southeast flow northward during summer (Sepulchre et al., 2006). As a result, climate patterns are highly complex and variable. In general, highlands flanking the Rift Valley intercept most of the monsoonal rainfall in the region, resulting in a strong moisture deficit at the rift floor, particularly near the lakes.

Table 3.1 East African rift lakes mentioned in the text, their location and key characteristics

	Longitude	Latitude	Altitude	Lake Area	Basin Area	Basin Area/ Lake Area	Hypsometric Integral	Precipitation	Potential Evaportranspiration	Aridity Index	Holocene Lake Level Rise	Normalized Holocene Lake Level Rise	Normalized Holocene Lake Level Rise	References
	deg	deg	m	km^2	km^2			mm/yr	mm/yr		m	(Lake Area)	(Basin Area)	
Nakuru-Elmenteita	36.08	-0.37	1,770	60	2,390	39.83	0.30	1,200	1,400	0.85	180	3.0000	0.0753	11, 28
Naivasha	36.34	-0.77	1,885	180	3,200	17.78	0.23	1,500	1,250	1.20	110	0.6111	0.0344	3, 27, 29
Awassa	38.43	7.03	1,680	129	1,455	11.28	0.23	1,028	1,000	1.03	40	0.3101	0.0275	1, 16, 25, 4
Suguta	36.55	2.22	275	80	12,800	160.00	0.30	1,000	2,309	0.43	300	3.5000	0.0219	9, 13, 18
Ziway-Shala	38.76	7.59	1,558	1,222	14,600	11.94	0.23	1,200	900	1.33	120	0.0982	0.0082	1, 15
Magadi-Natron	36.26	-2.33	600	440	10,930	24.84	0.36	1,000	1,750	0.57	48	0.0409	0.0016	5, 6, 10, 14, 26
Baringo-Bogoria	36.06	0.63	967	215	6,200	34.98	0.37	1,000	2,309	0.43	9	0.0419	0.0015	7, 18, 20, ,22, 24, 26
Manyara	35.80	-3.62	960	12,000	23,207	1.93	0.13	1,000	2,000	0.50	23	0.0019	0.0010	8, 21
Turkana	36.05	3.66	375	7,300	130,860	17.92	0.13	1,400	2,560	0.55	80	0.0110	0.0006	12, 17, 18, 19
Victoria	36.26	-2.33	1,134	68,800	184,000	2.67	0.18	2,400	1,690	1.40	18	0.0007	0.0027	19, 23

References **(1)** Alemayehu et al., (2006), **(2)** Ayenew (2003), **(3)** Ase et al., (1986), **(4)** Ayenew and Gebreegziabher (2006), **(5)** Barker (1990), **(6)** Bessems et al., (2008), **(7)** Burrough and Thomas (2009), **(8)** Casanova and Hillaire-Marcel (1992), **(9)** Castanier et al., (1993), **(10)** Darling et al., (1996), **(11)** Dühnforth et al., (2006), **(12)** Ferguson and Harbott (1982), **(13)** Garcin et al., (2009), (**14)** Knight Piesold (1992), **(15)** Legesse et al., (2002), **(16)** Makin et al., (1975), (**17)** Nicholson (1996), **(18)** Nyenzi et al., (1981), **(19)** Odada et al., (2003), **(20)** Owen et al., (2004), **(21)** Ring et al., (2005), **(22)** Rowntree (1990), **(23)** Spigel and Coulter (1996), **(24)** Tarits et al., (2006), **(25)** Telford (1999), **(26)** Tiercelin (1990), **(27)** Verschuren (1999), **(28)** Washbourn-Kamau (1970), **(29**) Washbourn-Kamau (1975)

3.3 Lake basins

The location and key characteristics of the ten study basins are summarized in Table 1. Each basin contains at least two modern lakes owing to fragmentation caused by faulting and volcanic eruptions within the basins that diverted or dammed surface drainage, hence multiplying the number of basins within a tectonic depression. The catchment areas of most of these basins are within the rift, most areas being supplied by streams descending from high marginal escarpments. Basin sizes range from a few hundred to thousands of square kilometres. Major rivers such as the Ewaso Ngiro which feeds Lake Natron, and the Kerio River which feeds Lake Turkana, are channeled N or S along fault-angle depressions. These basins are all closed and their chemistry ranges from fresh, alkaline to saline, depending on the input-output balance of each system. The fresh lakes are Naivasha, Awassa, Baringo, Ziway, Langano and Victoria, while the alkaline to saline lakes are Turkana, Suguta, Bogoria, Nakuru-Elmenteita, Magadi- Natron and Manyara.

Two of the basins, Ziway-Shala and Awassa, are located within the MER. The Ziway-Shala is a system of four interconnected, internally drained basins (Ziway, Langano, Abiyata, and Shala) in a NNE-SSW down-faulted structure, with the Somalian Plateau on the east and the Ethiopian Plateau on the west. Three of these sub-basins formed in tectonically controlled basins, whereas Shala occupies a deep caldera (Le Turdu et al., 1999; Legesse et al., 2002). Mean annual precipitation varies from 600 mm/yr close to the lakes to 1,200 mm/yr on the humid plateaus and escarpments. Ziway and Shalla receive water principally from the west escarpment. Langano is fed from the east escarpment, while Abiyata is mainted by overflow from Ziway and Langano (Alemayehu et al., 2006; Ayenew 2003). Basin evapotranspiration has been estimated at 900 mm/yr (Ayenew 2003). Evaporation ranges from 2,500 mm/yr in the rift floor to <1,000 mm/yr in the highlands (Le Turdu et al., 1999). South of the Ziway-Shala basin, at the southern edge of the MER, is the Awassa basin, located within a pair of collapsed Pliocene calderas, Awassa and Corbetti (Ayenew and Gebreegziabher 2006). The catchment area is smaller (1,455 km^2) and the lake area is 129 km^2. Maximum and mean depths are 21 and 10 m. Awassa receives surface input intermittently from the Shallo swamp, fed from the eastern wall of the rift valley. The lake has no surface outlet and is a freshwater system maintained by significant outflow of groundwater northwards (Darling et al., 1996). Rainfall is about 960 mm/yr (Ayenew and Gebreegziabher 2006) and pan evaporation estimates over the lake range from 1,600 to 2,140 mm/yr (Makin et al., 1976; Telford 1999).

The Turkana and Suguta basins (375 m asl) lie in the Turkana-Omo lows region, located between the Ethiopian and the Kenyan domes (Chorowicz 2005). Turkana is the largest lake in the eastern rift, with a catchment covering 130,860 km^2. The mean and maximum depths are 35 and 120 m, respectively. In this bottom rift setting, the lake receives about 300 mm/yr of rainfall (Nicholson 1996; Odada et al., 2003). The annual evaporation rate is about 2,300 mm/yr and evapotranspiration is about 2,500 mm/yr (Nyenzi et al., 1981; Ferguson and Harbott 1982). Lake Turkana is saline-alkaline and receives 90% of its water via the Omo River from Ethiopia, with minor inputs from the Turkwell and Kerio river systems to the south (Odada et al., 2003). Directly south of the Turkana basin lies the Suguta basin, separated by a transverse volcanic barrier currently occupied by Lakes Logipi and Alablab (Dunkley et al., 1993). In the

dry season, the water body is reduced to salt pans that are restricted to the deepest parts of both lakes. At its maximum extension, the lake depth varies between 3 and 5 m. Together the lakes cover 80 km^2 and the catchment covers 12,800 km^2. Rainfall varies from <300 mm/yr over the lake to 1000 mm/yr in the headwaters of the Suguta River, located in the south. There is considerable subsurface water inflow from the north as well (Castanier et al., 1993). Evapotranspiration is 2309 mm/yr (Nyenzi et al., 1981).

Baringo-Bogoria basin lies in the northernmost part of the Kenyan dome and developed in the main region with half-grabens. It has two closed lakes, Baringo and Bogoria. Baringo is fresh, whereas Bogoria is saline and alkaline. The entire basin covers 6,200 km^2 and is drained by five rivers. Lake Baringo is currently very shallow, with a mean depth of ca. 1.6 m and a maximum depth of 2.1 m. It is fed perennially by the Perkarra and Molo rivers from the south. The ephemeral rivers, Ol Arabel and Mukatan, enter it from the east and from the west, and several ephemeral rivers drain the Kamasia highlands (Tarits et al., 2006; Bessems et al., 2008). Lake Bogoria is deeper (10 m) and is fed by nearly 200 hydrothermal springs along the lakeshore, as well as four seasonal rivers (Waseges-Sandai, Loboi, Emsos and Mogun). The entire basin receives between 600 and 900 mm/yr of rainfall on the rift floor and >1000 mm/yr in the adjacent uplands. Potential evaporation exceeds 2,500 mm/yr (Nyenzi et al., 1981; Rowntree 1989; Owen et al., 2004).

The Nakuru-Elmenteita basin contains two shallow alkaline lakes, Nakuru and Elmenteita. The basin is set between east-dipping normal faults of the Mau escarpment and west-dipping faults to the east in the intra-rift Bahati-Kinangop plateau. The northern boundary comprises the Menengai Caldera, and to the south, the Eburru volcano separates it from the Naivasha basin. The catchment is about 2,390 km^2 in area. Mean annual rainfall is up to 1,200 mm/yr in the catchment and potential evapotranspiration is 1,400 mm/yr, whereas evaporation over the lake is about 1,736 mm/yr. Both lakes are shallow, with an average water depth of <3 m (Dühnforth et al., 2006). The basin is fed mainly by streams from the Mau escarpment. Naivasha basin (1,885 m asl) is the highest point of the Kenyan Rift. Naivasha is fed by three rivers that drain the Bahati-Kinangop ramp highlands, which receive up to 1500 mm/yr of rainfall and have evapotranspiration of about 1,250 mm/yr. Rainfall over the lake is about 600 mm/yr while evaporation is ca. 1800 mm/yr. The basin is confined by volcanoes that create three connected satellite basins, the main lake, Crescent crater and Oloidien. Crescent Crater Lake in the southeastern sector represents the deepest part of the lake (18 m) and a permeable sill separates the main lake from more alkaline Lake Oloidien in the southwestern sector (Ase et al., 1986; Verschuren 1999). The volcanic-tectonic origin of the lake accounts for its relatively circular shape.

The Victoria basin straddles the equator and is the second largest lake in the world, covering 68,800 km^2. The catchment area is 184,000 km^2. Lake Victoria formed as a result of river reversal and ponding as a consequence of rift margin uplift along the western branch in the late Pleistocene (~14.6 ka BP) (Scholz et al., 1998) and can thus be described as a tectonically induced lacustrine system. It is an open lake, receiving water from several rivers, the largest being the Kagera and the Katonga in the west and draining to the north through the Nile. Rainfall over the lake is about 1,200 mm/yr and up to 2,400 mm/yr in the catchment.

Evapotranspiration is about 1,690 mm/yr and river inflow makes a minor contribution (Spigel and Coulter 1996).

At the southern tip of the Kenya Rift is the Magadi-Natron basin that contains two lakes, Magadi and Natron, whose catchment covers 23,207 $km^{2.}$ Annual rainfall in the catchment is about 1,000 mm/yr and evaporation is about 1,750 mm/yr (Burrough and Thomas 2009). Lake Magadi is formed by an assemblage of several small basins defined by a complex system of N-S-, NNW-SSE- and NNE-SSW-trending faults. Magadi has no perennial inflowing streams at present and is fed by numerous (partly hot) springs as well as rainfall (Barker 1990). Lake Natron is a shallow water body covered by eight saline lagoons, with a maximum depth of about 2 m. It is fed mainly by two rivers, Peninj and Ewaso Ngiro, and some perennial streams (Knight Piesold 1992). Both lakes have extensive trona crusts that dissolve during the rainy season. Manyara basin lies in the Manyara Rift at the southern termination of the eastern branch of the East African Rift in Tanzanian Divergence Zone. This basin contains Lakes Manyara and Burungi (Ebinger et al., 1997; Chorowicz 2005; Ring et al., 2005). The lakes cover a surface area of about 440 km^2 with a maximum depth of 4 m. Mean rainfall ranges between 500 and 600 mm/yr. The catchment area is 10,930 km^2 and receives annual precipitation between 800 and 1,000 mm/yr and potential evapotranspiration is 2,000 mm/yr (Casanova and Hillaire-Marcel 1992; Nyenzi 1981). The main perennial rivers are located west of the lake.

3.4 Methods

We assessed the basin factors that can cause significant heterogeneity in paleoclimate records within the EARS:(1) geomorphic characteristics that best describe basin form and the accommodation space available for storage and preservation of sediment records, and (2) the aridity index (AI), which is an indicator of the effective moisture available to a basin relative to the demand under prevailing climatic conditions.

3.4.1 Geomorphic analyses

Hypsometric analysis describes the elevation distribution across an area of land surface, therefore it is an important tool for assessing and comparing geomorphic evolution of various landforms, irrespective of factors such as tectonics, climate, and lithology, which may be responsible for their creation (Hurtrez at al. 1999; Montgomery et al., 2001). Two products of these analyses are the hypsometric curve and the hypsometric integral (HI). The latter is a dimensionless parameter that allows different catchments to be compared. The absolute and relative vertical resolutions of the Shuttle Radar Topography Mission (SRTM) DEM in Africa are estimated as ±5.6 m and ±9.8 m, respectively (Rodriguez et al., 2006). This low error has little effect on hypsometric analyses of large catchments. Moreover, studies show that hypsometry is largely insensitive to grid scale, through comparison of results from a 10 m, 20 m and 90 m DEM (Hancock et al., 2006).

We used the 3 arc second or 90-m DEMs from the SRTM and processed 52 SRTM tiles covering the EARS. Where necessary, various tiles were “mosaiced” into larger grids and the

larger DEMs were re-sampled into a coarser grid before processing to save on computing time. Existing data gaps were filled by interpolation and data were smoothed using a 9x9-pixel moving average filter. We conducted watershed analyses for each basin. Then carried out morphometric analyses, developing hypsometric curves and integrals and swath profiles of East-West sections from the data.

The hypsometric curve for each basin was created by dividing into equal elevations the range of elevations and calculating the proportion of basin area within each interval. Elevations were normalized to the relief of the catchment so that they ranged from 0 to 1 The two ratios are plotted against each other. The hypsometric integral (HI) is the area under the curve obtained by numerically integrating this area. An alternative method uses the simple equation introduced by Pike and Wilson (1971):

$$HI = \frac{MeanElevation - MinimumElevation}{MaximumElevation - MinimumElevation} \quad (1)$$

This equation is widely used because it does not require rigorous computation of the hypsometry of the basin, but rather on three easily obtainable values, mean, maximum and minimum DEM values. This approach, however, is very sensitive to noise and outliers in the DEM. We compared both approaches by using the equation and integrating the area under the curve using the trapezoidal method “trapz,“ developed in MATLAB®.

3.4.2 Swath analysis and basin characteristics

To assess the topographic variations for each basin, we took swath profiles oriented approximately perpendicular to the main axis of the lake basins, from the resampled SRTM data. The area of the swath is defined by the rectangular grid sections that envelope each lake basin. For uniformity, we defined the extent of the swath as 300 m above the altitude of the current lake level because this is the highest inferred Early Holocene lake level, which is observed in the Suguta Valley (Garcin et al., 2009). For each swath area, we calculated the maximum, mean and minimum elevations. Swath profiles provide valuable insights into the geomorphologic means and variances of a basin and show depths and lake basin extent. These help define the graben- and pan-shaped basins in this study.

Table 3.1 shows the key characteristics of the lakes in the study. Because we are comparing several basins of various sizes, surface areas and volumes, we scaled them for comparison by their Early Holocene lake level to basin size and lake size. Early Holocene lake levels used were based on published paleoshoreline levels that had been identified by wave-cut notches, as shoreline cliffs, beaches, or shallow-water sediments with dated organic matter and stromatolites (References in Table 3.1).

3.4.3 Aridity index

The aridity index is used to define the moisture availability in a basin based on meteorological variables such as precipitation and air temperature. There are several indices currently in use. The De Martonne's aridity index is defined by the ratio between the mean annual precipitation (P) and temperature plus 10°C [P/(T+10)] (Paltineanu et al., 2007). The Thornthwaite index is defined by the ratio of the difference between precipitation and evapotranspiration to the potential evapotranspiration and given by 100((P/PE)-1). The water deficit (WD) is simply the difference between precipitation and evapotranspiration (P–ET), and the UNESCO aridity index is the ratio between precipitation and evapotranspiration. All these terms have some value in studying the potential impact of climatic change on water resources. The potential evapotranspiration according to the definition used by the UNESCO is calculated using the Penman formula, which requires meteorological data that are difficult to acquire for most basins in the world. This led to the introduction of a more simplified approach for calculating the potential evapotranspiration using the Thornthwaite formula. This index is widely known as the UNEP aridity index (Tsakiris and Vangelis 2005) and is defined as:

$$AI = \frac{P}{PE} \qquad (2)$$

Where P is the total annual precipitation (mm/yr) and PE is the potential evapotranspiration (mm/yr). According to this concept, regions where the aridity index is lower than unity are broadly classified as dry since the evaporative demand cannot be met by precipitation. Regions with an aridity index higher than unity are broadly classified as wet. We used published and known meteorological data of annual rainfall and potential evapotranspiration values for the lake basins in our study. Their areas are between 1,455 to 184,000 km^2, and annual rainfall over the catchments varies from 500 to 2,400 mm/yr. Potential evaporation ranges from 1,690 to 2,600 mm/yr, and the values were used as inputs to compute the UNEP aridity index (Table 3.1).

3.5 Results

3.5.1 Morphometric analyses and lake features

Averaged statistics for each E-W-oriented swath section, plotted against longitude (Figure 3.2A), illustrate the relationship between specific basin geometry and location along the EARS. The basins range from symmetric to asymmetric. The lowest mean and minimum elevation values are for the Turkana basin, and values increase significantly from the Turkana-Omo lows in both directions, southward to the Kenyan dome and northward to the Ethiopian dome. The swath profile reliefs gradually increase southward to the Suguta basin, through Baringo-Bogoria, Nakuru-Elmenteita basins and peak at the Naivasha basin. From there, southward along the rift, the mean and minimum values decrease through the Magadi-Natron basin to the Manyara basin. A similar pattern is observed north of the Turkana-Omo lows, the average minimum and mean elevations increase through the Awassa basin and terminate at

the Ziway-Shalla basin. There is, however, a great variability in averaged maximum elevations for each swath profile caused by the existence of volcanoes and features related to the en-echelon faults that influence the local topography, but have no distinguishing characteristics.

The swath profiles also show strong topographic differences, creating two main morphological shapes, distinct grabens and pan-shaped depressions. Examples of pan-shaped morphologies with gentle slopes are the Victoria, Turkana, Manyara, Magadi-Natron and Baringo-Bogoria basins. The Ziway-Shalla, Awassa, Suguta, Nakuru-Elmenteita, Naivasha basins show graben or half-graben morphologies with steeper slopes (Figure 3.2A).

Figure 3.2B shows results of hypsometric analyses. The hypsometric curves are typically sigmoidal or concave up, which can be grouped broadly into three categories of landmass distribution. The first category includes Lakes Manyara, Turkana and Victoria, which have relatively flat basins, and hence low hypsometric integral values. These lakes have low gradients and most of their relief occupies less than 50% of the highest altitude, giving them a lower local elevation range. The second category includes basins with pronounced step-like features in the higher altitudes and relatively higher hypsometric integrals. Examples in this category are Lakes Naivasha, Awassa, Ziway-Shalla and Suguta. The Ziway-Shalla, Suguta and Awassa catchments have shoulders in the hypsometric curve. The shoulders characterize abrupt rises in land surface as a series of fault steps that point to the tectonic activity of the EARS. Lakes in the third category have the highest topographic gradients and include Lakes Nakuru–Elmenteita, Magadi-Natron and Baringo-Bogoria. Lakes Nakuru-Elmenteita and Baringo-Bogoria have a high gradient in the hypsometric curve, i.e. they are characterized by a higher local elevation range. At 30% altitude, the hypsometric curves of lakes in the second category (Figure 3.2B) are comparable to the full profile of lakes Baringo-Bogoria, Magadi-Natron and Nakuru Elmenteita.

Hypsometric integrals for these basins range from 0.13 to 0.37 (Table 3.1). These values are relatively low, indicating that a greater proportion of the landmass within the catchment is at low or intermediate elevations. The results fall into three categories, similar to the hypsometric curve classification (Figure 3.2B):0.1-0.2, 0.21-0.3, and 0.31-0.4. The 0.1-0.2 category basins occupy the terminal end of the rift valleys. Both lakes Manyara and Turkana have hypsometric integrals of 0.13. Lake Victoria as a non-rift lake, but also falls in this category with a value of 0.17. Category II with HI values of 0.21-0.3, occupy the highest elevation in the EARS dome. Naivasha, Awassa, and Ziway-Shalla have integrals of 0.23, Suguta has an HI of 0.29 and the Nakuru-Elmenteita basin has a value of 0.3. Category III comprises the lakes in the intermediate area between the termination of the Kenyan rift and the dome. Examples are Lakes Magadi-Natron and Baringo-Bogoria, which have higher HI values of 0.36 and 0.37, respectively, and their hypsometric curves are almost linear. An exception to this rule, but also a member of this group, is the Suguta basin, which is located in an intermediate region, but has a lower integral (0.29). A plausible explanation for this lower value is its location. It is surrounded by volcanic formations to the north (the Barrier) and east (Tirr Tirr Plateau, Emuruangogolak), giving it high gradients similar to those of the Category II basins.

A strong correlation exists between relief and hypsometric integrals for the study area. The intermediate HIs of ca. 0.23-0.29 are typical for basins characterized by distinct graben

morphology and a tectonically active rift setting, whereas the lower and higher values describe pan-shaped basins in highly eroded, or tectonically less active settings.

Scaling by Holocene lake level rise to basin area enabled comparisons. Nakuru-Elmenteita emerges as having the largest change (0.0753) and the Turkana Basin had the least change (0.0006). Table 3.1 is arranged in descending order of normalized values. Victoria is last because it is a non-rift lake. By this classification, five lakes, Nakuru-Elmenteita, Naivasha, Awassa, Suguta and Ziway-Shalla, emerge as "sensitive," This finding is in agreement with the hypsometry and aridity index classification. Lakes Victoria, Baringo-Bogoria, Manyara, Turkana and Magadi-Natron experienced relatively minor increases in water levels during the Early Holocene wet episode in East Africa (Table 3.1).

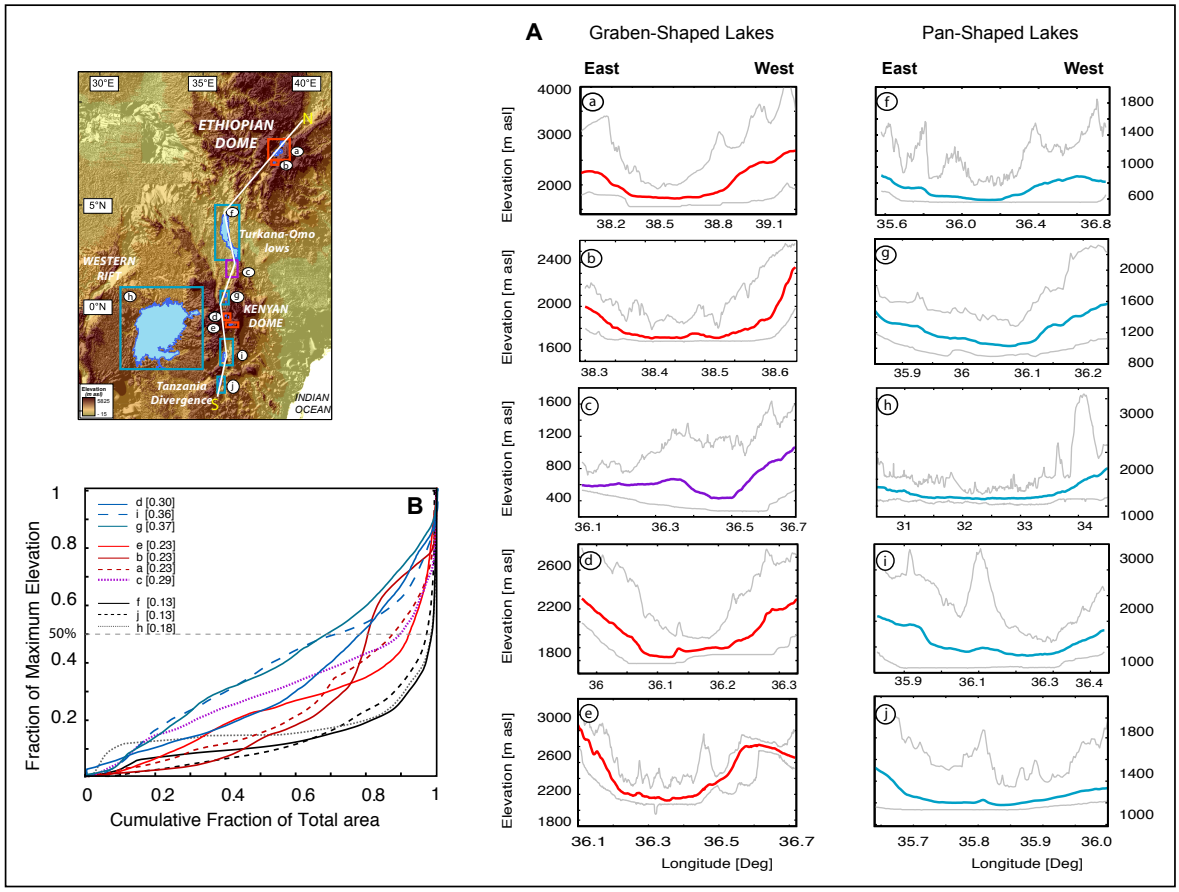

Figure 3.2 Morphometric characteristics from the SRTM (A) EW-oriented sections of swath profiles across the lake basins along the EARS derived from Shuttle Radar Topography Mission (SRTM) data. Each swath profile includes the lowermost 300 m of the lake basin. Bold lines indicate mean values of topography, thin grey lines are maximum (top) and minimum (bottom) elevations. Blue lines correspond to typical pan-shaped morphologies, whereas red profiles represent graben morphologies and the purple profile represents distinct half-graben morphology in lake basins (B) Hypsometric curves and hypsometric integrals of basins. The lowest values are for the lakes that lie at the northern and southern termination of the Kenya rift, while the intermediate values represent lakes in the Ethiopian and Kenyan domes. High values belong to the lakes in the intermediate elevations

3.5.2 Aridity index

Results for the study area range from 0.50 to 1.42. Lower values denote arid basins and higher values denote humid basins. There is a striking spatial pattern of the aridity index along

the N-S axis of the eastern branch of the EARS (Figure 3.3). The lowest AI values occur in the low-elevation basins in the Omo-Turkana lows and at the southern termination of the Kenya Rift, i.e. in the catchments of Lakes Turkana, Suguta, Baringo-Bogoria, Magadi-Natron and Manyara, with values of 0.55, 0.43, 0.43, 0.57 and 0.50, respectively (Figure 3.3). The AI values for lake basins at the domes of the Kenyan and Ethiopian rifts are higher (wet), e.g. the Ziway-Shalla, Awassa and Naivasha basins, which have indices of more than unity, 1.33, 1.03 and 1.20, respectively. The catchment of Nakuru-Elmenteita basin, however, which also lies in the Kenyan dome, has an aridity index of 0.85. We explain the exceptionally low value of this basin by the relatively small catchment area of the basin and its location north of Naivasha, lacking the high-elevation topography that captures high precipitation winds.

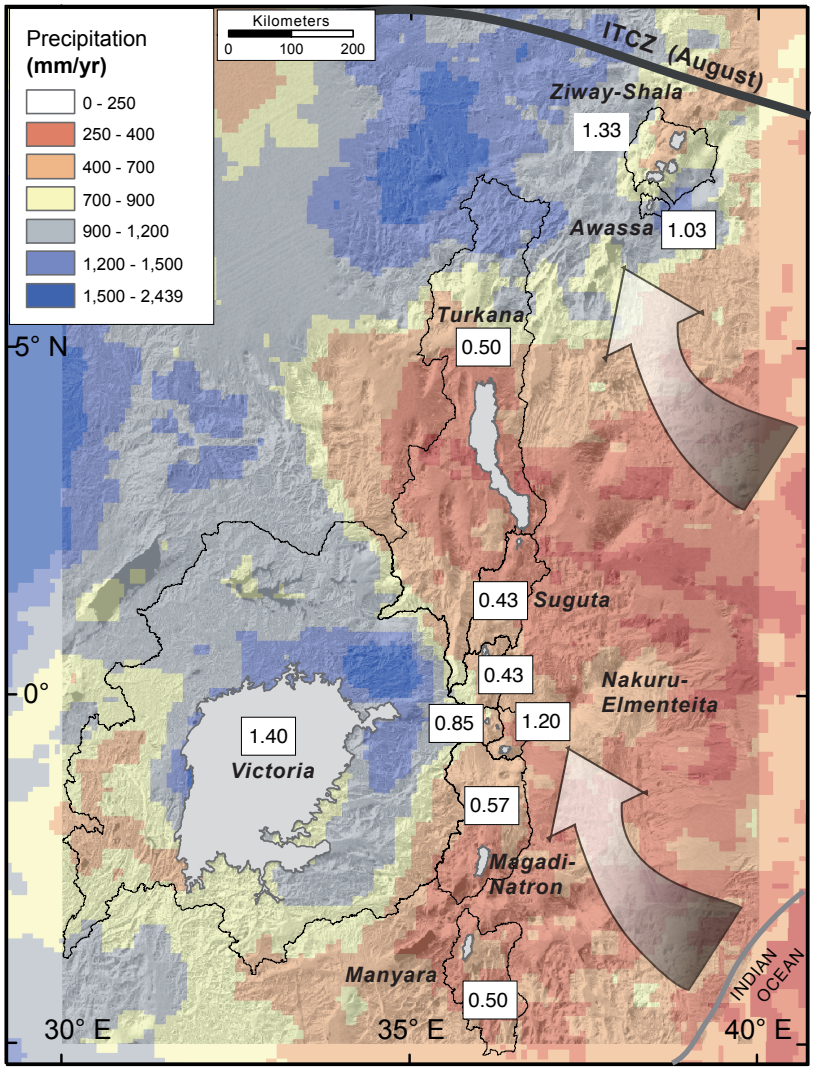

Figure 3.3 Spatial distribution of aridity index values in the EARS. The arrow shows wind direction from the Indian Ocean. High aridity index values are seen in the domes of Ethiopia and Kenya, which capture moisture-laden air from the Indian Ocean. Victoria is a large water body that is dominated by convective rainfall

The spatial distribution of AI is a result of orographic effects. The rift flanks deflect moist air upward causing rain in the highlands. The air descends into the valleys devoid of moisture.

Thus higher AI corresponds to high elevation and vice versa. Lake Victoria has an AI of 1.42, which is the highest value of all lakes in the study. This lake receives an enormous amount of rainfall in the 184,000-km^2 catchment that is not compensated for by high evapotranspiration in the lake area.

3.6 Discussion

In this study we used empirical measures to scale the sensitivity of EARS lakes with respect to their ability to record climate shifts. Using the geomorphologic and hydrologic settings of ten lake basins, we determined the key factors that amplify their sensitivity. The geomorphologic setting is described here by the hypsometry, whereas the climate setting is characterized by the aridity index. Traditionally, morphometric studies have been applied to sections of topography and individual drainage basins. To our knowledge, this is the first attempt to apply the approach in lakes of the East African rift system to classify them with respect to climate sensitivity.

Swath profiles of mean elevation show the topographic differences that exist east and west of the basins (Figure 3.2). In general, the mean elevations from the swath profiles of the lakes display either graben or half-graben shapes or pan-shaped basins. The shape affects the response and the preservation of the lake sediment record, and we used it to identify the potential for lake level amplification. No direct correlation exists between the swath profile shapes and the hypsometric analyses. The swath profiles, however, provide information about the slope and shape of lake basins and their catchments, both of which influence orographic rainfall distribution. From the swath profiles, we classified lakes as pan-shaped or graben-shaped. The former have greater oscillations in surface area relative to depth, while the latter have greater oscillations in lake level relative to surface area due to the constraining steep walls that bound them. The latter have high potential to yield good sediment records for paleoclimate studies, however the presence and preservation of biological and geochemical indicators of such climate changes depends on the chemistry of the lake.

The spatial distribution of HI values within the rift follows the general trend of the absolute elevation of basins above sea level (Figure 3.4), with the exception of the Victoria basin. High values are found within the Kenyan and Ethiopian domes, whereas low values are observed in the intermediate zones of the Turkana-Omo lows and Tanzania divergence. This finding points to tectonic control because both the domes and the basin-and-range-type tectonic setting of the Turkana-Omo area relate to the thermomechanical state of the lithosphere at the time of rifting and basin formation (Buck 1991; Ebinger 2000). Hot, weak lithosphere over the Turkana-Omo basin area developed broad rift zones bounded by low-angle border faults, creating pan-shaped basins with large basin areas (Figure 3.1), while cold, strong lithosphere developed narrow rift zones bounded by high-angle border faults at the crest of the domes, creating graben-shaped basins in, for example, the Nakuru-Elmenteita, Naivasha, Ziway and Awassa basins (Figure 3.4), with smaller basin areas (Table 3.1). A similar study by Hurtrez et al., (1999) found tectonic control to be dominant on drainage basin hypsometry in regions subjected to rapid tectonic uplift rates, in the Siwalik Hills of the Himalayas.

Using size and basin morphology to define sensitivity of lakes, various studies have shown that basins with large catchment-to-lake-surface area ratios have large amplification factors. Thus, they do not require a high input of water to maintain a positive hydrological balance (Burrough and Thomas 2009). In our study, it could explain the magnitude of paleolakes in the Suguta, Ziway-Shala, Naivasha, Awassa and Turkana basins (Table 3.1). However, we see a deviation to this rule in the Magadi-Natron and Baringo-Bogoria basins. For instance, Lake Manyara has a catchment-to-lake-surface area ratio of 24, but the highest lake level recorded was only 23 m above the current lake level. In some of these examples, overflow toward adjacent basins explains relatively low lake levels during periods of wetter climate. While important for some regions, size ratio is not the sole determinant of response to climate change for the lakes of the EARS (Table 3.1). Lakes with larger groundwater catchments than surface-water catchments cannot be classified with this method. These include such EARS lakes as Nakuru-Elmenteita, Magadi-Natron, Baringo-Bogoria. Thus both surface and subsurface input must be considered, along with information on size and morphology of the lake basins.

We used the aridity index to describe the effective moisture within basins. Using the UNEP classification scheme, regions with an aridity index >0.65 are classified as humid, while those <0.65 are divided into four arid subclasses, from dry sub-humid to hyper-arid. Sub-humid to sub-arid basins in the EARS are Suguta (0.43), Baringo-Bogoria (0.43), Manyara (0.50), Turkana (0.54) and Magadi-Natron (0.57). Humid basins are Nakuru-Elmenteita (0.85), Ziway-Shalla (1.33), Awassa (1.03), Naivasha (1.20) and Victoria (1.40). Because aridity indices correlate directly with precipitation and inversely with potential evapotranspiration, a low aridity index for a region means low rainfall because rainfall is hindered by greatly heated land surfaces and presence of dry descending air. Lower elevations (<1500 m asl), such as the intermediate zones between the domes and the flanks of the domes, correspond to lower aridity indices (drier conditions) due to rain shadowing from the Indian Ocean moisture and relatively high air temperatures. The Victoria basin, though only 1100 m asl, is relatively humid as it is not influenced by orographic rain shadowing and receives rainfall from the plateaus in both the western and eastern arms of the EARS, both at high elevations (~3,200 m). High-elevation lakes include the Nakuru-Elmenteita, Naivasha, Awassa and Ziway-Shalla basins, which have high aridity indices (Figure 3.5). Their landmass is distributed across the high-elevation plateaus (>2,500 m), which capture most of the moisture coming from the Indian Ocean.

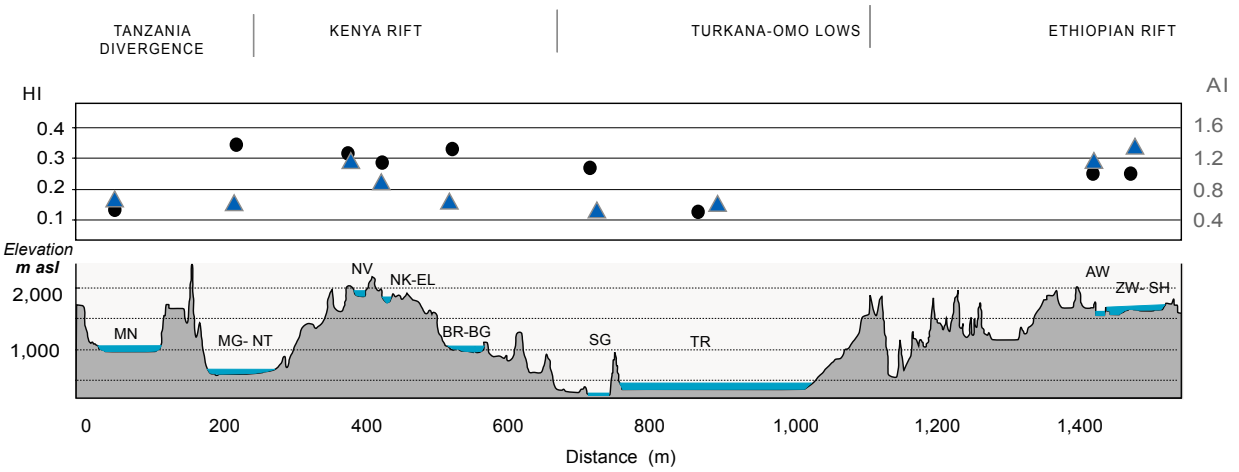

Figure 3.4 Topographic cross-section through the lake basins from south to north and the corresponding Hypsometric integral (HI; circles) and aridity index (AI; triangles) values of lake basins. The high values of HI and AI correlate with Ethiopian and Kenyan domes, whereas low values appear at the terminal end of the Kenya rift (ca. 4°S latitude) and between the Kenyan and Ethiopian rift at the Turkana-Omo lows (ca. 4°N latitude). The basins are labeled as follows:MN -Manyara, Mg-NT -Magadi-Natron, NV- Naivasha, NK-EL- Nakuru-Elmenteita, BR-BG -Baringo-Bogoria, SG -Suguta, TR -Turkana, AW -Awassa, ZW-SH -Ziway-Shalla

Climate in the EARS is influenced greatly by topography. Plotting the hypsometric integral (HI) and aridity index (AI) values against altitude illustrates this relation. The aridity index of the lakes increases with altitude (Figure 3.4). The Ethiopian and Kenyan domes create an orographic barrier that captures the moisture-laden air from the Indian Ocean and the highlands receive high rainfall, as observed in high-elevation (>1,500 m asl) lakes such as Naivasha (1,885 m asl), Awassa (1,680 m asl) and Ziway-Shala (1,636-1,557 m asl). The intermediate zones are in the rain shadow, thus their aridity index values decrease away from the crest of the domes in the Suguta, Turkana, Baringo-Bogoria, Magadi-Natron and Manyara basins. The AI of Lake Victoria (1.4) reflects high rainfall and relatively low evapotranspiration in a catchment that includes the plateau areas of both arms of the rift and the large lake area of 68,800 km^2, which is more humid as a result of local convectional rainfall.

We used early Holocene lake levels from published paleoshoreline studies (Table 3.1) to explore the sensitivity of lakes to climate change. In some basins, preservation of the sediment record is not perfect, especially in the pan-shaped basins, because of reworking and erosion of sediments during arid-to-humid transitions. The most dramatic change was observed in the Nakuru-Elmenteita and Suguta basins, where early Holocene lake levels were 45x and 75x higher than today, respectively. Both have graben shapes and HI of 0.23 and 0.29, respectively. Their basins receive lower rainfall (AIs of 0.85 and 0.45), and we suspect a significant contribution of groundwater from neighbouring basins kept water levels high. In the Kenyan rift, studies have shown that groundwater flows from the Naivasha basin to the north and south, following the hydraulic gradient created by the up-doming of the central section. Therefore, the amplifier effect of Lake Naivasha also contributes to the Lake Nakuru-Elmenteita system. Analogously, high-elevation Suguta lake received significant groundwater inflow or even surface overflow from the high Baringo-Bogoria system during the early Holocene (Garcin et al., 2009) that compensated for the extremely low aridity index of these basins.

The EARS's diverse lakes were valuable for sensitivity studies using empirical measures. According to this approach for evaluating sensitivity of lakes to climate fluctiations, lakes with a combination of an aridity index >1 and a hypsometric integral ~0.23 plot as the most sensitive (Figure 3.5) to local and regional climatic changes. These are rift lakes with graben morphologies and humid conditions, such as Naivasha, Awassa and Ziway-Shala. Their water balance is dominated by rainfall and surface inflow. Other lakes, such as Nakuru-Elmenteita and Suguta have graben morphologies and ideal hypsometry values, however they receive low rainfall, and thus do not make good archives of local arid-humid transitions, because they receive significant groundwater from neighbouring basins. They do however, archive regional climate changes. This helps explain why lake level changes during the early Holocene varied in magnitude among the lakes of the EARS. Because both basin morphology and climate are the consequence of up-doming and rifting in East Africa, this study highlights the importance of site-specific morphometry in tectonically controlled basins for unravelling climate histories from sediment records.

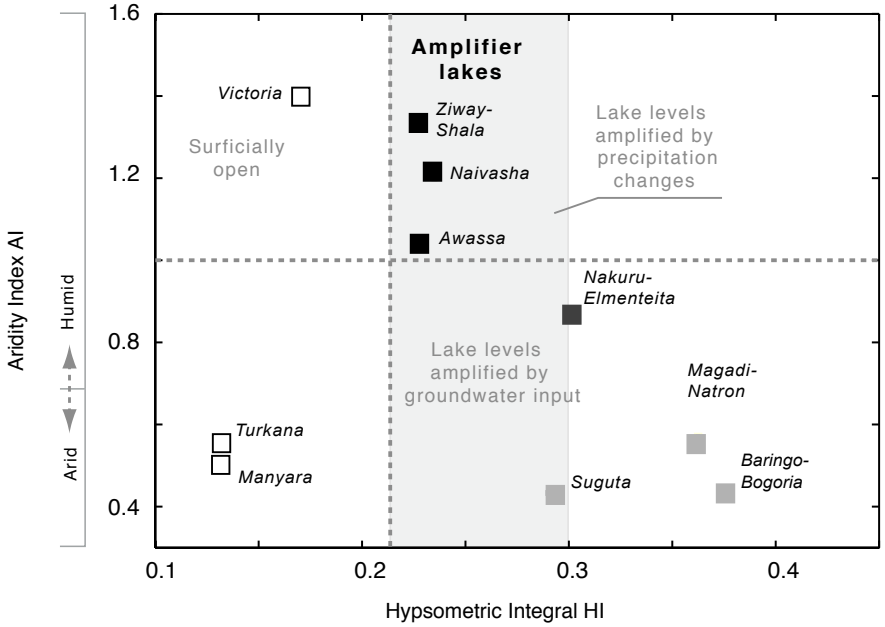

Figure 3.5 Hypsometric integral (HI) plotted against the aridity index (AI) of the basins of the EARS. Sensitive lakes plot in the top center, an ideal combination of a hypsometric integral of 0.23-0.30 and an aridity index >1. The most sensitive lakes lie at the highest point of both the Kenyan and Ethiopian domes

3.7 Conclusions

Previous shoreline studies of lakes in the EARS showed high water levels during the Holocene, though modeling results show only 25% more rainfall, which cannot account for the high lake levels. The “amplifier lake” concept was introduced by Street (1980) and Street-Perrott and Harrison (1985) to explain this phenomenon. We expanded upon this concept in our study by including a detailed morphometric analysis of basins using SRTM Digital Elevation Model and climate data. Considering the early Holocene high lake levels, we found that a lake basin with a hypsometric integral (HI) value between 0.23 and 0.30 and an aridity index (AI) >1 responds sensitively to climate changes. Both of these variables are directly linked to tectonics in the EARS. The rift lakes have distinct graben morphologies related to up-doming, rifting and volcanism within the EARS. The steep walls of such grabens inhibit wind-driven mixing, as opposed to the situation in pan-shaped basins. Of the ten lakes we examined, three are “amplifiers” and have provided adequate sediment records for paleoclimate studies. The non-uniform responses of lakes to climate change because of morphometric differences, dictates that caution be used in generalizing about climate inferences derived from a single lake in the EARS. Careful calibration of basins and modeling of lake responses can be used to better constrain the nature of lake responses to climate. Studies of modern lake responses to climate shifts is of interest to planning and management authorities who must deal with future climate-change scenarios. Our findings come from study of the lakes in the eastern arm of the EARS, but may also apply to similar geomorphologic and climatic settings elsewhere.

CHAPTER 4

SIGNIFICANCE OF GROUNDWATER FLOW FOR THE HYDROLOGIC BUDGETS OF PALEO-LAKES IN EAST AFRICA: **How closed are closed-basins lakes in rifts?**

Abstract

The hydrogeology of rift lakes is complex due to the potential influence of faults and porous volcanic and volcanoclastic media on groundwater flow. We conducted a comprehensive study that integrated geological and hydrogeological data as well as the application of a linear decay model to estimate the groundwater flow between the two of the best-studied lake systems in East Africa, the adjacent Lakes Naivasha and Nakuru-Elmenteita in the Central Kenya Rift. Whereas both lake basins host relatively shallow lakes today, paleo-shorelines and sediments suggest >100 m deep lakes during a wetter climate during the Early Holocene during the so-called African Humid Period. The linear-reservoir depletion model simulates the decline of the Early Holocene lakes in both basins to the modern levels. The altitude difference of ca. 100 m of both paleo-lake levels enables us to estimate the duration of the groundwater decline and the connectivity of the two basins via the Eburru/Gilgil barrier. The results suggest a decline of the groundwater levels during ca. 5 kyrs if there is no recharge, and between 2-2.7 kyrs based on the modern recharge of 0.52 m/yr as the end members of the delay time introduced by subsurface water flow to the hydrology of the lake system. The latter value suggests that ca. 40.95 cubic kilometres of water flowed from Lake Naivasha to Nakuru-Elmenteita at maximum lake level in the Early Holocene following the hydraulic gradient concurrent to the topographic slope. The unexpectedly large volume, more than half of the volume of the paleo-Lake Naivasha during the Early Holocene, emphasizes the importance of groundwater in hydrological modelling of paleo-lakes in rifts. Moreover, the subsurface connectivity of rift lakes also causes a significant lag time to the system introducing a nonlinear component to the system that has to be considered while interpreting paleo-lake records.

4.1 Introduction

Interpreting past climates from lake sediments is dependent on the accurate reconstruction of lake-level records. Various proxies from lacustrine environments such as:diatoms (Baker et al., 2002; Charlie and Gasse, 2002; Gasse, 2000; Dühnforth et al., 2006), ostracodes (Richardson and Dussinger, 1986), geomorphological signatures (Butzer et al., 1972; Washbourn-Kamau, 1975; Hillaire-Marcel et al., 1986; Casanova and Hillaire-Marcel, 1992), and terrestrial pollen for catchment conditions (Maitima, 1991; Olago, 1995; Olago et al., 2000; Olago, 2001) have been used to establish the existence of deep and large lakes during the Early Holocene in equatorial Africa. During this period, also known as the African Humid Period (AHP), the general long-term dry-wet-dry cycle between ca. 15-5 kyr BP and superimposed millennium-scale aridity events during Heinrich Events and the Younger Dryas suggest a mixed low-latitude insolation forcing and high-latitude glacial overprints as the most likely forcing for East

African climate variations on timescales from 10^3-10^6 years (Kutzbach and Street-Perrott, 1985; Barker et al., 2003, Brown et al., 2007).

However, although the timing and magnitude of the changes in hydrology are well known (Gasse, 2000; Baker et al., 2002; Bergner et al., 2003; Garcin et al., 2009), the climate conditions (rainfall and temperature) during these times are still not yet well established. Along with this growth in data is the recognition of the challenges of inferring climate from these records with the existence of spatio-temporal heterogeneity (Verschuren, 2003; Fritz, 2008). For instance, results from lake-balance modelling for the Early Holocene wet period provide estimates for mean-annual values of precipitation and air temperature but are contradictory in the magnitude of climate changes for adjacent lake basins. In the central Kenya rift (CKR) for instance, paleo-precipitation estimates of the Nakuru-Elmenteita system are higher (+20-55% precipitation) than the adjacent Naivasha (+16-32%) system (Hastenrath and Kutzbach 1983; Vincent et al., 1989; Bergner et al., 2003; Dühnforth et al., 2006). Although various intrinsic basin parameters such as morphological differences, the influence of local climate and groundwater flow have been identified to be responsible for such differences (e.g. Olaka et al., 2010), most paleohydrological reconstructions ignore their importance and paleo-lake fluctuations have been explained entirely in terms of shifts in surficial hydrology and hence precipitation-evaporation/evapotranspiration balance (Kutzbach, 1980; Street-Perrot and Harrison, 1985).

Unfortunately, studies on groundwater-surface water interaction in rift lakes have not received much consideration in paleo-lake level reconstruction and modelling studies in East Africa. The scarcity of measurable proxies to quantify groundwater influences on paleo-lakes has posed a hurdle for progress in this area of research. One traditional approach to avoid the problem of subsurface water flow is the assumption that the input of groundwater is equal to the outflow in many lakes. According to this approach, groundwater flow can be considered to be balanced out and must not to be included in hydrological modelling and paleoclimate studies (e.g. Bergner et al., 2003). At the same time, it points out that significant groundwater flow exists in rift lakes that can cause significant perturbations in the lake-level record used to reconstruct past climate change. As an example, Telford et al., (1999) observed high diatom inferred salinity in Lake Tilo in Ethiopia at the same time all paleoshoreline proxies show high lake levels suggesting a significant contribution of groundwater fluctuations on the overall budget of the lake and hence, significant variations in the flux of ions in solution in and out of the lake (Telford et al., 1999). Likewise, Sturchio et al., (1993) found evidence of elevated hydrothermal activity during the Early Holocene suggesting elevated water table and increased availability of meteoric water in the areas between Lake Baringo and south of Lake Turkana. Such large closed lakes that existed in the Holocene are thought to have drained by high groundwater discharge and evaporation after the water level was lower than the overflow sill (Garcin et al., 2009).

A couple of recent studies using instrumental data from modern lakes within the Ethiopian rift highlight the significant influence of groundwater on lake levels during both dry and wet episodes (Goener et al., 2009; Ayenew et al., 2007; Kebede, 2008). In Kenya, the freshness of Lake Naivasha as a surficially closed lake is thought to be a result of groundwater discharge out of the lake (Darling et al., 1990, 1996). Owing to its location on the up-domed

floor of the Central Kenya Rift, the potential exists for the lake discharge to occur in both northerly and southerly directions, which has been demonstrated to some extent using tracer stable isotopes (Darling et al., 1990, 1996; Ojiambo, et al 2001). Deeper groundwater flow can be mapped using subsurface imaging methods and recent developments such as Transient Electromagnetic Method (TEM) which is sensitive to subsurface conductivity (McNeill, 1990; Barsukov et al., 2004) can be employed.

Here, we present a comprehensive study of the hydrology of two adjacent lake basins in the Central Kenya Rift (CKR); Naivasha and Nakuru-Elmenteita, separated by a volcanic barrier (Mt. Eburru) composed of volcanic and volcanoclastic rocks, intensely faulted through the rifting process in the region (Clarke et al., 1990). It is ideal for ground-surface water dynamics studies and associated sensitivity to climate variability because of a uniform regional climate and amplifier lake morphology (Olaka et al., 2010). Conversely, water-chemistry and hydrological budget of both lakes differ significantly – Lake Naivasha is fresh, whereas Lakes Nakuru and Elmenteita are highly alkaline – and have changed dramatically since the AHP. Though the timing of past climate change during the Holocene is relatively well-studied in both basins (e.g. Richardson and Dussinger, 1986; Bergner et al., 2003; Dühnforth et al., 2006) the magnitude of precipitation/evaporation changes during the last dry-wet-dry cycle is controversial. A refined knowledge of the hydrostratigraphic properties of the CKR resolves this controversy by combining geotechnical information of the surface and subsurface to better understand the contribution of groundwater flow to the overall hydrological budget of Lakes Naivasha, Nakuru and Elmenteita in the course of Holocene climate change.

4.2 Setting

4.2.1 Geomorphology and geology

There are two basins in the Central Kenya Rift (CKR); Nakuru-Elmenteita and Naivasha, accommodating three distinct modern lakes: Naivasha (1880 m asl), Elmenteita (1786 m asl) and Nakuru (1770 m asl) covering a total area of ca. 5,590 km^2 (Figure 4.1). Characterized by relatively flat relief in the basin floor and topographic highs that mark the catchment divides. Its evolution history is marked by the initial formation of the full graben morphology of the rift between 12 and 3.7 Ma (Baker et al., 1988; Roessner and Strecker, 1997) and modifications by subsequent tectonic and three major volcanic events that led to the separation and closing-up of the two basins:first, the Eburru volcano (2820 m asl) separated the two basins at ca. 400 kyr BP), subsequently, Olkaria volcanic complex (2440 m) closed the Naivasha basin to south-west at ca. 320 kyr BP and finally, the Menengai Caldera (2278 m) closed Nakuru-Elmenteita basin to the north at ca. 180 kyr BP (Clarke et al., 1990). Volcanic and tectonic activity is on going.

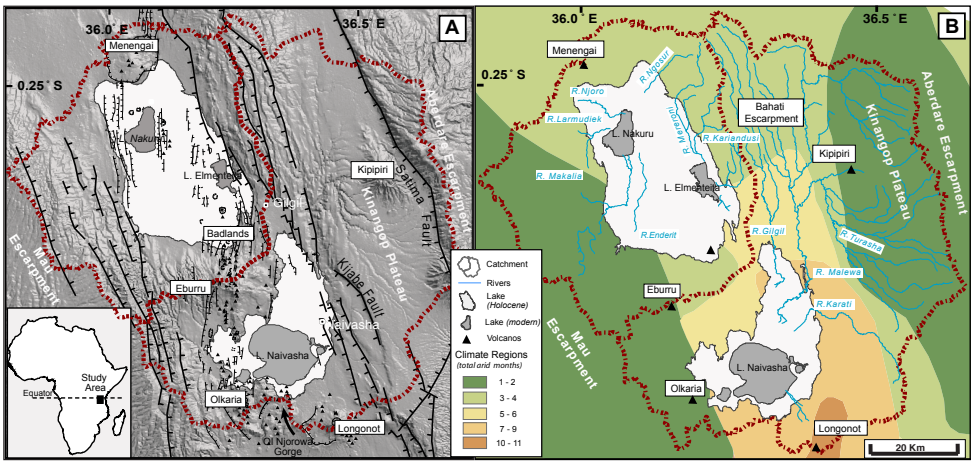

Figure 4.1. Regional map of the Central Kenya Rift (A) Geomorphology (B) Climate regions within the study area. The escarpments have only 1-2 dry months in a year, south of Lake Naivasha is the most arid area with up to 11 dry months. The approximate extent of the paleolakes during the African Humid Period (15-5 kyr) is highlighted in white around the modern-day lakes. Modern surface hydrology in the basins; North-South trending fault blocks deflect most of the rivers draining in the Aberdare Escarpment and the Kinangop plateau towards the south into the Naivasha basin. Only minor rivers drain into the Nakuru-Elmenteita basin draining the Mau Escarpment

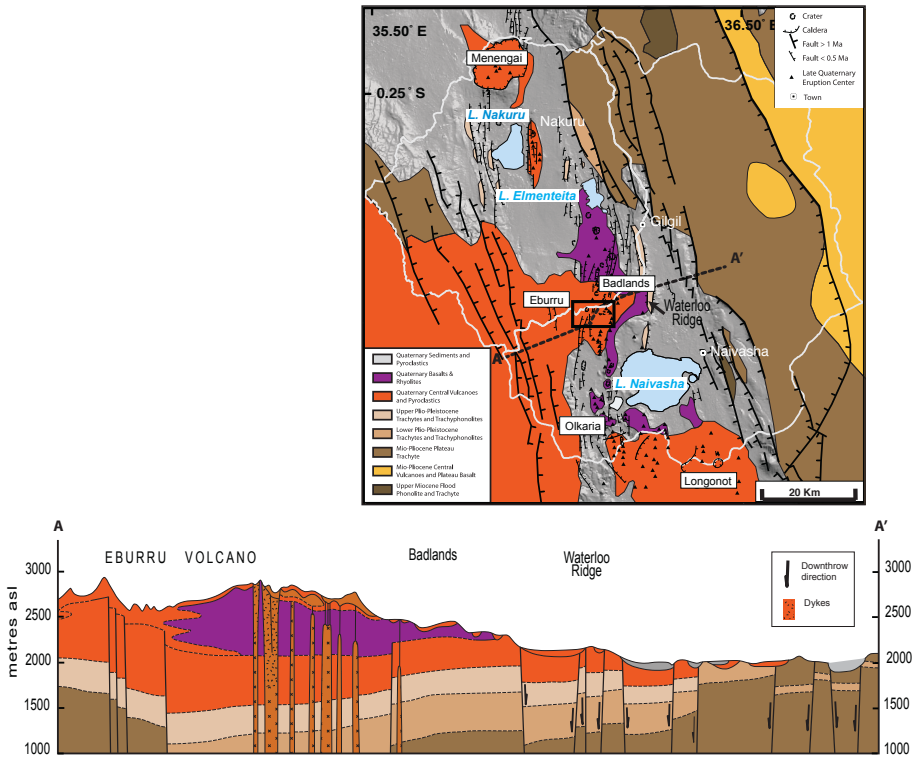

Figure 4.2. The Geological map of the CKR shows a NNW-SSE aligned rift-system structure with older faults and volcanic units on the rift-shoulders versus younger edifices and faults on the rift floor. A-A' is an E-W cross section profile through the Eburru Area, showing deep faults which dissect the inner graben. The existence of alignments of volcanoes such as the N-S alignment of Olkaria and Eburru and highly fractured rock create an environment of high groundwater flow through the rift. The black box indicates the TEM coverage in Figure 4.3. Geologic units, after Thompson and Dodson (1956), McCall (1959) and Clarke et al., (1990).

The geology of the CKR is characterized by trachytic, basaltic and rhyolitic lavas, and tuffs from numerous eruptive centres, as well as minor fluvial and lacustrine sediments of late

Pleistocene to Recent age (Thompson and Dodson, 1963; Clarke et al., 1990). Faults occur within the floor and mark the rift in a series of steps (Figure 4.2). At least two generations can be identified perpendicular to the changing rifting extension direction from NW-SE to N-S/ NNE-SSW. Linear features manifestations include faults bisecting eruptive centres, aligned volcanos and linear river sections (Barker et al., 1972; McCann, 1974; Strecker et al., 1990). Pronounced alignments of eruptive centres are inferred to be surface expressions of a system of deep axial faults which dissect the inner graben. One such alignment is the N-S trend of the Eburru-Olkaria craters to the west of Lake Naivasha, that incorporate the volcanic centres of Elmenteita, Ndabibi, Akira, Tandamara and Suswa (Riaroh and Okoth, 1994).

The Eburru volcanic complex is a 23 km wide ridge form projecting transversely from the western rift margin covering an area of 470 km^2. Maximum north-south extension is 18 km and a maximum elevation of 980 m above the adjacent rift floor. The main tectonic features in the Eburru area are marked by N-S striking normal, strike slip and oblique faults dissecting the volcanics (Clarke et al., 1990). The structural setting of the CKR likely controlsthe flowpaths of groundwater but not in simple ways. The deep faults that form the rift margins are considered to form pathways along which the deep geothermal aquifers are fed (Riaroh and Okoth, 1994). The existence of alignment features such as volcanoes and highly fractured rock and porous basaltic rocks create highly permeable environments for groundwater flow through the aquifers (Kebede et al., 2008), though extensive mapping within the CKR has not been done. Moreover, steam vents and other geothermal manifestations mainly occur along or near the fault/fracture lines on the flanks of the mountain.

4.2.2 Climate

Modern climate of the CKR is governed by the annual migration of the Intertropical Convergence Zone (ITCZ) and the seasonal development of the trade-wind/monsoon circulation over the Indian Ocean air masses and the Congo Basin (Nicholson, 1996) modified by local topography. Climate is humid to sub-humid in the rift highlands and semi arid in the rift floor (Figure 4.1). Rainfall is bimodal with peaks in April and October, the rift flanks receive up to four times more rainfall (ca. 2400 mm/yr) than the rift floor (ca. 600 mm/yr). Annual evaporation over the lakes, however, is at least three times the rainfall that these lakes receive (ca. 1800 mm/yr). Minimum monthly mean temperature is ca. 7°C and maximum monthly mean temperature is 26°C.

Inferred climate for the Late Pleistocene–Early Holocene reveal humid conditions between ca. 15-5 kyr BP. The rejuvenation of the African-Indian monsoonal circulation at this time is generally attributed to the increase in Northern Hemisphere summer insolation, and abruptness of the onset and termination of this period has also been attributed to strong biogeophysical feedbacks (Kutzbach and Street-Perrott, 1985; Olago et al., 2000). These wetter humid conditions are also supported by pollen data from the Naivasha basin, which show a dominance in forest pollen types between 12-6.5 kyr BP (Maitima, 1991). Dry conditions were initiated at 6.5 kyr BP, shown by an abundance of Podocarpus and Olea while tree taxa such as Rapanae and Pygeum disappeared from the pollen record (Maitima, 1991).

4.2.3 Hydrology and hydrogeology

Lake Naivasha is the largest of the three, with an average surface area of 190 km^2 while Lakes Nakuru and Elmenteita cover 40 km^2 and 18 km^2 respectively. These lakes are fed by a number of perennial and/or ephemeral streams from the highlands (Clarke et al., 1990) and also receive inputs from rainfall, surface runoff and in some cases cold and/or hot springs. Nakuru, is fed by five rivers all draining the Mau escarpment in the west, two of which sink to the subsurface and reappear near the lake:(i) Ngosur, which disappears in the Bahati Plain, (ii) Nderit disappears for some distance and reappears closer to the lake, Makalia, Lamuriak and Njoro rivers enter the lake to the West. Lake Elmenteita, located in the south of the same basin is fed by two rivers; Mereroni in the north and Kariandusi in the East and some warm springs south of the lake. Lake Naivasha, receives principle surface influx via the Gilgil and Malewa rivers. Minor discharge comes from the Karati river in the East (Figure 4.1). Both lakes are shallow with an average water depth of less than 3 m, fluctuating between 3 and 5 m. The Nakuru-Elmenteita catchment covers 2,390 km^2 which is 0.7 times the size of the Naivasha basin, thus it receives less hydrological inflow from its catchment than the large Naivasha basin with a catchment size of 3,200 km^2 (Dühnforth et al., 2006; Bergner et al., 2009).

Paleoclimate investigations have shown the existence of large lakes in the Nakuru-Elmenteita and Naivasha basins (Washbourn-Kamau 1970, 1971; Richardson and Richardson, 1972; Richardson and Dussinger, 1986). However, the existence of an even larger Lake Nakuru-Elmenteita-Naivasha covering the entire CKR basin at the time has been the subject of debate in the past decades (e.g. Nilsson, 1931; Butzer et al., 1972). Nevertheless, this Early Holocene Lake Nakuru-Elmenteita was a large lake; 760 km^2 and 180 m above the present lake level and had surface overflow northwards to the east of the Menengai crater (Washbourn-Kamau 1970, 1971; Richardson and Richardson, 1972; Richardson and Dussinger, 1986; Dühnforth et al., 2006). Lake Naivasha was ca. 685 km^2 in extent and 120 m higher than the present level, and when higher there was a surface overflow to the south through the Njorowa Gorge (Washbourn-Kamau 1970, 1971; Bergner et al., 2003).

The modern hydrogeology of the Central Kenya Rift is defined by aquifers within the volcanic and lacustrine deposits around the lakes with water tables ranging in depths from 1 m around lake Naivasha to about 250 m on the flanks of the rift or on volcanoes (Clarke et al., 1990). The shallower aquifers are important for lake water recharge and also for domestic and irrigation usage. Deeper aquifers are explored for geothermal steam production by the geothermal company at Olkaria, Eburru and in Menengai areas, these wells are drilled to depths of 1000-2600 m and have water temperatures of ca. 300 °C (Clarke et al., 1990). Over 300 active deep wells exist in the CKR; wells near Lake Naivasha shore usually have higher discharge yields (200 to more than 2,000 m^3/day) and transmissivities compared to those away from the lake (less than 100 m^3 /day) (McCann, 1974), whereas wells away from the lake tap aquifers along weathered contacts between different lithological units paleosurfaces or in fractured volcanic rocks (Clarke et al., 1990).

The main regional groundwater flow is from the flanks of the Rift Valley toward the rift floor, then southward into and out of the lake (Clarke et al., 1990) but it is diverted locally by

existing faults which form barriers or conduits (McCann, 1974). The Nakuru-Elmenteita system sits at about 100 m lower in altitude than the Naivasha basin causing a hydraulic gradient to the North. Thus, whereas the surface and subsurface connectivity smoothes the geomorphic differences out, the hydrological deficit of the Nakuru-Elmenteita basin is compensated for by a significant flow from Naivasha (Darling et al., 1996). Hydrologic indicators such as the aridity index and disequilibrium indices show the Nakuru-Elmenteita catchment have a lower hydrological budget compared to the Naivasha basin (Dühnforth et al., 2006; Olaka et al., 2010).

The salinity of these closed lake basins today varies depending on the water balance. Lake Naivasha's conductivity is only 0.378 mS/cm and fresh, while Nakuru and Elmenteita are 29.5 mS/cm) and 14.83 mS/cm respectively and highly saline (Water Resources Management Authority database). Interestingly, the differences in the hydrological budgets and lake salinities did not exist during the African Humid Period as inferred from diatom studies (Richardson and Dussinger, 1986, Bergner at al., 2004, 2009). Current knowledge of the hydrology is that principle discharge from lake Naivasha is occurring in the south; the wells immediately south of Lake Naivasha have a higher proportion of lake water input into their systems (Ojiambo, 2001; Clarke et al., 1990), whereas shallow wells immediately north have shown higher proportion of river water and high-elevation eastern rift water from the north (Ojiambo et al., 2001). Because such processes are highly dynamics depending on the water level. The current knowledge gap is in the dynamics of lake-groundwater and interbasin transfer for the adjacent basins in the course of synchronous lake-level variations in the course of humid-arid conditions and the lag interposed to the sensitivity of the receiver system (Nakuru-Elmenteita).

4.3 Methodology

We investigate the hydrodynamic and hydrogeological properties of the subsurface to map groundwater flow and surface-groundwater interaction within the CKR. Consequently we make estimations of aquifer depletion between the two basins since the AHP through the Eburru barrier and the associated lag imposed on the response time Nakuru System by the aquifer. The study is conducted in two scales:a regional scale, involving the entire CKR basin and two localised scales - the Eburru barrier for its conductivity and on the River Gilgil for surface water-groundwater interaction. We analyse geological information, geophysical resistivity measurements derived from the Transient Electromagnetic Method (TEM), modern water table information from boreholes and paleohydrological inferred levels during the Early Holocene for the two lake basin and river discharge data from two downstream stations on the Gilgil River.

4.3.1 The subsurface and hydrogeology

To understand the complexity and dynamics of the surface-subsurface hydrological system, knowledge of the regional geology, permeability of the underlying rocks and the structures governing the occurrence and movement of groundwater is required. From the geological map, the lithology was divided into eight units according to their age and type. The term

"lineament" was adopted according to O' Leary et al., (1976), who consider a lineament as a simple or composed linear feature whose parts are aligned in a rectilinear or curvilinear way, which differ from the adjacent feature patterns presumably as a reflex of a sub-superficial phenomenon. We developed a lineaments map by digitizing all faults from the available geological maps at 1:100,000 scale by Clarke et al., (1990) and ETM Landsat satellite imagery for area. Additionally, all linear features with or without a visible ground displacement that are more than 100 m long were traced too from the satellite images and included in this map. Field surveys were carried out in May 2009 to ground-truth the lineaments digitized from the satellite imagery and also to map out the surface manifestations of discharge/ recharge areas such as river flow direction. Their orientation and densities were calculated within a GIS environment. High porosity and permeability of the rocks in the CKR is inferred from the lineament densities and interconnectivity. Furthermore, in the Eburru area additional resistivity information for the upper 600m depth from the central loop Transient Electromagnetic Method (TEM) is used. The TEM data was acquired by Olkaria Geothermal project of KenGen company in 2006 from an area of about 30 km^2 of ground-based soundings in the Eburru field, at three depths of 300 m intervals:2400, 2100 and 1800 m asl. TEM has provided high-resolution data in the near surface (<1 km), and has been used to identify hydrothermal fluid circulation and aquifer systems. In general good correlation exists between electrical properties of the rocks and fluid content of geological formations (Fitterman and Stewart, 1986; McNeill, 1990; Barsukov et al., 2004). The correlation of borehole data and TEM sounding depths for low resistivity regions on Kilauea volcano, Hawaii, and Newberry volcano, Oregon, have shown the effectiveness of this method (Fitterman et al., 1988; Kauahikaua, 1993; Lenat et al., 2000; Manzella et al., 2004). Nevertheless, care is required to assure that estimates of depth to the water table are not affected by clay alteration in the stratigraphic section or perched water zones.

The groundwater data are acquired from the National Water Resource Management Authority of Kenya (WRMA); ca. 300 boreholes exist in the CKR for domestic and industrial use. Technical borehole information in the database includes well yield and depth, depth to water table, casing length, water strike and rest levels, well use and location. An absolute groundwater level map was interpolated within a GIS environment using the depths of water level subtracted from the borehole-top altitudes and piezometric levels in confined aquifer systems. Groundwater head and the flow direction were estimated from the hydraulic gradient information.

Lineaments influences on the hydrological features such as river path direction were mapped and spatially correlated with groundwater depths to identify; a) zones of deep groundwater depending on lineaments interconnectivity b) regional flow influence by faults and c) groundwater and surface water interaction and possible recharge/discharge areas enhanced by faults. For this third example we used data from Gilgil River that drains into lake Naivasha. The data exists for only the period between 1958-1965. Fortunately, for this time period anthropogenic perturbations related to water abstraction and obstruction are significantly minimal in the area. The Gilgil River flow along a linear path of a fault within the rift floor between the two lower gauge stations. The influence of tectonics on the flow path is very characteristic for most rivers in the Rift Valley.

4.3.2 Paleohydrogeologic model

We apply a hydraulic-head decay model developed by DeVries (1984) to estimate the groundwater lowering duration of the AHP aquifer of Lake Naivasha into Lake Nakuru-Elmenteita via the Eburru barrier by using the depth to groundwater distribution and subsurface geological and inferred resistivity information of the Eburru volcano. This linear-reservoir depletion approach is based on the Dupuit approach (Almendinger, 1990); with a number of essential assumptions since our paleo-hydrogeological information has a low resolution for this time period. We suppose that the fractures and pores of the volcanic formations and the alluvial/lacustrine sediments bordering and underlying the AHP lakes were saturated with water at the time when the lake was at least 120 m higher than present. The current hydraulic gradient is assumed to have followed the existing topographic surface and the groundwater table must have been above the valley floor to facilitate high discharge which implies a hydraulic head of about 0.1 at the beginning of the Holocene. A schematic model of the vertical profile of groundwater decay is drawn from this level. The evolution of the hydraulic gradient was examined from the fully saturated Early Holocene stage to the present-day condition by a finite-difference scheme for a section through the Eburru barrier covering both the Naivasha to the Nakuru-Elmenteita basin.

4.4 Results

4.4.1 Subsurface architecture

At a local scale, the resistivity values from TEM measurements reveal a heterogeneous lithologic structure in the Eburru barrier, with units varying in setting, properties and thicknesses:from a few to hundreds of metres. At 300 m depth interval slices (at 2400 m asl, 2100 m asl and 1800 m as), resistivity values range from 5 Ωm (low) to 579 Ωm (high) (Figure 4.3). 1) At the surface (2400 m asl), the resistivity values span the highest range from 10-579 Ωm. A pronounced low resistivity (< 25 Ωm) anomaly with a NNE-SSW alignment exists. 2) Deeper at 2100 m asl, resistivity values of the units range from 10 to 451 Ωm. At this depth, rocks to the west of the Eburru peak create a zone of high resistivity (>242 Ωm) and those to the north, and north-eastern area around Lion Hill have lower resistivity values (less than 20 Ωm. 3). At 1800 m asl, the resistivity values are lower, distributed between 5 and 479 Ωm, the spatial distribution of low and high resistivity, however, is almost similar to that at 2100 m asl with minor perturbations. A region of high resistivity extends eastwards, oriented approximately NNW-SSE relating to a volcanic intrusion at depth while the rocks with low resistivity are still confined to the north (Figure 4.3).

Overall, the high resistivity rocks of the Eburru barrier taper to the east with depth, possibly related to the fault there creating a high conductance (low resistivity) region. At 2400 m asl, a conductive zone exists that is larger southwards and links the northern to the southern part of the area, with depth it correlates with the high resistivity values (> 400 Ωm), which are related to the cold lavas and intrusives. From the TEM at 2100 and 1800 m asl, the low resistivity area is shifted northwards and is confined to the north creating a northward dip of low resistivity with depth, which indicate higher conductive area.

The lineaments in Eburru area formed by continued tectonic activity of the inner rift and range in length from a few to hundreds of metres. They have a strong westward component, have an azimuth to the W, SW, S and NW, and are significantly longer.

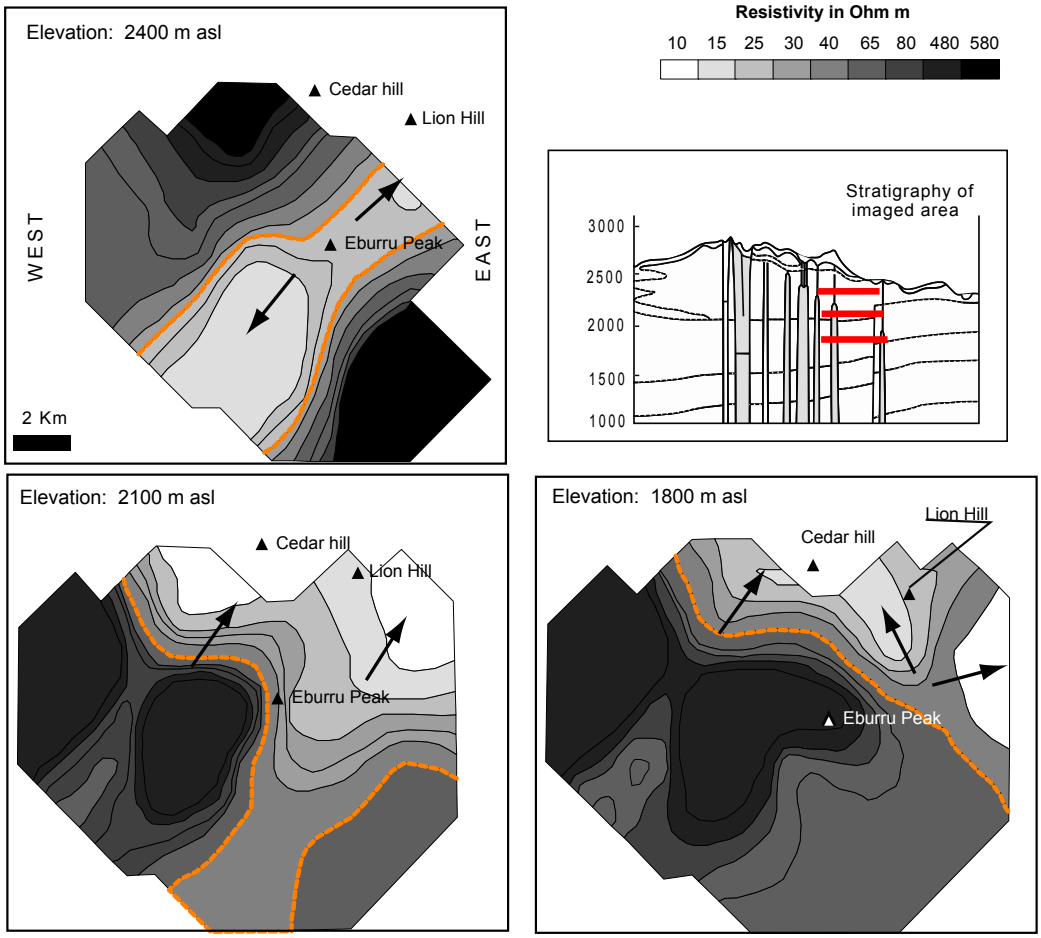

Figure 4.3. The geological cross section of the Eburru and resistivity iso map from the Transient Electromagnetic Method (TEM), at three depths:- 2400 m asl, 2100 m asl and 1800 m asl. Resistivity distribution at 2400 m asl shows an anomaly of low resistivity values that has a NNE-SSW alignment. This anomaly changes to a more N and NE location at depths 2100 and 1800 m. asl the low resistivity areas is highlighted with the dashed line (modified after Wameyo, 2007).

4.4.2 Modern hydrogeology

Groundwater levels within the CKR are reported as both below depth from the surface and as elevation above sea level. They vary from near surface to >2000 m deep. By definition shallow and deep groundwater is divided at a depth of 200 m. Groundwater is shallower in the rift floor around Lake Naivasha, to the west of Lake Elmenteita and south of Lake Nakuru occurring at a few metres below the surface to 40 m depth (Figure 4.4). Additionally, a perched water table is seen located to the west of Lake Elmenteita, and southeast of the Nakuru basin, which is about 18 m higher than Lake Nakuru. The Mau Escarpment, which is the western boundary of the CKR, has intermediate water tables between 2000 and 1900 m asl while the Aberdare Ranges and Kinangop Plateau, its eastern boundary, have deeper water levels.

Groundwater contours of the study area show eight regions having depressed groundwater, that is where groundwater levels have a sharp drop from the surrounding level

highlighting pockets of deep groundwater , labeled with numbers 1 to 8 in Figure 4.4. Three pockets are within the Naivasha catchment; the first one is in the south east (No. 1), within the Karati watershed slightly eastwards of the NW extension of the Longonot volcano. The second pocket is located south west of the lake that extends beyond Ndabibi area and Lake Sonachi (Green Crater Lake, No. 2). The third pocket is in the north within the Bahati escarpment (No. 3). At the Eburru barrier, which is the drainage divide of Naivasha and Nakuru-Elmenteita, is the largest zone of deep groundwater within the study area. The other zone of deep groundwater is located west of Lake Elmenteita (No. 5). The next three zones of deep groundwater are found in the vicinity of Lake Nakuru; a shallower one occurs to the west (No. 6), a small but deep one is found immediately north of Lake Nakuru (No. 7) and another one further north at the foot of Menengai Caldera (No. 8). The contours in the zones of depression are up to 2000 m below ground (100-700 m asl). It is likely that the zones of depressions recharge deeper geothermal aquifers. What is not clear, however, is how they are hydraulically connected with the shallow groundwater at < 200 m depth (1900-2600 m asl). The General flow of the groundwater is from the escarpments to the rift floor, then adopts a northwesterly flow north of lake Naivasha.

Groundwater contour spacing is not uniform throughout the study area indicating lateral changes in aquifer properties that create differing hydraulic gradients within the CKR. This feature is not surprising due to the inherent inhomogeneity caused by the fractured rock and the existence of dykes. In the Eburru area, groundwater levels occur between 2202 and 2450 m asl where the hydraulic gradient typically is 0.04 in the existing boreholes (Figure 4.4). The western part of Eburru has lower gradients of 0.02 to 0.04, while the eastern section of Eburru has slightly higher gradients between 0.02 to 0.07. These groundwater contours indicate a groundwater flow from the Naivasha basin at a shallower level to the east and west (1750 m. asl). This flow is part of a deeper system in central Eburru that is sucked into the deeper groundwater aquifers, at No. 4 in Figure 4.4 through the Pleistocene-Holocene Eburru volcanoclastic rocks.

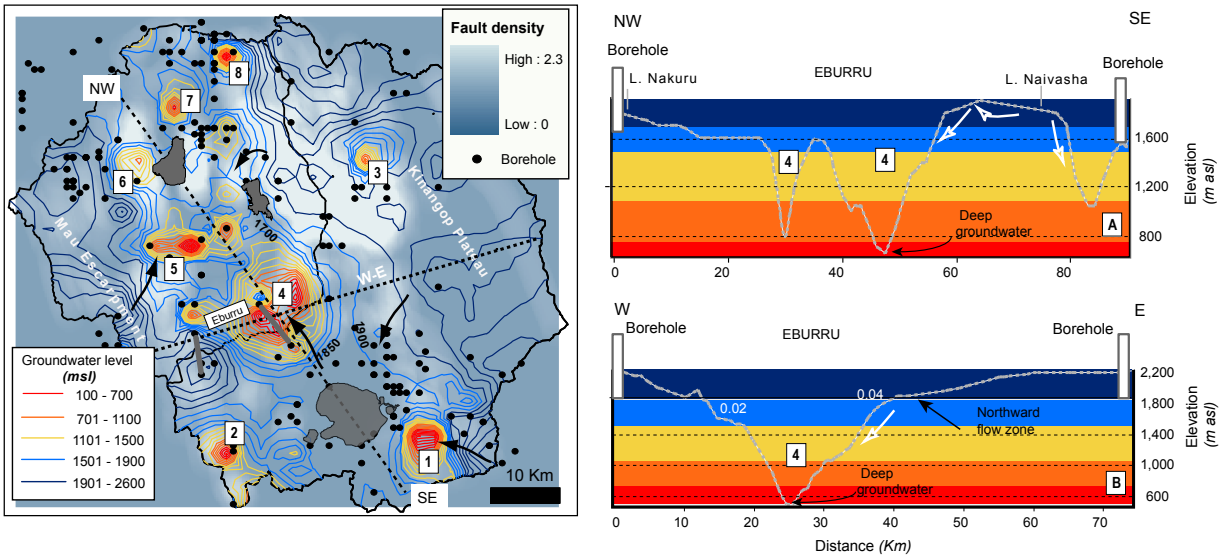

Figure 4.4. Groundwater levels map with boreholes, overlaid on the fault lineament densities. Regions with groundwater depressions with deeper aquifers are the bright red and yellow colours marked with numbers 1-8. The blue contours mark areas with shallower groundwater levels. A) NW-SE cross section of the water levels between two wells and B) is the W-E cross section. The Hydraulic gradient to the East and west of the Eburru are highlighted as 0.02 and 0.04.

4.4.3 Groundwater-surface water interaction

Groundwater recharge and discharge within volcanic bedrock such as in the CKR has been enhanced by the existing fractures. Fractures are either major regional faults on the escarpments that bound the drainage basins to the East and West or as small scale faults within the inner rift graben, oriented in NS direction. We investigated fault manifestation that enhance groundwater permeability and flow. The surface expression can be seen in linear river sections and alignments of volcanoes. Some of these faults around the lakes were inundated by the large Holocene lakes and are now exposed and pose as less resistance paths that rivers selectively follow. Three rivers have linear sections which are likely to be related to faulting within the rift; about 10 km of the lower section of Gilgil River before it enters Lake Naivasha, and Makalia and Enderit rivers that drain into Lake Nakuru (Figure 4.1). These faults seem to have been important for recharge and discharge of water into the lakes during the high lake levels in the Early Holocene. In modern times, however, rivers loose water and recharge the local and regional aquifers in the system and some disappear before reaching the lakes:At Lake Nakuru (i) Ngosur disappears in the Bahati Plain, (ii) Enderit disappears for some distance and reappears closer to the lake, Makalia, Lamuriak and Njoro rivers enter the lake to the West. Lake Elmenteita, in the south east of the same basin, is fed by two rivers; Mereroni in the north and Kariandusi in the East and some warm springs in the south.

River-groundwater interaction is revealed in discharge data of Gilgil River, covering 1958 to 1965, which shows up to 150 m^3 of the river water recharges the alluvial aquifer of the southernmost part of the Gilgil River basin (Figure 4.5) which is between 20-50%. The difference is minimal in drier years than in the wetter years. Anomalies exists in 1965, 1973,

1984 and 1986 when the lower Gilgil station recorded more discharge than the upper Gilgil station. The Gilgil River therefore reveals a peculiar character in which it both recharges and discharges shallow, water-table aquifers depending on amount of river water. The years when the lower Gilgil station receives more discharge than the upper Gilgil station, correspond to years when a lowering was recorded on the lake. That is during a drought the lower Gilgil River gains while during a normal/wet year it looses water. This is similar to the observation by Olago et al (2009), that higher surface runoff may alter lake water balances and raise their water level. If this happens, then Lake Naivasha, for example, may increase its proportion of recharge to the surrounding aquifers relative to surface runoff, river influents, and direct rainfall infiltration components. This is rather related to temporally short and transient occasions where the rift floor receives more precipitation than the rift flanks, raises lake level which discharges into surrounding areas then rapidly lowers when the event is over. The fracture zones forms an interlaced network of high transmissivity and acts as groundwater conduits in massive rocks in inter-fractured areas. The faults and fracture network on the tuffs of Bahati and Gilgil area act as conduits for regional groundwater recharge, and that water is more than 120 m deep from the surface.

To the south-eastern section of the study area (Figure 4.4), within the catchment of Karati river, an area with deep groundwater exists. This river runs along the Kijabe fault and is also where the Late Miocene trachytes and phonolites, the Pliocene trachytes and the Holocene volcanic trachytes occur.

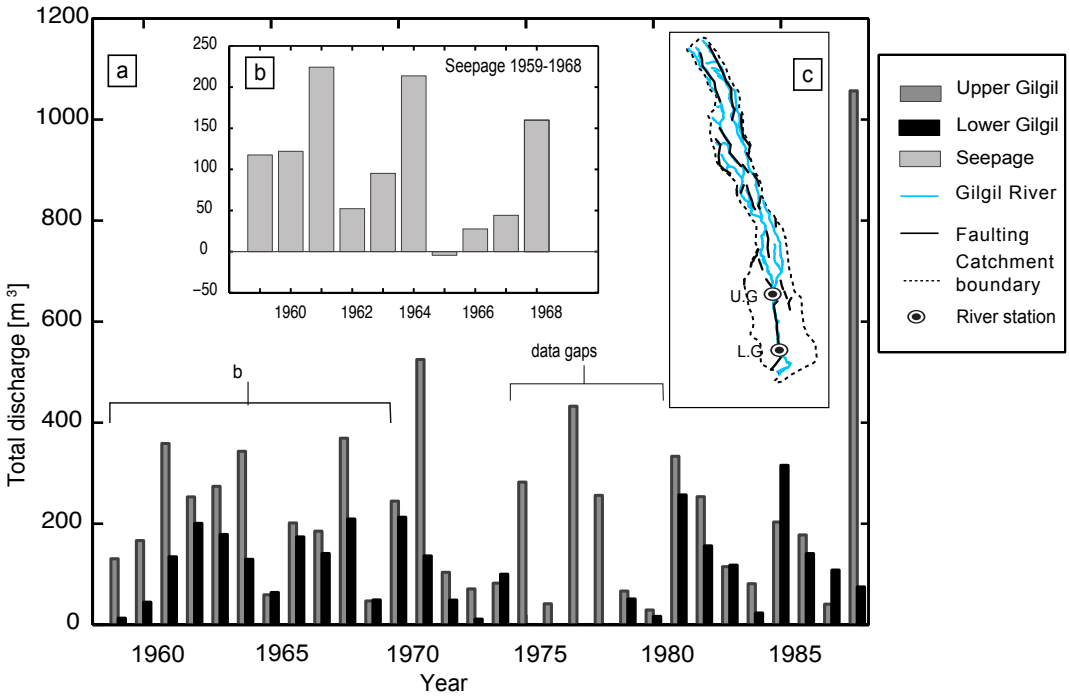

Figure 4.5. Graphs showing the loss of water between upper and lower Gilgil gauge stations trough subsurface seepage in the lower section the river runs along a 20 km N-S striking fault. An average of 150,000 litres per year between 1960 and 1964 is lost. C is the catchment boundary of the Gilgil River

4.4.4 Drying out the lake system

At the drainage divide in the vicinity of Eburru, the paleo-shorelines of Naivasha and Nakuru-Elmenteita derived from the digital elevation models (DEM) during the AHP are estimated to have been 6 to 20 km apart from east to west. The hydraulic head of the groundwater that determines interbasin flow is located in this area which is on average about 10 km from either paleo-shoreline, across this highly fractured and conductive zone. It is in this zone that the groundwater head in the unconfined aquifer has dropped by at least 150 m thickness since the AHP. Using 21% as the specific yield for tuffs (Johnson, 1967) the total volume of the saturated area can be estimated by the formula VT = Total volume of saturated deposits x Specific yield. Thus using the formula for a trapezium ½(6+20)*10*0.15 x 21/100 = 40.95 km^3.

We then use a linear-reservoir depletion approach to estimate the time needed to produce the decay of 40.95 km^3 volume of unconfined groundwater at the drainage divide from 2000 to 1850 m asl due to a decrease in recharge from the Early Holocene wet period to the present-day average annual recharge of 0.52 m at the fringing area. For continuity

$$Sdh = (N - q)dt \tag{1}$$

where S is the specific yield; h is the average head above the discharge base (L); N is the recharge (LT -1); q is the discharge (LT-1). Using the Dupuit assumptions, the parabolic groundwater table is thus

$$h = 2/3(h_m) \tag{2}$$

where h_m is hydraulic head at the divide. The specific drainage resistance R (T) is

$$R = h_m q \qquad \text{thus} \qquad dh_m = Rdq \tag{3}$$

The parameter R is the function of the length of the considered flow path and the transmissivity. Substituting Eqs (2) and (3) in Eq. (1) gives

$$2/3(SR)dq = (N - q)dt \tag{4}$$

or

$$dq = j(N-q)dt \tag{5}$$

where

$$j = 1.5(S.R)^{-1} \tag{6}$$

j is the reaction factor or reservoir outflow recession constant (T^{-1}). Integrating equation (4) with boundary conditions $q = q_0$:$t = 0$ and $q = q_t$:$t = t$ with N = constant gives:

$$q_t = q_0 e^{-jt} + (1-e^{-jt})N \tag{7}$$

recalling Eq. 3:

$$h_t = h_0 e^{-jt} + (1 - e^{-jt})N \quad (8)$$

where h_t is present head above the drainage base at the divide: 1850 – 1700 = 150 m, h_0 is the height at the divide above drainage base at the beginning of depletion (t = 0):2000 - 1700 = 300 m.

We presume the groundwater head level at the drainage divide between Naivasha and Nakuru-Elmenteita has dropped by 2000 m - 1850 m = 150 m since the AHP. Assuming the present conditions are close to steady state, then to reduce the groundwater thickness by 1m in a steady linear decay model would take approximately 67 years within the 10,000 year period. However, this is more of an ideal scenario, whereas when climatic extremes and anthropogenic activities that impact on groundwater are also considered, then this rate of replenishment changes.

To find the specific drainage resistance, we substitute the present average recharge, which is based on helium isotope studies by Ojiambo et al., (2001) in Olkaria region, which has similar hydroclimatic setting as Mt. Eburru, N = 0.12 m/yr and the present hydraulic head ht =150 m in Eq. (3) gives R = 1250 yr. Assuming a specific yield of 11.7 % for the Eburru region and substituting this value with R in equation (6) gives j = 1.0 x 104. Substituting these values in Eq (8) gives a decay in groundwater head of 2%. The time lapse for zero-recharge during the depletion period is about 5,000 years (Figure 4.6) representing the calculated hydraulic-head decay for 10 kyr, i.e., since the end of the last high lake period under the condition of no replenishment (N = 0). The current recharge of the Eburru area is estimated as about 0.52 m/yr from rainfall and it is at least 150 m lower than during the AHP while to maintain the positive water balance that kept lakes high the recharge must have been higher than this present value.

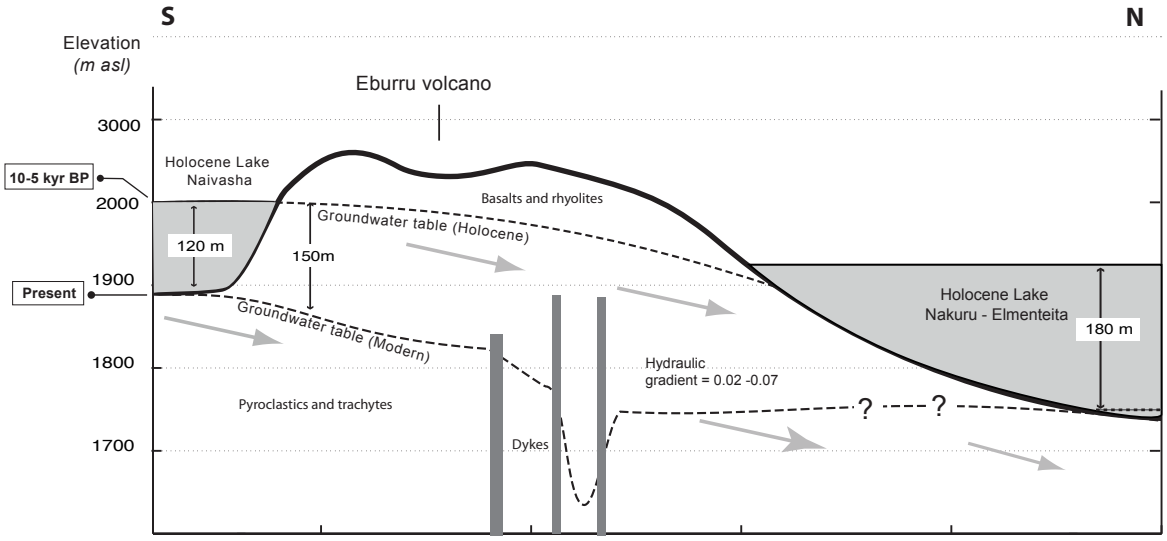

Figure 4.6 S-N schematic topographic-hydrological section through the Central Kenya Rift lake catchments, showing groundwater head decay from the Early Holocene to present day. The arrows show the direction of groundwater flow.

4.5 Discussion

Subsurface analysis generates the necessary information for estimating and assessing groundwater occurrence and flow through the fractured volcanic rocks within the CKR. This background is used to estimate the depletion duration and interbasin transfer of the AHP groundwater via the Eburru barrier from the Naivasha basin to the Nakuru-Elmenteita basin.

Faults within the CKR are predominantly NS oriented. In places at depth, volcanic and pyroclastic rocks are highly fractured and displaced to the east or west depending on the direction of throw on the governing fault that have predominantly N-S orientation. Resistivity values at the Eburru barrier give insight of the litho-hydrostratigraphy and possible pathways of flow with depth; up to 600 m deep, the low resistivities correspond to high conductivity:(1) at 2400 m asl there are younger Eburru trachytes (<0.45 My BP) and the region with low resistivity has a slight NNE-SSW orientation, which is highly conductive whereas areas of high resistivity values in the north and south west are attributed to the intrusive bodies that exist in these sections. Such intrusions generally have hydrothermally altered rims around them, which tend to exhibit lower resistivity (2) below 2100 m asl, a zone of high resistivity (>80 Ωm) exists on the western part of the imaged area; this could be attributed to the cold unaltered rocks of the older volcanic centre of western Eburru; (3) low resistivity values have a northward dip to Nakuru-Elmenteita catchment with depth. Corresponding to highly conductive zone governing interbasin groundwater flow between Lakes Naivasha and Nakuru-Elmenteita.

Lineaments are often considered as zones of enhanced permeability compared with the surroundings (Yin and Brook, 1992). The main lineaments have a N-S to NNW-SSE orientation within the CKR. The highest density of lineaments (2.3 lineaments per km^2) is in the Bahati Kinangop area, west of Lake Elmenteita at the eastern boundary between Naivasha and Elmenteita catchments. Another region with high density of lineaments bound Lake Nakuru to the East and West within the inner rift (Figure 4.7). These structures are related to normal faults that created the basins at about 2.6 Ma and further tectonic activities (Strecker et al., 1990) and subsequent volcano-tectonic faulting. These areas somewhat correlate with areas with groundwater zone of depression (Figure 4.4). The Eburru barrier has moderate fracturing, nonetheless the groundwater level goes quite deep, over 2000 m in some areas. This difference could be reflecting the depth of the faults. Deeper reaching faults create deeper water levels as opposed to shallow reaching faults, as in the Bahati-Kinangop area case, with a high density of faults and shallow groundwater. The faults that cut through the Eburru volcano generally trend in NS direction and formed during an E-W extension and were previously reported as having smaller throw and almost sub vertical orientation with a ca. 70-degree dip (Nylor, 1972). This near vertical orientation enhances faster vertical groundwater flow. The complex fracture systems and related variability of the hydraulic transmission properties of the rocks in the CKR make delineating the flow of groundwater and recharge a challenging task, however some general estimations can be made. In the Eburru region, groundwater flow northward is not a uniform pattern. Shallow flow occurs in a narrow zone of about 10 km width in the eastern section and deep flow is in the central section (Figure 4.4). The existence of numerous dykes and the concentration of obsidian and pantellerite flows, which are related to the NS trending fractures of the area, seem to perturb the groundwater

flow in the central region causing small scale irregularities in the groundwater head that we see further north of Eburru in the Nakuru-Elmenteita catchment.

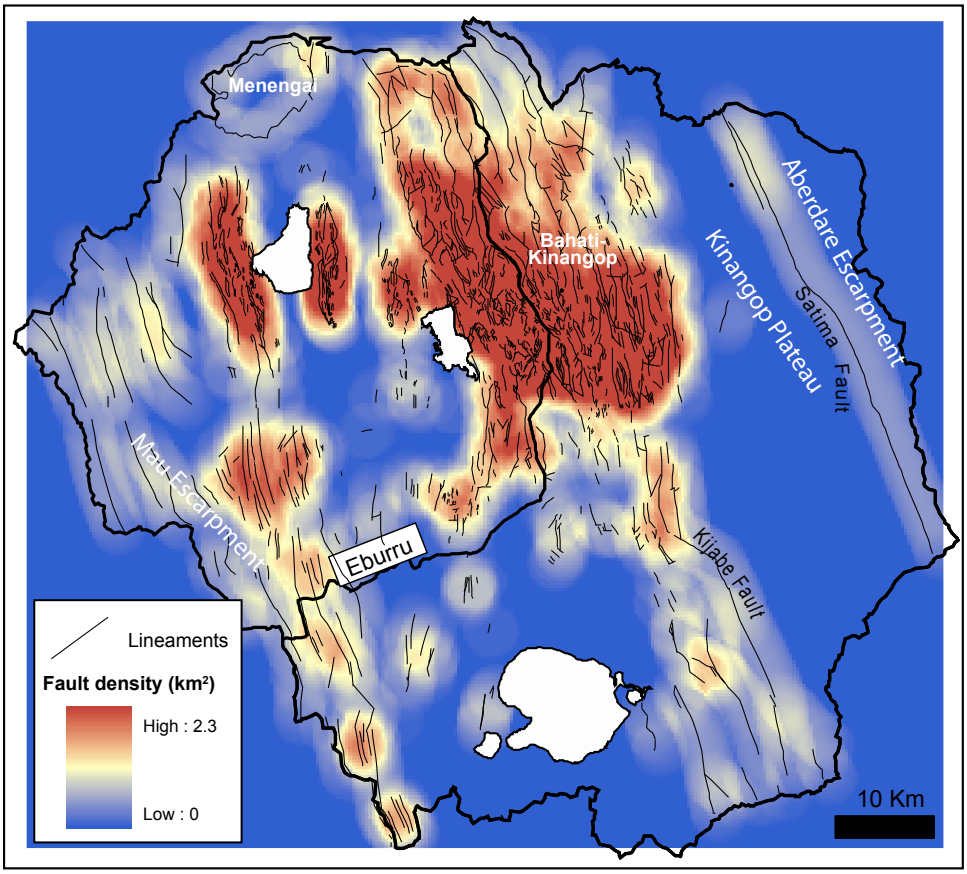

Figure 4.7 Lineament density map of the Central Kenya Rift. Higher densities outline the rift axis. Highest densities (>2 km^2) are found in the Bahati Kinangop area, defining the drainage divide between Nakuru-Elmenteita and Naivasha in the north. Note the lower density of lineaments in the Eburru barrier region is discussed in the text.

The groundwater map's head somewhat mimic topography with groundwater flow following the regional topography from the rift escarpments to the rift floor and subsequently to the north and south following the NW-SE rift orientation in the CKR. The influence of the NS trending faults on the rift floor is also seen with steeper hydraulic gradients (ca. 0.07) to the east of Eburru barrier than to the west of it (ca. 0.03). This also confirms stable isotope studies of Darling et al., (1990, 1996) where they detected lake water about 12 km to the north in the Eburru volcanic ridge from geothermal wells at 1850 m below the surface. In fractured rock units, the direction of groundwater flow is completely constrained by the direction of the fractures. There may also be intrinsic permeability in directions not parallel to a set of fractures. Basalt flows are highly anisotropic, as they parallel the dip of the flow as it moves in the interflow zones (Fetter, 2001). Quaternary basalts occur in the east of Mt. Eburru and the south of Lake Elmenteita in a region with many eruptive centres called the badlands and also numerous hotsprings occur (Figure 4.2). Research in other mountain-bounded lowland aquifers in arid regions have established the relative importance of the recharge component coming from mountains as groundwater inflow, compared to recharge from precipitation in the

valley or from stream loss (e.g. Manning and Solomon, 2005). Groundwater inflow is dependent on the hydrogeology of the interface between the mountains and the valleys including the nature and depth of bounding faults, the presence of transverse faults connecting the mountains and the valleys, the permeability of the mountain mass etc (Manning and Solomon, 2005).

Recharge of the aquifers occurs either by rainfall infiltration or in some cases influx of river and lake discharge. Annual river discharge from two stations on the Gilgil River revealed significant surface water and aquifer interaction east of the Eburru barrier (Figure 4.5). It seems that river water infiltrates into a hydraulically connected aquifer during a rising flood stage and its reverse motion during stream flow recession recharges the stream (Singh, 1968; Todd, 1980). Stream flow infiltration is common in the central Kenya rift rivers. The total annual stream flow infiltration occur in the Gilgil River of which we estimated as 150 cubic metres, which is between 20-50% of the total annual discharge. Other rivers in the Nakuru-Elmenteita catchment disappear and reappear along their course to the lake. River discharge records are scant and, therefore, we are not able to give quantifiable values for all the rivers. However, a similar behaviour is expected within this geological field depending on the gradient of the groundwater flow. It is an area for further work to make quantitative estimates by long-term river monitoring and tracing through different seasons.

A NS schematic model of the groundwater connectivity can be drawn based on this knowledge of the subsurface and paleo-lake levels (Figure 4.6). The present hydraulic gradient and the level of groundwater can be explained as a result of groundwater decay that started after the high Lakes Naivasha and Nakuru-Elmenteita that existed between 10-8 kyr BP and 10-7 kyr BP, respectively (Butzer, 1972). Low lake levels existed from 5 kyr BP in the Naivasha basin and 4 kyr BP in the Nakuru basin. Under no recharge condition on the groundwater aquifers in the Eburru region, we get a decay time of 5 kyr needed to lower the groundwater from the elevation of 2000 m to its present level of 1850 m asl. This implies that, if there was significant recharge of the aquifers and the groundwater levels still dropped, then it must have taken a short time to drain the aquifers. No published data is available on the age of the deeper waters in the Central Kenya Rift, however, in the Ethiopian Rift deeper groundwaters in the rift floor have 14C ages ranging between 2.3 and 3 kyr BP (Kebede et al., 2008).

Both the Kenyan and Ethiopian rifts have similar volcano-tectonic and climatic history that affect hydraulic transmissivity, hence we speculate that the current groundwater within the Eburru could be of similar age with the Ethiopian Rift implying that it would have taken between 2-2.7 kyr to drain the rift aquifers after the high lake period in the Holocene. Lake sediment studies have shown that paleo-Lake Nakuru-Elmenteita declined about 1 kyr after Lake Naivasha (Butzer, 1972). However, their spatial proximity to each other is too close to explain for a significant difference in their hydroclimate. With the similarities in the physiogeographic setting we do not expect major climatic differences in these two basins. Such peculiarity can be sustained by existence of a groundwater connection driven by the hydrological gradient between the two catchments and creates a lag in lowering of Lake Nakuru-Elmenteita for the same regional climatic forcing. Depending on the height of the hydraulic head, the surface catchment divide between the two basins at the Eburru barrier can

either be congruent or incongruent to the groundwater divide boundary. During high lake levels, the groundwater divide is highly incongruent and vice versa.

Resistivity values are generally interpreted as relating to effective porosity. Low resistivity values correlate to high conductivity in groundwater. However, in geothermal systems such as the Eburru volcanic complex, resistivity variations can be caused by hydrothermal alteration. Clay products such as smectites that cap the outer margins of such a reservoir, have lower resistivity. The succession of a low resistivity region (i.e., the clay cap) and a high resistive surrounding (the core below) are somehow consistent with geothermal reservoirs, making porosity estimations in the Eburru area using the TEM method alone insufficient. We make up for this by juxtaposing these results with the data of geology and structures of the area to get a non-biased impression of the conductivity. We observe a narrow zone of about 10 km wide to the east of Eburru that has a higher density of NS trending faults which we observe as influencing the physical and mechanical characteristics of rocks and also control fluid movement and storage in the subsurface (Figure 4.7).

Because groundwater influences on a lake is not static but dynamic depending on the water level and location. From the hydrostratigraphy, our results suggest that during the Early Holocene +120 m lake levels, the two basins were connected by a groundwater system that would have had an influence on the water and solutes following the existing hydraulic gradient. The modern outflow from lake Naivasha to the North, however, recharges the deeper aquifers in the Eburru area with minimal flow to the Nakuru-Elmenteita system within the current low lake levels – a constellation that developed after the lowering of the Holocene lake levels. These results have implications for paleo-/limnological reconstructions of arid/humid transitions in groundwater influenced lake systems. In such areas a clear delineation of the hydrologic setting is necessary to reconstruct the likely responses of selected proxies for climate reconstructions.

4.6 Conclusion

The study of the hydrogeological properties of the CKR has highlighted the viability of groundwater control on the surface water balance and hence influencing lake hydrology. In our reconstruction of the water table decline after the AHP by northward outflow from the Naivasha aquifers into the Nakuru-Elmenteita basin, estimates show that through the Eburru barrier, the aquifer volume of 40.95 km^3 would require between 5 kyr and 2.7 kyr to deplete from the AHP levels. This depletion and hence the lag is enhanced by three factors; (1) the highly fractured volcanics that enhance surface and subsurface water interconnectivity and flow, (2) the reduced recharge as a result of change from humid to arid conditions after the mid Holocene, and (3) the high hydraulic gradient existing between the two catchments enhances northward flow. The findings highlight that groundwater flow within the CKR is an important component of the hydrological system of rift lakes and can therefore not be neglected in lake-balance modelling studies and the specific groundwater responses of each basin has to be carefully calibrated to improve the paleo-precipitation estimates.

Acknowledgements

This project was funded by grants to L.A.O. by the German Academic Exchange Service (DAAD), by grants awarded to M.R. Strecker (Gottfried Wilhelm Leibniz Prize)and by the DFG Graduate School GRK1364 led by M.R. Strecker and M.H. Trauth and the German Research Foundation (DFG) to M.H.T. We thank the Government of Kenya (Research Permits MOST 13/001/30C 59/10, 59/18 and 59/22), the Ministry of Water and Irrigation of Kenya and the University of Nairobi for research permits and support. We thank S. Higgins, Y. Garcin, G. Muchemi, M. Strecker, A. Junginger, K. Stoof, and the graduate students at the GRK1364 for inspiring discussions. We also would like to acknowledge KenGen Ltd. Olkaria for providing the geophysical data and access to their library.

CHAPTER 5

CONTRIBUTIONS TO CLIMATE PROXY SITES OF EAST AFRICA:
Intraseasonal precipitation variability in the last decade

Abstract

As paleoclimate proxy records from East African lakes grow, distinguishing local from regional climatic processes is becoming increasingly important to improve interpretations of past regional dynamics. Inter basinal comparison of high frequency precipitation offers the ability to distinguish the effects of local dynamics on the mesoscale circulation/controls. This study uses satellite rainfall estimates data from FEWSNET available at dekadal (10 days) scale and 8 km resolution for the period between 1996-2010. The seasons are grouped as MAM, JAS, ON and DJF. Basin's averaged precipitation are used to investigate the spatial and temporal dynamics for each season on eleven lake basins with contrasting topography, located within the East African rift system. The eleven from North to south are Lakes Tana, Ziway, Awassa, Abaya, Turkana, Suguta, Baringo, Nakuru, Naivasha, Natron and Manyara. Each season is invesigated for the impact of the prevailing climate dynamic such as ENSO/IOD, QBO, ISM, ITCZ, CAB, Solar flux.

The results are preliminary and they show great complexities at high frequency and there is no dominant rainfall mechanism acting in the 14-year period however we see differences in magnitudes of the catchments. The JAS season is the most complex. Spatial heterogeneity however relates to onset, intensity and duration of each of these climate oscilators. A few lakes emerge as indicators of strengths of specific mechanisms. For example, Lake Natron has shown very good biennial circulation while Lake Tana in the EP reveals good correlation to the strength of the CAB and the onset and strength of the ISM. Rainfall in Nakuru and Naivasha differ greatly in JAS as a result of recycled moisture from Lake Victoria. Effect of topography and catchment configuration play a significant role in the East African plateau basins. Understanding these disparities is of interest in deceiphering trends and fluctuations in paleo- climate proxies.

5.1 Introduction

In East Africa, lake basin sediments have yielded diverse proxy records for investigating the Pleistocene-Holocene climate dynamics and establishing major arid-humid transitions. However, regional comparison of these records show spatial heterogeneity in the timing and magnitude of regional scale events or trends from these records (Verschuren et al., 2000; Russel and Johnson, 2007; Garcin et al., 2009, Junginger and Trauth, subm.) and is a challenge to establishing patterns of palaeoenvironmental change across the East African Rift System (EARS). These differences in the records could be attributed to dating uncertainties or sensitivities of applied proxies or catchment characteristics. In East Africa the rift feature and associated volcanos plays a major role in modifying the amount of effective moisture for each basin. Climate variability in tropical Africa manifests as moisture-related arid-humid transitions,

rather than temperature changes that characterize the higher latitudes. An understanding of mechanisms responsible for present day interannual to interdecadal climate variability is required in order to enhance interpretation of climate variations from paleo-climate records(Wang et al., 2005).

East African rainfall is generally associated with the latitudinal migration of the Intertropical Convergence Zone (ITCZ) between ca. 10° north and south of the equator and associated seasonal eastward shift of the Congo Air Boundary (CAB) over parts of East Africa (Nicholson 1996, see details in section 5.2). Significant precipitation anomalies are usually linked with sea-surface temperature (SST) anomalies in the Indian and Pacific Ocean associated with the Indian Ocean Dipole (IOD; Saji et al., 1999; Clark et al., 2003) and the El Niño Southern Oscillation (ENSO; Camberlin et al., 2001; Camberlin and Philippon, 2002) phenomenon. Additional to these well-known phenomena, SST variations in the Atlantic Ocean, the quasi-biennial circulation (QBO; Indeje and Semazzi, 2000), the strength of the Indian summer monsoon (ISM; Camberlin, 1997; Junginger and Trauth, subm.) and regular fluctuations in solar flux (Neff et al., 2001; Wang YI et al., 2005; Kodera et al., 2007; Meehl et al., 2009) also contribute to variations in East African precipitation. Further, the existence of highly variable topography, vegetation and large inland lakes are also cited to cause significant spatial variability in the rainfall pattern of East Africa (Nicholson, 1996; Indeje and Semazzi, 2000; Chan, 2008). However, the direct contribution of these features to disperse precipitation pattern has not been extensively investigated. Such a study offers the potential to improve interpretations of climate proxies from these lake basins.

Generally, estimates of aerial precipitation for hydrological applications are made from point observations. in East Africa, the rain gauge density is quite low, though, interpolation of the existing rain gauge data provide relatively accurate estimates at a few point in a region, rain-fields for tropical regions where most rainfall has a convective origin with high spatial variability at the daily level exhibit a great deal of uncertainty (Meisner and Arkin, 1987; Dai, 2001), linked to local effects such as complex terrain and sea-breeze circulations (Oki and Musiake, 1994; Yang and Slingo 2000), or the long, nocturnal life cycle of mesoscale convective systems (MCSs; Wallace, 1975; McAnelly and Cotton 1989; Dai et al., 1999; Sherwood and Wahrlich, 1999). Recent technological advances in remote sensing techniques, provide rainfall measurements at high spatial and temporal resolutions and offers possibilities to overcome the uncertainties of interpolation.

Here we use rainfall estimates from remotely sensed data to investigate the intraseasonal precipitation variability on the EARS basins, for the time period January,1996 - February, 2009. We intend to provide insights into the complex interaction of local and regional climatic processes in catchments along the topographically complex Rift system. We also attempt to identify the governing atmospheric circulation patterns leading to intraseasonal rainfall distribution in East Africa. The results of this study foster a better understanding of intraseasonal disparity among catchments and the resultant perturbation of regional climate signatures recorded by climate proxies. Such studies have potential to improve calibration of Regional climate models (RCM's) currently required for future predictions efforts for rainfall and hydrological systems in this area (Stute et al., 2001; Donders et al., 2008). The current

population growth rate is of East africa is 2.9% (UNFPA, 2010). and relies predominantly on rainfed agriculture.

5.2 Setting

5.2.1 Climatic setting of East Africa

East Africa is one of the most meteorological complex part of Africa due to the interaction of highly variable topography, large inland water bodies and maritime influence with several convergence zones, resulting in climate patterns that change over short distances (Nicholson, 1996). The general climate is controlled by the annual latitudinal migration of the ITCZ around the equator, between 10° north and south latitudes, following the overhead position of the sun with a time lag of 4-6 weeks (Nicholson, 1996). This migration produces a bimodal precipitation cycle along the equator with the so-called ‘long rains’ in March-May (MAM) and ‘short rains’ in October-November (ON). Although both of the rainy seasons are related to the seasonal migration of the ITCZ, they are not the mirror image of each other. This might be related to the longer march of the ITCZ northwards from February to August, whereas the southern retreat occurs faster between August to November (Suzuki, 2011). The ‘long rains’ therefore show heavier rainfall than the ‘short rains’, but the ‘short rains’ experience a larger degree of interannual variability relative to climatology (Hastenrath et al., 1993), hence the long rainy season is the most important East African agricultural season along the equator (Camberlin and Philippon, 2002). In contrast, the limits of the ITCZ migration path receive maximum rainfalls within only one rainy season, from December-February (DJF) and July-September (JAS) south and north of the equator, respectively (Fig. 5.2). This general picture is slightly blurred for northern East Africa, where a northern protrusion of the March-May rains known as ‘Belg’ rains into northeast Ethiopia occurs, often starting as early as February and lasting until April/May (Camberlin and Philippon, 2002). Especially, the area along the eastern rim of the northern central highlands is known to be highly vulnerable to rain failures during ‘Belg’ rains or the ‘Kiremt’ rains, which occur from July onwards (Camberlin and Philippon, 2002).

Precipitation associated with the ITCZ has its origin in large-scale moist advection from the Indian Ocean (Levin et al., 2009). Precipitation anomalies are therefore supposed to be linked to Indian Ocean SSTs anomalies attributed to the IOD with intensified (reduced) rains during high (lowered) SSTs in the western Indian Ocean (Saji et al., 1999). The highest rainfall variability in the course of IOD events is reported to affect East Africa in October/November (Saji et al., 1999). Under certain conditions ENSO and IOD occur simultaneous, but the exact relationship between these two events is not fully understood yet.

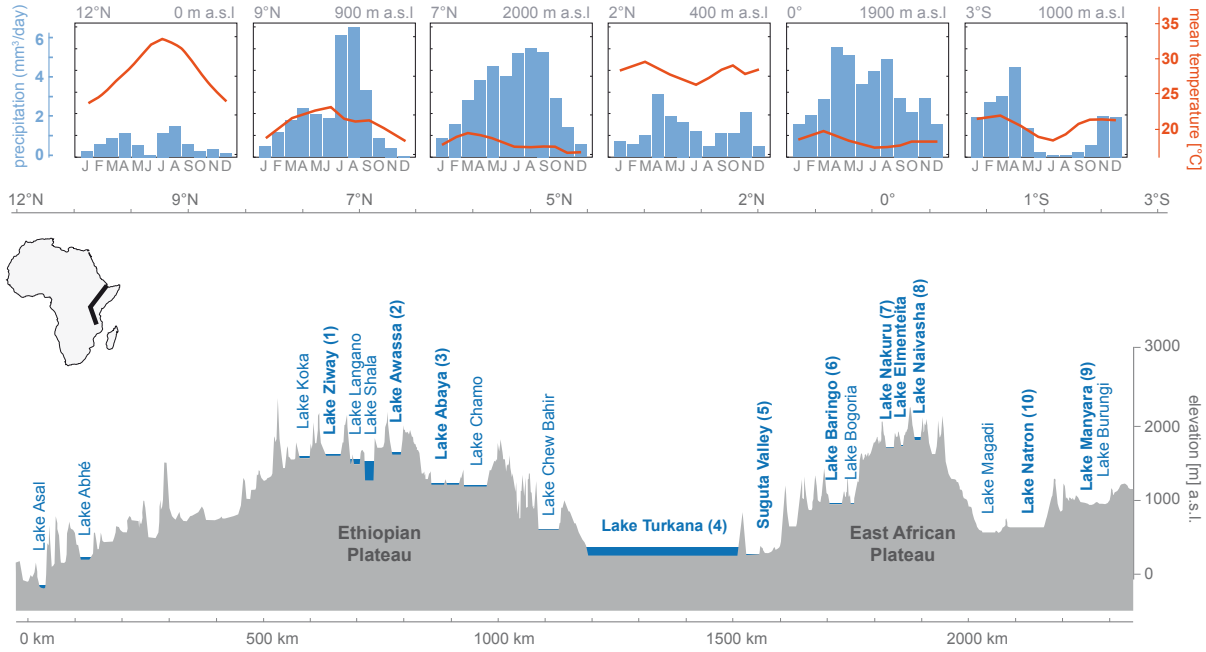

Figure 5.1 Location of lake basins and regional climate of East Africa. Cross-section of the eastern branch of the East African Rift System (EARS) showing the location of lake basins in relation to the geographical distribution of rainfall regimes across East Africa. Present lake depths of most of the lakes are less than 8 m. Numbered (bold) lake basins (1-10) refer to studied sites in this study. Lake Tana (not displayed) is not within the EARS, but also on the Ethiopian Plateau westwards at the same elevation as Lake Ziway. Insets - show monthly mean temperature-rainfall regimes (means are from 1961-1990 data) along the transect provided by http://iridl.ldeo.columbia.edu/maproom/ (March 2011).

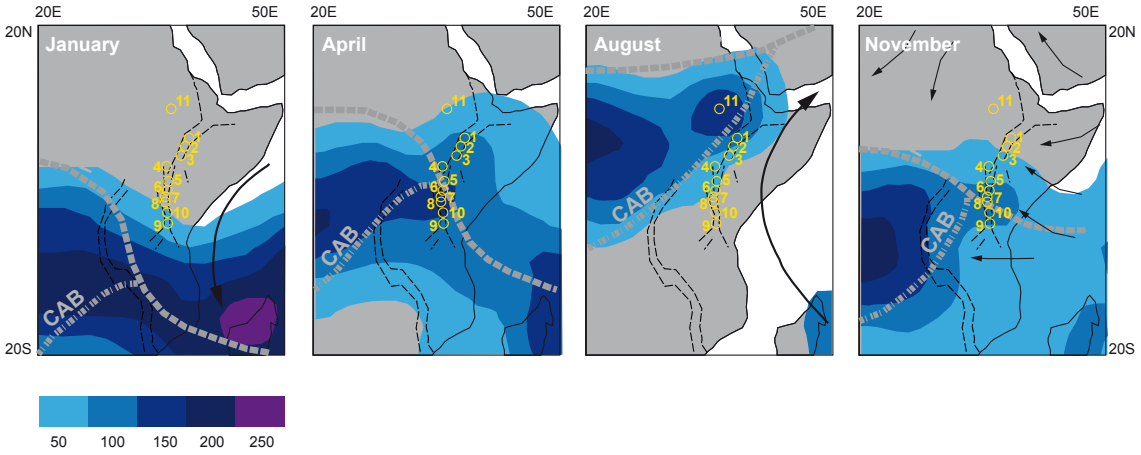

Figure 5.2 Synoptic climatology of tropical East Africa for four representative months of the seasons discussed in this study. The blue shaded area (contours at 50 mm intervals) corresponds to the approximate location of the Intertropical Convergence Zone (ITCZ) and associated rain belts across the studied region. The distribution is based on gauge data over land, and satellite estimates over sea. Dotted grey lines show the mean position of the Congo Air Boundary (CAB) and ITCZ. Black dashed line outlines the East African Rift System and yellow numbered dots the studied lake basins. 1-Ziway, 2-Awassa, 3-Abaya, 4-Turkana, 5-Suguta, 6-Baringo, 7-Nakuru, 8-Naivasha, 9-Manyara, 10-Natron, 11-Tana. Rainfall distribution was provided by: http://iridl.ldeo.columbia.edu/maproom/.Regional/.Africa/.Climatologies/Precip_Loop.html (March 2011).

Additional precipitation on equatorial and northern East Africa occurs when the northern most position of the ITCZ in July/August allows the southwestern humid Congo air stream, with recycled eastern Atlantic moisture brought from the Congo basin through the West-African

monsoon, to reach parts of East Africa (Fig. 5.2; Nicholson 1996, Camberlin 1997; Okoola, 1999). This unstable flow from the Atlantic converges with drier air from the Indian Ocean along a northeast-southwest-trending convergence zone known as the Congo Air Boundary (CAB). The CAB is considered to bring during times of a strong Indian summer monsoon (ISM) wet spells in the JAS months to East Africa (Camberlin, 1997; Okoola, 1999). Camberlin (1997) showed that an anomalous deep low over western India enhances the east-west pressure gradient between Africa and India, which results in enhanced westerly winds from the Congo basin that cause the shift of the CAB further eastwards. Thus, the CAB is considered to play a major role in interannual variability (Camberlin and Philippon, 2002).

5.2.2 Topography

The East African rift System is a prominent feature in East Africa extending for several thousands of kilometres. The eastern arm of the rift aligns NS with topography ranging from -155 m in the Danakil depression in Ethiopia to over 5000 m asl. This rift expression has two main domed ares which we refer to as plateaus in this study: the Ethiopian plateau and the Kenyan plateau, separated by the Turkana-Omo depression. Along the rift there are numerous volcanic centres and high escarpments associated with it. Mount Kenya (5200), and Kilimanjaro (5964) and Elgon (4321) occur on the vicinity of the EAP. The tectonic evolution in the rift has led to segmentation of the rift basins into various sizes. Creating a highly rugged terrain (Chorowicz, 2005). The highlands are thought to block the relatively moist unstable westerly flow of the Congo from reaching the coastal areas (Nicholson, 1996). Most great lakes in Eastern Africa are located in the rift valley bounded by roughly NS striking faults. The basins are bordered on the two sides by high relief comprising almost continuos parallel mountain lines and scarps and sometimes called volcanic massifs. The catchments within the rifts are generally defined with boundaries in the escarpment and open lakes in the rift floor of various sizes. The catchment characteristics and location map are shown in table 5.1 and figures 5.1,5.3

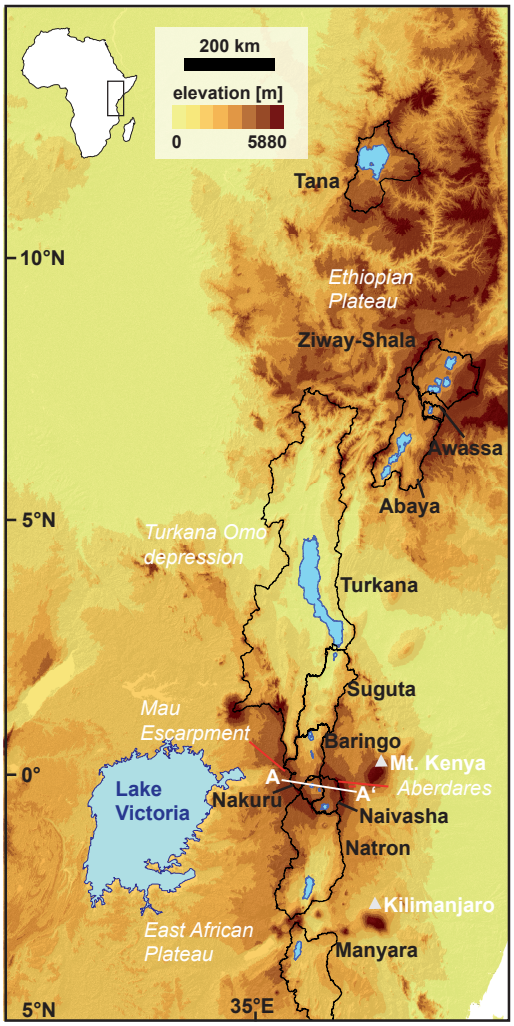

Figure 5.3 Topography and location map of catchments within the East African Plateau and the Ethiopian Plateau. The moisture transport along the cross section A-A' is described in figure 5.8

Table 5.1 Lake catchment characteristics.

Lake Basin name	Lake basins included	Latitude [deg.]	Longitude [deg.]	Basin Floor [m asl.]	Basin Area [km²]
Tana	Tana	11°59'59N	37°17'53E	1785	16,500
Ziway	Ziway, Shala, Abiyata, Langano	07°58'48N	38°49'44E	1558	14,600
Awassa	Awassa	07°01'57N	38°25'50E	1680	1,455
Abaya	Abaya, Chamo	06°24'42N	37°52'38E	1268	33,060
Turkana	Turkana	03°39'53N	36°03'35E	375	130,860
Suguta	Suguta	02°13'41N	36°33'23E	275	12,800
Baringo	Baringo, Bogoria	00°38'03N	36°03'44E	997	6,200
Nakuru	Nakuru, Elmenteita	00°22'15S	36°05'23E	1770	2,390
Naivasha	Naivasha	00°46'29S	36°20'54E	1885	3,200
Natron	Natron, Magadi	02°19'50S	36°01'44E	600	184,000
Manyara	Manyara	03°37'25S	35°48'31E	960	23,207

5.3 Materials and Methods

Rainfall measurements by conventional rain gauges provide relatively accurate estimates at a few points of a region. Interpolating the available rain-gauge data to the remaining area of interest can approximate the actual rain-field. In places with relatively low gauge density, such interpolated rain-fields will exhibit a great deal of uncertainty. This is especially true for tropical regions where most rainfall has a convective origin with high spatial variability at the daily level. Estimates of rainfall by remote sensing can be very useful in regions such as East Africa, where rain-gauge density is very low and rainfall highly variable.

The data utilized in this study are rainfall estimates (RFE) acquired from the National Atmospheric and Oceanic Administration (NOAA) repository for the period 1996-2009 with a spatial grid resolution of 8 km. This high-resolution data in temporal and spatial domains provide good opportunity to study the rainfall characteristics especially in the humid tropics. The data before 2001- RFE 1.0 were used as algorithm that interpolated Meteosat and Global Telecommunication System GTS data and included warm cloud information for the dekadal estimates. From 2001, RFE 2.0 is an improvement from RFE 1.0. The method uses cloud top temperature and station rainfall data that formed the basis of RFE 1.0. Meteosat 7 geostationary satellite infrared data is acquired in 30-minute intervals, and areas depicting cloud top temperatures of less than 235K are used to estimate convective rainfall. WMO Global Telecommunication System (GTS) data taken from ~1000 stations provide accurate rainfall totals, and are assumed to be the true rainfall near each station. Two new satellite rainfall estimation instruments are incorporated into RFE 2.0, namely, the Special Sensor Microwave/Imager (SSM/I) on board Defense Meteorological Satellite Program satellites, and the Advanced Microwave Sounding Unit (AMSU) on board NOAA satellites. All satellite data is first combined using a maximum likelihood estimation method, and then GTS station data is used to remove bias (FEWS NET). The data output used is the total dekadal (10 day) data. For details on the method please refer to http://www.cpc.ncep.noaa.gov/products/fews/rfe.shtml.

We selected eleven regions in East Africa for this study because the rainfall distribution in this area exhibits high seasonal variability. The eleven regions are catchment boundary extent of lakes along the two plateaus of the EARS with highly variable topography from N-S. The lake basins selected are; Ziway-Shalla, Awassa, Tana, and Abaya in the Ethiopian Plateau, Turkana, Suguta, Baringo, Nakuru-Elmenteita, Naivasha, Magadi-Natron and Manyara in East African Plateau these basins are analysed as watershed averages (Fig. 5.3). To understand the seasonal variability of precipitation characteristics, the dekadal estimates are combined for four seasons designated as December-January-February (DJF) March-April-May (MAM), July-August-September (JAS), and October-November (ON). DJF is considered as months showing the variability related with the maximum southward location of the ITCZ, MAM and ON the transitional times of the ITCZ over the equator, where ON is regarded to show highest variability during IOD/ENSO events, and JAS are considered to be the months of maximum northward position of the ITCZ and CAB's most eastern position causing high variable rainfall rather associated with ISM strength and largely independent from ENSO or IOD. We used the monthly Nino3.4 index for comparing ENSO events (http://

www.cpc.ncep.noaa.gov/data/indices/nino34.mth.ascii.txt) and the monthly dipole mode index (DMI) dataset from HadISST for summarizing IOD events (http://www.jamstec.go.jp/frsgc/research/d1/iod/). Solar flux data are based on the solar flux radio data set F10.7 (ftp://ftp.ngdc.noaa.gov/STP/SOLAR_DATA/SOLAR_RADIO/FLUX/Penticton_Adjusted/monthly/MONTHPLT.ADJ).

5.4 Results and Discussion

5.4.1 IOD/ENSO, QBO, ISM & the 11-year solar cycle 1996-2010

Figure 5.4 and 5.5 display the various mesoscale influencing mechanisms to East African Rainfall variability. For an easier identification of IOD and ENSO events in following figures, we categorized them by their parallel or single occurrence: We defined a 'no anomaly' stage (A), when SST variations in the Indian and/or Pacific Oceans ranged between -0.5 and 0.5°C. A 'balanced' mode (B) was reached when the opposite phases of IOD and ENSO co-occur (i.e. a positive ENSO with a negative IOD and vice versa). We also selected pure positive and negative IOD and ENSO (C-F) events as well as events where the same phases of IOD and ENSO (G-H) occurred contemporaneously. Stronger June-September ISM occurred 1996, 1998, 2005-2007 according to the ISMIDX with no obvious relation to the solar flux and occurrence of IOD and ENSO events.

The direct comparison of occurring IOD and ENSO events between 1996-2010 shows a complex pattern of combined and single events with no obvious relationship to each other. Different anomalies seem to develop within one year and show some indications of dependence to variations in the solar flux. Most of the events are suppressed during higher solar flux between 2000-2002 with the longest event occurring from July 2001 to March 2002, where ENSO is in a neutral state and IOD is largely suppressed. The broad suppression of oscillator events during higher solar flux indicates a kind of dependency. This hypothesis appears to be supported by the build up of very large IOD and/or ENSO events during times lower solar flux, especially along the transition zones between low and high solar activity. The explanation for this observation needs to be supported by longer data sets and would go beyond the scope of this paper. However, the possibility of enhanced solar flux to the suppression of ENSO or IOD events are regarded to be possible (Neff et al., 2001; Wang Y.I. et al., 2005; Kodera et al., 2007; Junginger and Trauth, subm.).

A

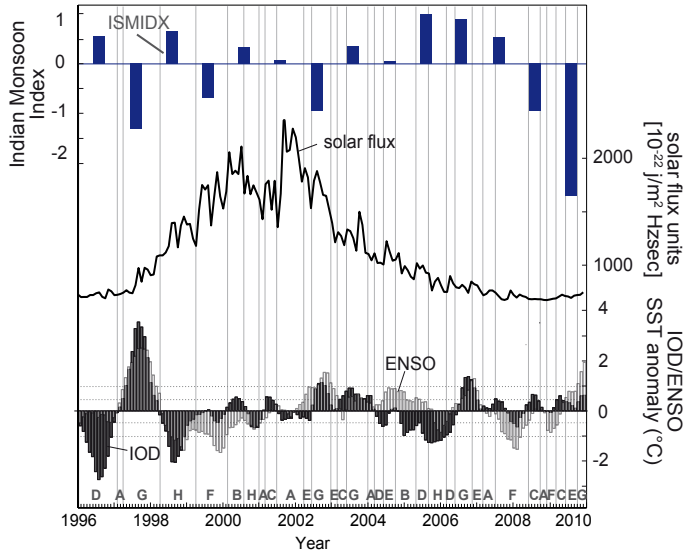

B

Category	Occurrence months	Strength [SST anomaly °C]
	Jan-Feb 1997	-0.3 IOD; -0.3 ENSO
(A) no anomaly	Jan-Feb 2001	-0.3 IOD/ENSO
	Jul 2001 - Mar 2002	-0.3 IOD
	Mar-Jun 2007	+0.1 IOD;-0.2 ENSO
	Oct-Nov 2008	0 IOD/ENSO
(B) balanced	Mar-Jul 2000	+0.7 IOD; -0.7 ENSO
	Oct 2004-Apr 2005	+0.7 ENSO; - 0.8 IOD
	Mar-Jun 2001	+0.6 IOD
(C) pos. IOD	Mar-May 2003	+0.9 IOD
	Jan-Feb 2004	+0.1 ENSO; 0.5 IOD
	Apr-Jun 2005	+0.6 IOD
	Mar-Jun 2007	+0.1 IOD;-0.2 ENSO
	Jun-Sep 2008	+0.6 IOD
	Mar-May 2009	+0.7 IOD
	Mar-Dec 1996	-3 IOD; -0.5 ENSO
(D) neg. IOD	Mar-May 2004	-0.6 IOD; +0.2 ENSO
	May-Aug 2005	-1.2 IOD; 0.2 ENSO
	Mar-May 2006	-0.6 IOD, +0.2 ENSO
	Jun-Sep 2004	+1 ENSO
(E) pos. ENSO	Jan-Feb 2003	+0.8 ENSO
	Apr-May 2002	+0.8 ENSO; -0.2 IOD
	Dec 2006 - Feb 2007	+0.4 IOD;+0.9 ENSO
	Jun-Sep 2009	+0.9 ENSO; -0.3 IOD
	Mar 1999 -Feb 2000	-1.5 ENSO; -0.5 IOD
(F) neg. ENSO	Jul 2007 - May 2008	-1.5 ENSO; -0.5 IOD
	Dec 2008 - Feb 2009	-0.9 ENSO; 0 IOD
	Mar 1997 - May 1998	+3.5 IOD, +2.7 ENSO
(G) pos. IOD/ENSO	Jun-Dec 2002	+1 IOD/ENSO
	Jun-Dec 2003	+1 IOD, +0.7 ENSO
	Jun-Nov 2006	+1.2 IOD/ENSO
	Oct-Dec 2009	+0.7 IOD; +2 ENSO
	Apr 1998 - Feb 1999	-2 IOD, -1.2 ENSO
(H) neg. IOD/ENSO	Aug-Dec 2000	-0.8 IOD/ENSO
	Sep 2005 - Feb 2006	-1.2 IOD, -1 ENSO

Figure 5.4 (A) Distribution of ENSO and IOD events during one 11-year solar cycle between 1996-2009 in comparison to the Indian Monsoon strength. Shaded areas in monsoon indices indicate above average strength. Dotted line shows ±0.4 restriction for no-anomaly regarded events. Blue line 2001-2002 is regarded to show the normal stage with no IOD and ENSO anomaly is existing. (B) Categorisation of ENSO and IOD events used for discussion of Figure 5.6. Letters in Figure 5.3A refer to events described in Figure 5.4B. Database: ENSO: monthly Nino.3.4 (http://www.cpc.ncep.noaa.gov/data/indices/nino34.mth.ascii.txt); IOD: monthly dipole mode index (DMI) from HadISST dataset (http://www.jamstec.go.jp/frsgc/research/d1/iod/). Solar flux: solar flux radio data set F10.7 (ftp://ftp.ngdc.noaa.gov/STP/SOLAR_DATA/SOLAR_RADIO/FLUX/Penticton_Adjusted/monthly/MONTHPLT.ADJ). Indian Monsoon Indexes from http://iprc.soest.hawaii.edu/users/ykaji/monsoon/seasonal-monidx; ISMIDX June-September (Wang and Fan, 1999; Wang et al., 2001).

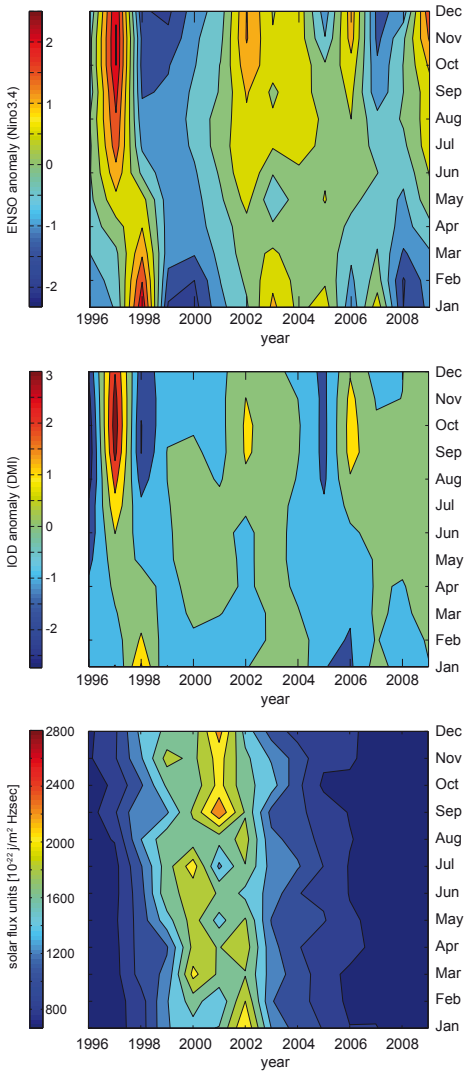

Figure 5.5 Monthly overview of the development of (A) ENSO and (B) IOD events compared to solar irradiation changes (C) between 1996-2009. Data sources in Figure 5.3.

A ‘balanced’ seasonal appearance of pos. ENSO and neg. IOD or vice versa, as it was the case in March-July 2000 and October 2004 to April 2005 is a very important observation as it shows indications of IOD independence from ENSO. Another ‘balanced’ event, which has been mentioned in the literature as evidence for the IOD to operate independently (e.g. Abram et al., 2008), occurred in the boreal summer months in 2007. However, we do not relate this particular event to our category, since it was within the boundaries of no impact.

5.4.2 Seasonal lake basin precipitation

This study aims to provide a detailed picture of the causes of present local precipitation variations within the EARS under consideration of the complex topography and the existing prevailing atmospheric conditions in order to help paleo-climate proxy studies to better interpret discovered trends and fluctuations. The following discussion is supported by Figures 5.6, 5.7, 5.8 and S1. Information about sizes of lakes, catchment and geographical position are summarized in Table 5.1.

5.4.2 1 West-Ethiopian Plateau – Lake Tana

Catchment features | Lake Tana is located at the northern most position (11°N) of the studied area outside the general eastern branch of the East African Rift System (EARS) on the western side of the EP (Fig. 5.1, 5.3). The elevation of lake Tana is similar to the highest lakes in central Ethiopia at 1785 m asl and its catchment is with 16,500 km^2 only slightly larger than the one from Ziway or Abaya east of it also showing a rather circular shape.

Seasonal observations Tana

Tana in MAM from 1996-2009 received usually around 50 mm/MAM rainfall in its catchment, with three exceptions in 1996, 1997 and 1999 (Fig. 5.6). During the developing strong positive IOD/ENSO event (+1°C SST anomaly) in 1997 (Fig. 5.4) anomalous high rainfall (+150 mm/MAM) received this area. Interestingly, rainfall was also enhanced during the developing negative IOD in 1996 (-1°C SST anomaly) and the long lasting large La Niña (-1°C SST anomaly) event in 1999. Comparatively events occurred in MAM 1998 and 2002 (Fig. 5.4) with both only showing no impact to MAM rainfalls. A clear impact of IOD and/or ENSO events can therefore not be the explanation for anomalous high rainfall in 1997 and 1999.

Precipitation during JAS in the Tana basin is highest and fluctuates between 300-400 mm/JAS with one exception of anomalous high rainfall (600 mm/JAS) in 1996 during peak SST anomalies (-2.9°C) of a negative IOD event. Fluctuations in rainfall during this season do not correlate with SST anomalies and rather indicate amplitude alterations of a biennial precipitation pattern.

Mean precipitation in ON fluctuates in Tana around 50±20 mm/ON within an interval of 3 years with no preferred direction during and IOD or ENSO event. This pattern is typical of a triennial pattern of rainfall Such a triennial pattern was reported to affect rainfall in South Africa (Mason and Tyson, 1992; Kane, 2009). Further investigations are needed to understand this phenomenon on the western Ethiopian plateau and how distinct it is from the other Ethiopian basins in the rift. The absence of such a clear pattern in other basins might only occur in basins that are not influenced by the ITCZ during this season During DJF, precipitation in Tana basin is not apparent in the entire study period. According to Figure 5.7 and S1, no rainfall centers developed north of 10° latitude.

Discussion & conclusion Tana | Annual rainfall anomalies in Tana are generally not directly related to SST anomalies causing ENSO and IOD events during the studied time period. The only larger fluctuations in MAM occurred in 1997 and 1999 might therefore be related to either a broadening or faster movement of the ITCZ northwards or an early penetration of the CAB eastwards. This situation would be achieved when the onset of the ISM was anomalous early in the year the mechanisms that trigger and maintain the ITCZ over continental Africa are still unclear (Suzuki, 2011). Internal precipitation variations in JAS are not related to the strength of the ISM. Fluctuations must be related to internal intensity variability of CAB (Jury, 2010) most likely associated with Atlantic SST anomalies or recycling dynamics over the Congo basin. What is also significant is that the floods recorded in Ethiopia between 2006 – 2006 (Jury, 2010) seem to have been recorded in the other lakes basins and not in Tana. In general,

mechanisms that influence JAS and MAM moisture availability are the most important in driving Tana's basin precipitation.

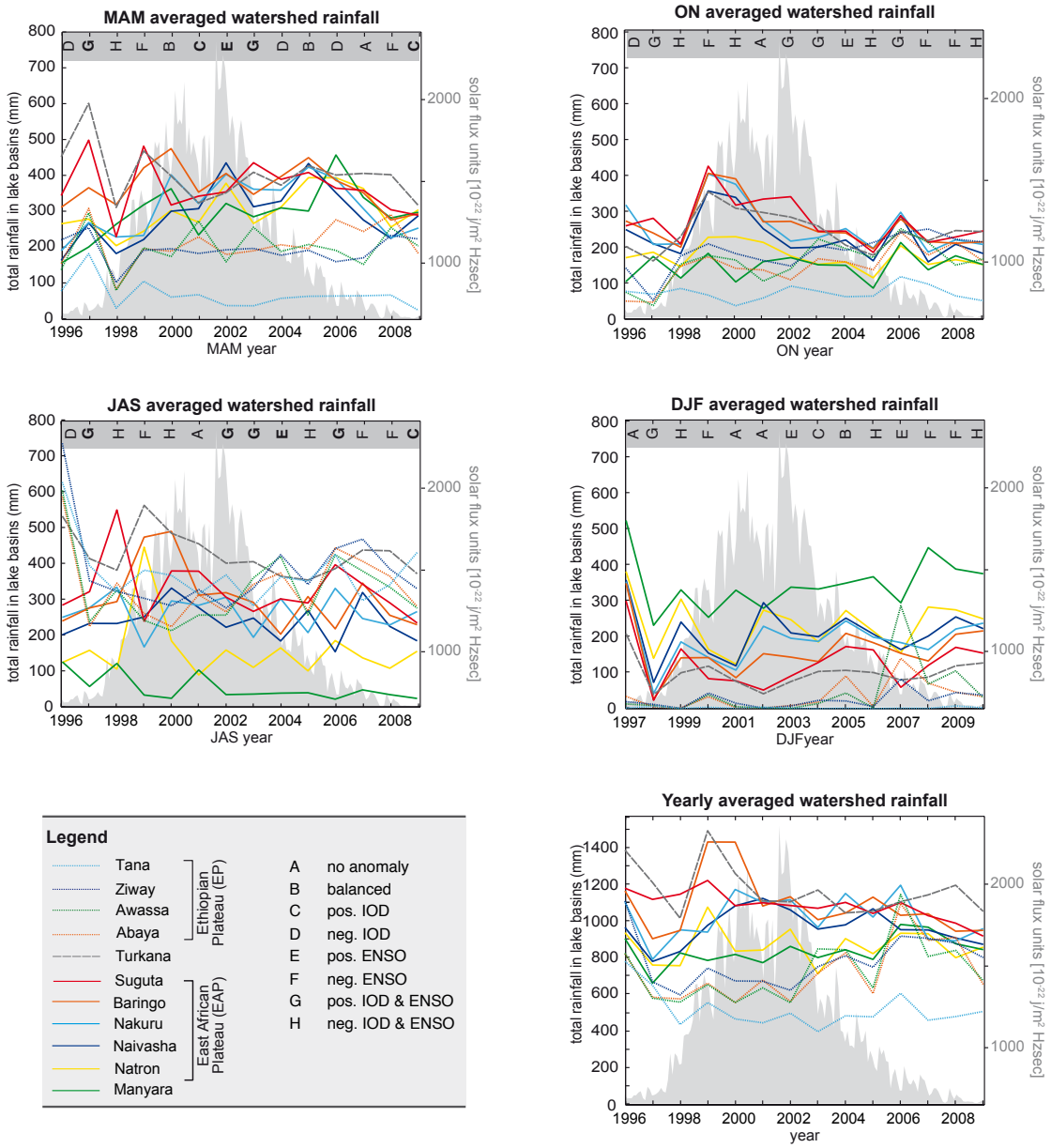

Figure 5.6 Seasonal averaged watershed mean and total rainfall for the 11 watersheds of East African lake basins within one 11-year solar cycle (grey shaded area, 1996-2009) and their relationship to ENSO and/or IOD events (Letters on upper x-axis). MAM - March-April-May, JAS - July-August-September, ON - October-November, DJF - December-January-February. Bold letters indicate positive IOD and/or ENSO events.

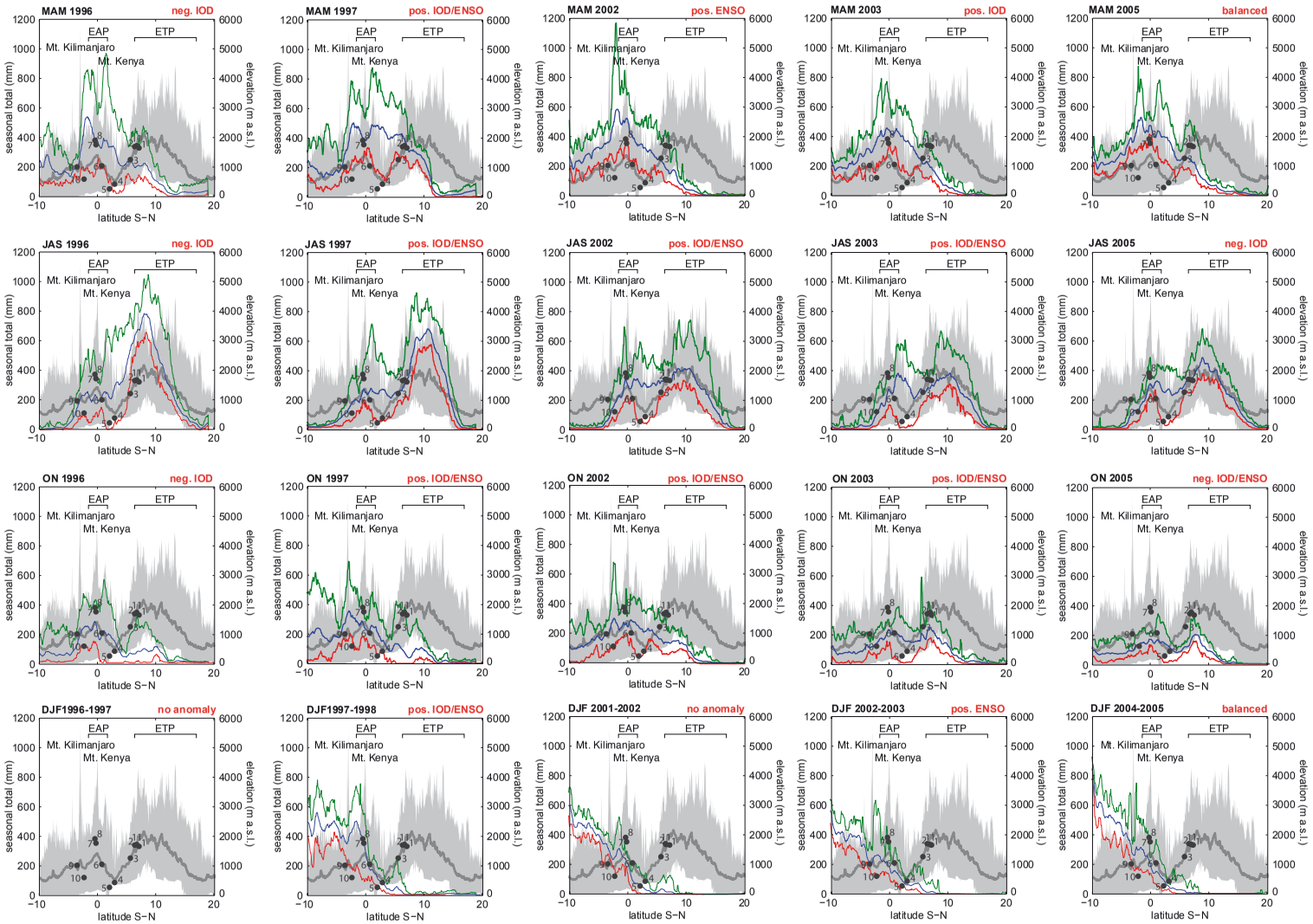

Figure 5.7 Topographic and precipitation swath profiles along the East African Rift System between 35-40 ^{0}E. Topography (grey) is derived from SRTM data, mean topography is shown by the bold grey line, whilst the grey band represents the minimum and maximum elevations. Precipitation, for the four years discussed in the text is shown by green (maximum), blue (mean) and red (minimum) lines. the relative location of the lake basins are marked as 1-Ziway, 2-Awassa, 3-Abaya, 4-Turkana, 5-Suguta, 6-Baringo, 7-Nakuru, 8-Naivasha, 9-Manyara, 10-Natron and 11-Tana. Note the shift in locality and distribution of peak precipitation for each season.

5.4.2.2 Central-Ethiopian Plateau – Rift lakes

Catchment features | The investigated lake basins Ziway, Awassa and Abaya are located very close to each other in the central sector of the Ethiopian Rift, of whom the highest elevated basins are Ziway and Awassa (1558 and 1680 m asl, respectively; (Figs. 5.1 and 5.3). The catchments of Ziway and Abaya are of similar size (14600 and 14487 km^2, respectively) whereas Awassa's basin area is very small with 1455 km^2. The catchments of Ziway and Awassa are broadly circular shape, with Ziway's extending over the western and eastern rift shoulder. and Awassa extends more to the eastern Rift escarpment (Fig. 5.3 catchment). Abaya's catchment is elongated and covers both escarpments of the the Ethiopian highlands from ca. 2000 m asl down to ca. 1000 m asl between 7.5°N to 6°N (Fig. 5.1, 5.3).

Seasonal observations

The central EP lake basins in MAM follow generally in this season the same trends similar to the Tana basin, only with a higher amount of precipitation. Abaya and Ziway show stable precipitation amounts of ca. 200 mm/MAM between 1999-2005. Interestingly, within the same period, Awassa basin, located in between Ziway and Abaya (Fig. 5.3) shows two peaks of 100 mm more rainfall in 2001 and 2003 than in the other basins during the two minor pure positive IOD events (Fig. 5.4, 5.6). From 2005-2009 precipitation remains similar in Ziway, with Awassa following, but Abaya at the southern located study area now receives ca. 100 mm more rainfall in 2006-2008 during negative oscillator events. During the developing positive coupled IOD/ENSO event in 1997 rainfall was enhanced by 100 mm in all three basins and largely suppressed by 100 mm in 1998 during the developing large negative coupled IOD/ENSO. La Niña (1999, 2008) causes higher precipitation in all basins. Homogeneous stable rainfall conditions produce the occurrence of opposite SST anomalies in the Pacific and Indian Ocean as in 2000, 2002, 2004, and 2005.

JAS is known as the Kiremt main rainy season in central Ethiopia and brought highly variable precipitation to the study area that can be summarized into 3 time periods, namely 1996, 1997-2003, and 2004-2009. In 1996 anomalous high precipitation (600-700 mm) fell during the peak times of the largest pure negative IOD event in the past 14 years. 1997-2003, rainfall and its variations were largely suppressed ranging from 220-350 mm/JAS. Maximum precipitation in 1998 and 2001 occurred here during both a large coupled neg. IOD/ENSO event and only very small negative SST anomaly in the Indian Ocean. 1997 and 2000, when the rainfall was lowest, coincide with coupled or pure positive anomalies in the Indian and Pacific Oceans. Average higher precipitation and higher amplitudes (250-450 mm) describe the time slice 2004-2009. 2004 and 2006 were the years with highest rainfalls, coinciding with pure and coupled positive SST anomalies in the Indian and Pacific Ocean. 2005 and 2009 were the driest months that occurred during both a negative IOD and pos. ENSO, respectively. Generally, Ziway receives the highest amounts of rainfall followed with almost no differences in Abaya and Awassa, which is interesting since Awassa catchment is by far the smallest (Fig. 5.2, Tab. 5.1). The ISM strength largely is positively correlated to internal fluctuations in rainfall, with exceptions in 2000, 2005, and 2007.

ON rainfall in the rift basins of the EP is homogeneous distributed (mean 200 mm/ON) with very low variability, except of a pronounced drought in 1997. Internal variability only

shows minor correlation to positive ENSO or IOD events. Positive events produced drier conditions in 1997-2002, whereas a positive correlation occurred from 2003-2009. No similar trends appear in the Tana basin.
Rainfall in DJF is very low 1997-2004 (0-50 mm/ON) and highly variable from 2005-2009 (0-300 mm/ON), which not follows SST anomalies in the Pacific or Indian Ocean. Interestingly, the highest rainfall and variability experienced Awassa basin that is the smallest basin in the studied area and located in between Ziway and Abaya (Fig. 5.3). No similarity with trends in the Tana basin are observed.

5.4.2.3 Central East African Plateau – Baringo, Nakuru, Naivasha

Catchment features | The basins are located on the East African plateau in close proximity to each other but with significant differences in their catchments (Fig. 5.3). Baringo is the largest catchment (6200 km^2) while Naivasha (3200 km^2) and Nakuru (2390 km^2) have smaller catchments. The catchments of Nakuru and Naivasha are located almost along the same latitude and receive water from the western and eastern rift margins, respectively. In contrast, Baringo basin can receive from both sides of the rift margin precipitation similar to Abaya from the central EAP highlands ca. 2000 m down to 1000 m asl from 0.5°S to 1.5°N (Fig. 5.1, 5.2

Seasonal observations

MAM rainfalls in the central EAP basins show similar trends over the entire study period but the amplitudes of variability are quite different (Fig. 5.6). Whereas Baringo received high precipitation (400-500 mm/MAM) before 2001, Nakuru and Naivasha generally received lower amounts (200-300 mm/MAM). After 2001, precipitation amounts among the basins are similar (350-400 mm/MAM), with amplitudes in interannual variations are shown in the Naivasha catchment, especially in 2002 and 2005. We observe a general decline in precipitation to 250 mm/MAM after 2005.

MAM precipitation are highest in the western parts of the EAP. This conclusion comes through the direct comparison of rainfall amounts in the lake basins of Nakuru and Naivasha that have a similar size and drain only the western and eastern part of the rift, respectively. Baringo, whose catchments covers both sides of the rift supports this hypothesis since its precipitation amounts somewhat follow the one of Nakuru than Naivasha. The amounts are slightly enhanced in Baringo though, because of larger catchment size. Highest amplitudes in the Naivasha basin such as in 2002 and 2005 might explain a protrusion of additional moisture sources towards the eastern escarpments. These peak precipitation are restricted to the central EAP basins and Natron only, which receives most of its moisture also in the area of the central EAP. This restriction to the EAP basins is nicely shown in a swath profile in Figure 5.7, where we see a very narrow band of high precipitation around the equator in 2002 that correlates with the position of the ITCZ at this time of year. The location of the high rainfall peak appears between the high mountains Kilimanjaro and Kenya, which seem to induce an orographic effect by capturing the moisture. The rainfall during this season in centred over the central EAP basins and related catchments, giving them a higher peak rainfall. We don't know yet exactly what the mechanisms behind these variabilities are, but they must be related to the changes in the ITCZ dynamics. An explanation of possible circulation variables to the

observed east-west rainfall variabilities is under investigation and will completed before journal submission of the manuscript.

During the JAS season we see that Naivasha and Baringo basins are showing the same trend with a clear sign of biennial precipitation between 2001-2008 (See Figure 5.6), this biennial precipitation pattern is absent pre 2001. In the Baringo basin, the mean precipitation is between 200- 300 mm however, a departure from this trend is seen between 1999 and 2000 where precipitation doubled to 500 mm. Between 2002 and 2008, variations in Nakuru catchment are out of phase with the adjacent Baringo and Naivasha catchments. Which also coincides with the biennial precipitation pattern of Baringo and Naivasha. This out of phase pattern on Nakuru is however in phase with the trends we see in the northern EP basins after 2002. These differences could be attributed to the local effects of imposed by the topographic architecture of this area. Its bound on the west by the lower elevated Mau Escarpment (3,200 m asl) and higher elevated Aberdares escarpment (> 4000 m asl) in the East of these catchments. We can only speculate that this is connected to the local topography and distribution of air mass from lake Victoria, it is known that lake Victoria which is to the west of these basins has the highest convective activity northward and has high evaporation in the months of July and August (Nicholson and Yin, 2004). Our interpretation is that, the low level moisture laden winds from the western impinging air mass are partially blocked by the 3,200 m. asl Mau escarpment and rain out on the Nakuru catchment on the Mau, the rest move across the rift to east and are forced to ascend above the higher Aberdares mountains (4000 m asl) which causes higher rainfall on the Eastern escarpment which is the watershed of Naivasha. Additionally easterlies converge with the westerlies here hence developing rain clouds. The descending air absorbs moisture again in the valley from the moisture lifted from the lake surface by convection. The presence of complex topography most likely plays a major role in distributing the moisture of both local surface winds and high. This is a very interesting observation, probably consistent with the hydrological difference between the Naivasha and Nakuru basins mainly because of the moisture sources (Bergner, 2009; Dühnforth 2006). Additionally, the biennial pattern of precipitation seen here with the catchments alternating between strong and weak years might be related to the QBO's easterly and westerly phases. Naivasha seems to be a good example however Baringo seems to be overprinted by some other interacting mechanism as well. The ISM is known to have a strong influence during this season on the precipitation of East Africa, it is probable that the trends we see after 2002 are related to the strong ISM that persisted then (Figure 5.4). Additionally the QBO is thought to control the variability of the ISM. The ISM is stronger during the westerly phase and weaker during the easterly. The connectivity of JAS rainfall and QBO and ISM is an interesting topic for discussion with a longer time series.

During the ON season, all the EAP basins have the same trends and the mean precipitation for this season is about 200 mm with the exception in 1999-2000. We expect high rainfall during the positive phase ENSO and IOD and droughts during the negative phases especially in 1996 and 1998 respectively. This signal is not as high as in the MAM season. The absence of peak precipitation in 1997 in the watershed means in surprising. However, looking at the spatial map of the rainfall distribution for this season (Figure S1) we see the two regions of high rainfall are located on the coast of Somalia and further off shore on the Indian ocean

and the second is located around the Victoria Catchment. Its seems here that though the region received high precipitation, its distribution along the rift was lower than the non rift locations. The distribution of rain in the La Nina 1998 and 1999 is quite different as visible in figure S1. What is interesting to point out for this season is the difference in distribution of rainfall during a negative IOD e.g. in 1999 where a small anomaly of the IOD is existing (0.5) compared to a strong La Nina is very varied which leads to the different catchment rainfall variabilities. Nevertheless, although ENSO is often to blame for rainfall anomalies in the East African region, other studies have presented contradictory results indicating the independence of ENSO and East African precipitation (e.g. Webster et al., 1999).

In 2006 all the basins receive almost comparable precipitation which is during a coupled positive IOD/ENSO. We see that only large ENSO IOD events (greater than 1) seem to affect the EAP. Previous studies have cited the high variability that exists in this season, sometimes classified with as the September October November (SON). The spatial maps in figure S1 show this too. However, what is new is the location of the region of intense rainfall depending on the strength of the SST overprinting the ITCZs influence better seen on the spatial map.

In the DJF season, we see that all the EAP basins are in phase and all of them have the same trends, Naivasha basin is the one that receives high rainfall than all of them of about 200± 50 mm. The ENSO signal not seen in the ON season is however recorded here in 1997 for example with about 350 mm while the 1998 drought results in about 50 mm. We see a somewhat triennial precipitation pattern where high rainfall is followed by 2 years of reducing rainfall

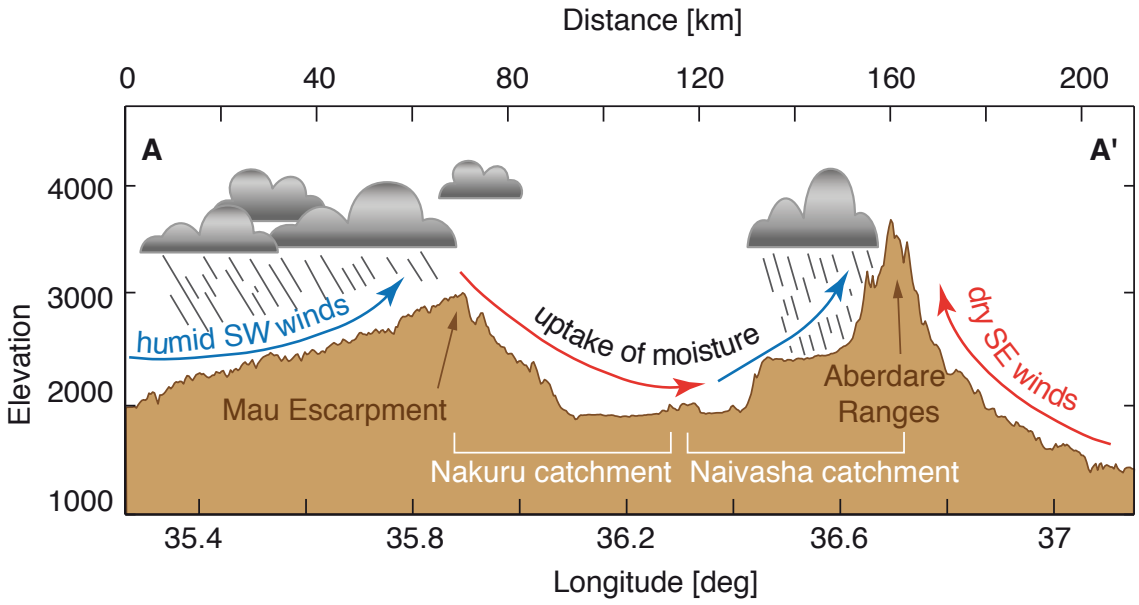

Figure 5.8 Schematic diagram of moisture transport across the East African Plateau. the cross section is from Mau Escarpment to the Aberdares over lakes Nakuru and Naivasha This explanation is tied with the JAS season when evaporation over lake Victoria is highest. Lake victoria surface evaporation values are estimated by Nicholson and Yin, 2004.

5.4.2.4 Southern East African Plateau Lakes - Natron and Manyara

The Natron (2°S, 600 m asl) and Manyara (3°S, 960 m asl) catchments are the southern most basins of the study area. They occupy areas of lowest elevation at the terminal end of the Eastern arm of the EARS (Fig. 5.1, and 5.3). Both catchments are elongated in their N-S direction, but Natron is the larger with 184,000 km^2 whereas Manyara only covers an area 23,207 km^2. An additionally feature most likely important for rainfall distribution is, that Natron's catchment originates in the northwestern escarpment of the EAP south of the Mau Escarpment (0.5°S) while Manyara's catchment boundaries is marked by the Mbulu Plateau and various volcanoes farther south (5°S) of the terminal lake.

During MAM season the ITCZ location is northwards and causes precipitation along the equator. The mean precipitation in the watersheds ranges between 300±100 mm. Although the two basins are adjacent to each other, significant variability in rainfall exists with respect to the two basins, which are partly in and out of phase with each other. Opposite phases occur in 1998 where Manyara received high precipitation while Natron was low and in 2005 when the opposite situation occurred. Lake Natron exhibits similar variability to the central EAP lake basins in the North with amounts and trends following the one from Naivasha with exceptions in 2001 where better correlations with the Nakuru basins are observed (Fig. 5.6). An example for an event only restricted to the southern lake basins occurred in 2006, when peak precipitation reached 400 mm/MAM, despite the onset of the drying trend in the central EAP basins. Though 2006 MAM was generally dry in EA, figure S1 shows highly irregular distribution of rainfall with a small core SE of lake Victoria.

The northern boundary of Natron catchment is located near Nakuru catchment, however it shows a higher correlation in amplitudes and trends with the Naivasha basin which receives significant precipitation in its Eastern margin, might be attributed to its catchment covering both sides of the rift valley on the highland of the EAP. Although Natron's catchment is largely draining the northwestern escarpment, expected higher precipitation does not occur. This distribution could explain, that additionally to the general amount of moisture delivered by the ITCZ some additional moisture sources could reach the eastern rift shoulder.

An explanation for the 2006 event, where only the basins of Natron and Manyara received anomalous high rainfalls can be attributed to a number of possibilities. For example, circulation pattern over Madagascar are known to cause precipitation highs around the Kilimanjaro region (Chan et al 2008). Moist air masses entering the EARS from the southeast might bring precipitation only to the southern basins. One major role might play the Kilimanjaro as moisture barrier leading low and mid level moisture-laden winds around and therefore control flow directions. This is an interesting hypothesis that can be further investigated by stable isotopes studies.

However, a detailed investigation of possible mechanisms leading to the observed east-west rainfall variabilities and also the in and out of phase relations of these two basins is under consideration and will completed before submitting to the journal. Additionally to the build up of circulation patterns over northern Madagascar, we assume, that since this season's rainfall is principally controlled by the location and strength of the ITCZ, variations in these parameters might drive in or out of phase relation between these two basins. Maybe ENSO/IOD, ISM,

QBO, solar variations might affect the ITCZ strength and precipitation distribution.

5.4.2.5 Lakes in between two plateaus - Lakes Suguta & Turkana

Catchment features | These basins are located in the depression between the two plateau regions of the EAP and EP. The Turkana catchment is with 130,860 km^2 about 10 times greater than Suguta. The catchment of Turkana has a long N-S extension and covers both the EAP and the EP while the watershed of Suguta, which is also elongated, is mainly located on the EAP east of the Turkana catchment (Fig. 5.3). Lake Turkana is the largest lake in the studied regions with an area of about 73,000 km^2 and is known to experience very strong diurnal winds lasting about 9 hours from late evening to mid morning. The pronounced diurnal pattern of winds likely arises from interactions between local thermal circulation patterns and the prevailing trade winds over the region (Ferguson & Harbott, 1982; Johnson and Malala, 2009).

Seasonal observations

In the MAM season we see very good correlation Between the Suguta and Turkana basin rainfall. However high fluctuations of between 250 and 600 mm exist during 1996 – 2000. After 2001 the rainfall trends seem to be exhibit less variability with about 400 mm of rain being received. We see similarity in the rainfall between these two basins, this is surprising due to the apparent difference in size between the two basins. Our explanation relates to the position of the ITCZ around the Equator during this season, where both catchment have their catchment boundaries. This is also confirmed by the similarity in trend to the EAP basins located at the path of the ITCZ at this time. This is also closely correlated to the EP basins.

In the JAS season Turkana and Suguta basins show large variabilities and hardly similar trends and even opposite phase trends in precipitation between 1996-2000 with high amplitudes between 300-550 mm. This picture changes after 2001 where precipitation in Turkana is higher than Suguta and also less variable. Regional precipitation during this season in East Africa is governed by the convergence zones of the ITCZ and the CAB which are also dependent on the strength of the ISM during this season. We see a quasi correlation between the ISM and the Suguta variability, however such mechanisms require longer time series to investigate.

During the ON season, Suguta receives more rainfall than Turkana, during the entire study period apart from 2008 and 2001. Which is somewhat surprising and we still cannot offer an explanation. However all the basins have somewhat similar trends and peak precipitation recorded by all EAP basins is in 1999. Peak rainfall in Baringo in 1999 we cannot explain. These basins react to the same mechanism that cause a high rainfall in 2009. Though from our data the, this seasons exhibits the least variability among basins, it the one that offers surprising results relating to these basins a feature we cannot yet explain.

During the DJF season both Suguta and Turkana exhibit in phase variability in this season only that the Suguta has higher amplitudes between the years. Turkana on the other hand appears stable. The main drivers of meso scale precipitation during this season are the ITCZ and sea surface temperatures Indian and Pacific Oceans. The ITCZ during this season is at its most southerly location. We also see a visible sign of influences of negative phases of

IOD and ENSO correlating to the high rainfall in the Suguta and vice versa for positive phases. For a large lake as Turkana, convective cloud lifting is eminent which are probably swept away by the existing winds related to the convergence if the ITCZ or they are pushed by lower winds southwards based on its lower elevation.

5.5 Preliminary Conclusions

Climate dynamics of the EARS is an interesting topic that is still under investigation in order to distinguish regional from local processes to improve climate proxy interpretations and forecasting. By using rainfall estimates from remotely sensed data between January 1996 and February 2010 we have observed interesting dynamics that we think are behind high precipitation gradients in this topographically complex region. Though, the analysed period is too short to make conclusive statements, some preliminary inferences can be made. A rather complex picture, with considerable spatial variation in watershed precipitation, has been observed along the EARS. The nature of variability among the watersheds can be grouped as those that exhibit low or high amplitudes in intraseasonal variability; those that are in or out of phase with each other and also biennial to triennial precipitation patterns in different basins i.e alternating between strong and weak years. The variability is driven by a) their position relative to the high escarpment and also b) by the shape and length of catchments. For example, the elongated catchments of Natron and Turkana that start around the equator in the high EAP record both regional and localised signals. The strength of variability is governed by the onset, timing and intensities of moisture-laden winds and maritime convergence zones juxtaposed on the topography and inland lakes convection.

The relative height of the catchment bounding escarpments imposes variability in the EAP, whereby In the JAS season we see the difference in basin precipitation between the Nakuru catchment and the Naivasha catchment despite their spatial proximity. Orographic barrier of the Western escarpment causes raining out on the western side out of the Nakuru catchment while the descending air absorbs moisture within the rift floor bypassing the Nakuru, Elmenteita and Naivasha lake bodies and then raining out on hitting the Abedares escarpment which is part of the Naivasha catchment, thereby causing this difference. Precipitation, at low levels on the Easterlies from the Indian Ocean and westerlies from the Atlantic Ocean and Congo in the CAB and recycled air mass the lake Victoria This difference is not observed in the other seasons related with the overpass of the ITCZ. Although we can report evidence for an E-W, N-S rainfall gradient in the past 14 years with some degree of confidence, our hypotheses regarding the pattern's underlying causes are speculative and will be investigated with well designated transects of stable isotope analysis.

The investigations of the October and November rainfall alone leaving out September totals reveals a vulnerability of this 'short rain' season to the onset and intensity of the annual solar cycle. A high intensity in the solar cycle after September results in a homogenized rainfall over all the entire study area due to a broadening of the Hadley cell. Enhanced rainfall during a pos. ENSO/IOD event therefore affects the entire area. Outside highest solar flux, higher amounts of rainfall is restricted to the northern EAP and positive oscillator events only

enhance rainfall amounts along this area, whereas the basins north of it in Ethiopia experience droughts

The DJF season uniquely displays a stratification of decreasing rainfall northwards. The DJF season in the EARS is largely controlled by the width of the Hadley cell, that is controlled by the solar flux. During highest solar flux in addition to positive ENSO/IOD, Ethiopian lake basins, except of Tana, receive very low precipitation whereas the precipitation is slightly reduced in the southern basins Outside higher solar flux, precipitation anomalously high precipitation occurs in the EP watershed such as in 2007 whereas there is no significant anomaly in the EAP basins.

Outlook

We now have identified the topographic effects of each catchment, which is key to explaining regional moisture redistribution and the subsequent east-west and north-south precipitation gradients. The next step would be to test these hypotheses with isotopic studies.

These intraseasonal precipitation differences in the catchments have significant implications on the hydrological budgets and hence limnological environment and catchment ecology. On longer times, these changes lead to migrations and modification of species. It is intriguing to speculate morphological or DNA changes in species to adapt with their changing environment. population and species succession of rotifers of the genus *Brachionus* have been shown in some of the EAP lakes by Epp et al., (2010).

Acknowledgements

I thank Annette Junginger PhD student at the Graduate school GKR1364 potsdam whom we spent many hours trying to understand the mechanisms of intraseasonal rainfall variability in the East African System and preparing this manuscript. I thank DAAD and the GKR 1364-DFG Graduate school for funding. I thank Ephrem Gebremariam for his assistance.

CHAPTER 6

CONCLUSIONS AND GENERAL PERSPECTIVES

Lakes in tectonically-active settings such as the East African Rift System (EARS) typically have a complex hydrogeology related to the tectonically-induced extremities in topography, the occurrence of faults and fissures, enhanced porosity in the volcanoclastic rocks and springs contributing to surface and subsurface water bodies. The interplay of these rift-related influences on lake hydrology often hampers the inference from lake-level records to climate change on all time scales, ranging from intra- to interannual changes with rather immediate implications on humans, to time scales of hundreds or thousands of years providing the boundary conditions for multiple generations of human populations of a larger region.

Understanding the relationship between climate and hydrological fluctuations is critical to our understanding of future impacts of climate change on societies. Lakes as recorders of such environmental change, have usually been described from a purely climate perspective, i.e., the precipitation-evaporation (P-E) balance. In my doctoral project, I have performed comprehensive geomorphometric, hydroclimatic and hydrogeological analyses to better understand the exceptional sensitivity of rift lakes to climate change, referred to here as amplifier lake phenomenon. The results of my work provide a step towards developing robust basin specific transfer functions for better interpreting and calibrating climate proxies within the EARS lakes.

Using Holocene shorelines, the study identifies amplifier lakes that are very sensitive to relatively moderate climate changes and non-amplifier lakes that do not show this behaviour. The amplifier lakes are defined as having a distinct graben-shaped basin morphology and are typically located on the crest of the Ethiopian and Kenya domes (Naivasha, Ziway-Shalla). On a bivariate plot of morphometric vs. hydroclimatic properties, these sensitive lakes are characterized by a hypsometric integral of 0.23-0.29 and an aridity index <1, respectively. The non-amplifier lakes on the other hand have pan-shaped basins and occupy the lower elevation regions between the two East African domes, their hypsometric and climate indices are outside the range of their amplifiers counterparts. Their locations correlate to the inherent tectonic processes and resultant orographic features. The implications of these morphological differences to the aquatic ecology are large shifts of the littoral zone within panshaped basins

while graben shaped basins have slightly diffuse response to lake volume changes.

A specific example of the hydrology of sensitive lakes in the Central Kenya Rift (CKR) raises an awareness of interbasin connectivity that can be used to reduce some of the uncertainty in constructing hydrological balance models for lakes with subsurface water connectivity. The groundwater connection for rift lakes imposes a significant lag which is not used by most studies for various reasons (Vincent et al., 1989; Hastenrath and Kutzbach 1983; Bergner et al., 2004; Dühnforth et al., 2006). Though surficially closed, the dome topography of the CKR creates a high hydraulic gradient from the dome crests in freshwater lake Naivasha basin, and high density of faults in the rift floor from volcano-tectonic activity increase permeability and hydraulic connection of groundwater. This finding cautions against the 'closed lake' systems modelling and reconstruction approach held with regarding most EARS lakes. The high frequency dynamics of groundwater connection is not investigated in this study since longer monitoring and precise water tracing and stable isotopes studies is needed. A topic which I hope to answer in my postdoc project funded by the Volkswagen foundation which seeks to determine vulnerability of the groundwaters within the CKR to climate variability.

At high seasonal and annual timescales, rainfall in East Africa is quite variable. Using 8 km gridded NOAA rainfall satellite data of the last 14 years, analysis of the high-frequency variability in space is possible, minimizing the biases of sparsely-distributed station data in such an area with convective storms. The length of the study prevents definitive conclusions from being drawn, however, it at least includes one complete solar cycle (11 yrs), and three IOD and two ENSO extreme events, and therefore shows typical features of rainfall anomalies in the course of solar influences and sea-surface temperature anomalies. The occurrence of extreme weather conditions during the last 14 years caused transient response on both hydrological and solute budgets of lakes and groundwaters and had dramatic consequences for the infrastructure and agriculture in East Africa.

Though the EARS has receive a lot of attention in paleolimnological research to better understand the climate-environment interaction and make predictions for the future. Most studies have concentrated on the surface hydrology based on sediments and strandlines, whereas studies on lake-subsurface water dynamics have lagged behind, that contributes uncertainties of maximum one third of the hydrological budget, within the CKR as quantified by this study. The differential influence of groundwater and the identified E-W intraseasonal climate gradient existing in this area, generates a recharge lake (fresh) in the Naivasha system and is a mix between recharge and thourough flow lake in the Nakuru system. This has now been demonstrated by a linear decay model. To quantify the geochemical enrichment hypothesis, of transient changes of groundwater chemistry to intraseasonal variability is the subsequent study that will be carried out by employing numerical modelling with physical hydro(geo)logical monitoring data - currently unavailable for these lakes. Funds for the study have already been awarded to me by the Volkswagen Foundation.

Despite these challenges and drawbacks, the insights from this study and the results are encouraging and not only provide measures that are important for limnological lake comparisons within the EARS but also provide significant information for lake management authorities to enable planning. Moreover it has singled out areas I hope to pursue further and

contribute to a better understanding of the hydrological vulnerability of lakes in Africa to climate change .

BIBLIOGRAPHY

Abram NJ, Gagan MK, Cole JE, Hantoro WS Mudelsee M (2008). Recent intensification of tropical climate variability in the Indian Ocean. *Nature Geoscience* 1: 849-853.

Abram NJ, Gagan MK, Liu Z, Hantoro WS, McCulloch MT, Suwargadi BW (2007). Seasonal characteristics of the Indian Ocean Dipole during the Holocene epoch. *Nature* 445:299-302.

Alemayehu T, Ayenew T, Kebede S (2006). Hydrogeochemical and lake level changes in the Ethiopian Rift. *J. Hydrol* 316:290-300.

Alley RB, Marotzke J, Nordhaus WD, Overpeck JT, Peteet DM, Pielke Jr RA, Pierrehumbert RT, Rhines PB, Stocker TF, Talley LD, Wallace JM (2003). Abrupt Climate Change, *Science* 299: 2005-2010

Almendinger JE (1990). Groundwater control of closed-basin lake levels under steady-state conditions. *J. Hydrol*, 112:293-318.

Ase LE, Sernbo K, Syren P (1986). Studies of Lake Naivasha, Kenya and its drainage area. Naturgeografiska Institutionen Stockholms Universitet Forskningsrapport 63:1-75.

Ashok K, Guan Z, Saji NH, Yamagata T (2004). Individual and combined influences of the ENS and Indian Ocean Dipole on the Indian summer monsoon. *J. Clim.* 17: 3141-3155.

Ashok K, Guan Z, Yamagata T (2003). A look at the relationship between the ENSO and the Indian Ocean dipole. *J. Meteor. Soc. Japan* 81: 41-56.

Ayenew T (2003). Environmental Implications of changes in the levels of lakes in the Ethiopian Rift since 1970. *J Hydrol* 279:83-93.

Ayenew T, Becht R, Van Lieshout A, Gebreegziabher Y, Legesse D, Onyando J (2007). Hydrodynamics of topographically closed lakes in the Ethio-Kenyan Rift:The case of lakes Awassa and Naivasha. *J Spatial Hydrol* 7:81-100.

Ayenew T, and Greegziabher Y (2006). Application of a spreadsheet hydrological model for computing the long-term water balance of Lake Awassa, Ethiopia. *Hydrol Sci J* 51:3.

Baker B H, Mitchell JG, Williams LA (1988). Stratigraphy, geochronology and volcano-tectonic evolution of the Kedong–Naivasha–Kinangop region, Gregory Rift Valley, Kenya *Journal of the Geological Society* 145:107-116.

Baker BH, Mohr PA, Williams LAJ (1972). Geology of the eastern rift system of Africa. *Geol Soc Am* Spec Pap 136:67.

Barker PA (1990). Diatoms as palaeolimnological indicators:A reconstruction of Late Quaternary environments in two East African salt lakes. Unpublished Ph.D. thesis, Loughborough University of Technology, Leicestershire.

Barker PA and Gasse F (2003). New evidence for a reduced water balance in East Africa during the Last Glacial Maximum:implication for model-data comparison. *Quaternary Science Reviews* 22:823-837.

Barker P, Telford R, Gasse F, Thevenono F (2002). Late Pleistocene and Holocene palaeohydrology of Lake Rukwa, Tanzania, inferred from diatom analysis. *Paleogeography, Paleoclimatology, Paleoecology* 187:295-305.

Barsukov PO, Fainberg EB, Khabensky EO (2004). Joint inversion of TEM and DC soundings, Near Surface. 10th European Meeting of Environmental and Engineering Geophysics, Utrecht, The Netherlands.

Bhattacharyya S and Narasimha R (2007). Regional differentiation in multidecadal connections between Indian monsoon rainfall and solar activity. *J. Geophys. Res.* 112, doi:10.1029/2006JD008353, D24103.

Beer J. Blinov A, Bonani G, Finkel RC, Hofmann HJ, Lehmann B, Oeschger H, Sigg A, Schwander J, Staffelbach T, Stauffer B, Suter M, Wötfli W (1990). Use of 10Be in polar ice to trace the 11-year cycle of solar activity. *Nature* 347:164-166 .

Berger A and Loutre MF (1997). Inter tropical latitudes and precessional and half-precessional cycles. *Science*, 278:1476-1478

Berger WH, Yasuda M, Bickert T, Wefer G, Takayama T (1994). Quaternary time scale for the Ontong Java Plateau:Milankovitch template for Ocean Drilling Program Site 806. *Geology* 22:463-467.

Bergner AGN, Trauth MH, Bookhagen B (2003). Paleo- precipitation estimates for the Lake Naivasha Basin (Kenya) during the last 175 k.r. using a lake-balance model. *Global Planet Change* 36:117-136

Bergner AGN and Trauth MH (2004). Comparison of the hydrological and hydrochemical evolution of Lake Naivasha (Kenya) during three highstands between 175 and 60 kyr BP. P*aleogeography, Paleoclimatology, Paleoecology* 215:17-36.

Bessems I, Verschuren D, Russell JM, Hus J, Mees F, Cumminge BF (2008). Palaeolimnological evidence for widespread late 18th century drought across equatorial East Africa. P*aleogeography, Paleoclimatology, Paleoecology* 259:107-120.

Birks HJB (1998). Numerical tools in palaeolimnology–progress, potentialities, and problems. *J Paleolimno*l 20:307-332. doi:10.1023/A:1008038808690.

Bjerknes J (1969). Atmospheric teleconections from the Equatorial Pacific. *Mon. Wea. Rev.*, 97:163-172.

Bomblies A, Duchemin JB, Eltahir EAB (2008). Hydrology of malaria:Model development and application to a Sahelian village, *Water Resour. Res.* 44, W12445, doi:10.1029/2008WR006917.

Buck R (1991). Modes of continental lithospheric extension. *J Geophys Res* 96:20161-20178.

Burns SJ, Fleitmann D, Mudelsee M, Neff U, Matter A, Mangini A (2002). A 780-year annually resolved record of Indian Ocean monsoon precipitation from a speleothem from south Oman. *J. Geophys. Res.* 107, D20, doi: 10.1029/2001JD001281.

Burrough SL and Thomas DSG (2009). Geomorphological contributions to paleolimnology on the African continent. *Geomorphology* 103:285-298

Butzer KW, Isaac GL, Richardson JL, Washbourn-Kamau C (1972). Radiocarbon Dating of East African Lake Levels. *Science,* 175:4027.

Cai W, Pan A, Roemich D, Cowan T, Guo X (2009). Argo profiles a rare occurrence of three consecutive positive Indian Ocean Dipole events, 2006-2008. *Gephys. Res. Lett.* 36, L08701, doi: 10.1029/2008GL037038.

Camberlin P and Philippon N (2002). The east African March-May rainy season : associated atmospheric dynamics and predictability over the 1968-97 period. *J. Clim.* 15:1002-1019.

Camberlin P, Janicot S, Poccard I (2001). Seasonality and atmospheric dynamics of the teleconnections between African rainfall and tropical sea-surface temperature: Atlantic vs. ENSO. *Int. J. Climatol.* 21:973-1005.

Camberlin P (1997). Rainfall anomalies in the source region of the Nile and their connection with the Indian summer monsoon. *J. Clim.* 10:1380-1392.

Camberlin P (1995). June-September rainfall in North-Eastern Africa and atmospheric signals over the tropics: a zonal perspective. *International Journal of Climatology* 15:773-783.

Casanova J and Hillaire-Marcel C (1992). Chronology and paleohydrology of Late Quaternary high lake levels in the Manyara Basin (Tanzania) from isotopic data ($^{18}0$, ^{13}C, ^{14}C, Th/U) on fossil stromatolites. *Quaternary Research* 38:205-226.

Castanier S, Bernet-Rollande M, Maurin A, Perthuisot J (1993). Effects of microbial activity on the hydrochemistry and sedimentology of Lake Logipi, Kenya. *Hydrobiologia* 267:99-112

Charlie F and Gasse F (2002). Late Glacial Holocene diatom record of water chemistry and lake level change from the tropical East African Rift Lake Abiyata (Ethiopia). P*alaeogeography, Palaeoclimatology, Palaeoecology* 187:259-283

Charles CD, Cobb K, Moore MD, Fairbanks RG (2003). Monsoon-tropical ocean interaction in a network of coral records spanning the 20th century. *Marine Geology* 201:207-222.

Chiang CHJ (2009). The Tropics in Paleoclimate. *Annul. Rev. Earth Planet. Sci*. 37:263-297

Chorowicz J (2005). The East African Rift System. *J Afr Earth Sci* 43:379-410.

Christensen JH, Carter TR, Rummukainen M, Amanatidis G (2007). Evaluating the performance and utility of regional climate models:the PRUDENCE project. *Clim. Change*, doi:10.1007/ s10584-006-9211-6ice-ocean model and the strategy for the coupling of the three spheres.

Clark CO, Webster PJ, Cole JE (2003). Interdecadal Variability of the Relationship between the Indian Ocean Zonal Mode and East African Coastal Rainfall Anomalies. *J. Clim* 16:548-554.

Clarke MCG, Woodhall DG, Allen D, Darling G (1990). Geological, Volcanological and hydrogeological controls on the Occurrence of Geothermal activity in the area Surrounding Lake Naivasha, Kenya. British Geological Survey and Ministry of Energy, Nairobi, Kenya.

Cohen AS (2003). Paleolimnology: The history and Evolution of lake systems. Oxford University Press. 500 p.

Crowley TJ and North GR (1991). Paleoclimatology,Oxford University Press, New York, 339 pp.

Darling WG, Allen DJ, Armannsson H (1990). Indirect detection of subsurface outflow from a Rift Valley lake. *J. Hydrol* 113:297-305.

Darling WG, Gizaw B, Arusei MK (1996). Lake groundwater relationships and fluid rock interaction in the East African rift valley, isotopic evidence. *J Afr Earth Sci* 22:423-431.

Dai A 2001. Global precipitation and thunderstorm frequencies. Part II: Diurnal variations. *J. Clim* 14:1112–1128.

Dai A, Giorgi F, Trenberth KE (1999). Observed and model-simulated diurnal cycles of precipitation over the contiguous United States. *J. Geophys. Res.* 104:6377–6402.

De Vries JJ (1984). Holocene Depletion and active rechanrge of the Kalahari groundwaters- A review of an indicative model. *J. Hydrol*. 70:221-232.

De Vries JJ, Selaolo ET, Beekman HE (2000). Groundwater recharge in the Kalahari, with reference to paleo-hydrologic conditions. *J. Hydrol*. 238:110-123.

Digerfeldt G, Almlendinger JE Björck (1992). Reconstruction of past lake levels and their relation to groundwater hydrology in the Parkers Prairie sandplain, west-central Minnesota. *Paleogeography, Paleoclimatology, Palaeoecology,* 94:99-118.

Donders TH, Wagner-Cremer F, Visscher H (2008). Integration of proxy data and model scenarios for the mid-Holocene onset of modern ENSO variability. *Quaternary Science Reviews* 27:571-579.

DonovanJJ, Smith JA, Panek VA, Engstrom DR, Ito E (2002). Climate-driven hydrologic transients in lake sediment records:calibration of groundwater conditions using 20th Century drought. *Quaternary Science Reviews* 21:605-624.

Dunkley PN, Smith M, Allen DJ, Darling W G (1993). The geothermal activity and geology of the northern sector of the Kenya Rift Valley. Research Report SC/93/1. Keyworth:British Geological Survey.

Dühnforth M, Bergner AGN, Trauth M.H (2006). The hydrological budget of the Nakuru- Elmenteita basin, Central Kenya Rift, during the Early Holocene wet period. *J Paleolimno*l 36:281-294.

Ebinger CJ, Yamane T, Kelley S. (1993). Volcanism and extension between the main Ethiopian and Gregory Rifts. In:Thorweihe U, Schdelmeier H (eds), Geoscientific Research in Northeast Africa. Balkema. Rotterdam, p. 301-304.

Ebinger CJ, Poudjom Y, Mbede E, Foster F, Dawson JB (1997). Rifting Archean lithosphere:The Eyasi-Manyara-Natron rifts, East Africa. Geol Soc London Special Publications 154, p 947-960.

Ebinger CJ, Yamane T, Harding DJ, Tesfaye S, Kelley S, Rex DC (2000). Rift deflection, migration, and propagation:Linkage of the Ethiopian and Eastern rifts, Africa. GSA Bull 112:163-176.

Eggermont H, Heiri O, Verschuren D (2006). Subfossil Chironomidae (Insecta:Diptera) as quantitative indicators for past salinity variation in African lakes. *Quaternary Science Reviews* 25:1966-1994.

Egorova T, Rozanov E, Manzini E, Haberreiter M, Schmutz W, Zubov V and Peter T (2004). Chemical and dynamical response to the 11-year variability of the solar irradiance simulated with a chemistry-climate model. *Geophys. Res. Lett* 31:1-4.

Enfield DB (1989). El Nino, past and present. *Reviews of Geophysics* 27:159–187.

Epp LS, Stoof KR, Trauth MH, Tiedemann R (2010. Historical genetics on a sediment core from a Kenyan lake: Intraspecific genotype turnover in a tropical rotifer is related to past environmental changes *J Paleolimno*l. 43:939-954

Ferguson AJD, Harbott BJ (1982). Geographical, physical and chemical aspects of Lake Turkana. In Hopson AJ (ed), Lake Turkana:A Report on the Findings of the Lake Turkana Project, 1972 - 1975, Vol. 1. London, Overseas Development Administration, 1-108

Fetter CW (2001). Applied hydrogeology, Pearson Education international. Upper Saddle River, New Jersey

Fitterman DV, Stewart MT (1986). Transient electromagnetic sounding for groundwater. *Geophysics* 51:995-1005

Fitterman DV, Stanley WD, Bisdorf RJ (1988). Electrical structure of Newberry Volcano, Oregon, *J. Geophys. Res.* 93:10119-10134.

Fleitmann D, Burns SJ, Mudelsee M, Neff U, Kramers J, Mangini A, Matter A. S (2003). Holocene Forcing of the Indian Monsoon Recorded in a Stalagmite from Southern Oman. *Science* 300:1737-1739.

Fritz SC (2008). Deceiphering Climate histories from lakes *J Paleolimno*l 39:5-16

ftp://ftp.ngdc.noaa.gov/STP/SOLAR_DATA/SOLAR_RADIO/FLUX/Penticton_Adjusted/monthly/MONTHPLT.ADJ (March 2011).

Garcin Y, Junginger A, Melnick D, Olago DO, Strecker MR, Trauth MH (2009). Late Pleistocene–Holocene rise and collapse of Lake Suguta, northern Kenya Rift. *Quaternary Science Reviews* 28:911-925

Garcin Y, Vincens A,Williamson D, Guiot J, Buchet G (2006). Wet phases in tropical southern Africa during the last glacial period. *GRL,*. 33, L07703, doi:10.1029/2005GL025531.

Gasse F (2000). Hydrological changes in the African tropics since the Last Glacial Maximum. *Quaternary Science Reviews* 19:189-211.

Gasse F (2006). Climate and hydrological changes in tropical Africa during the past million years *Human Palaeontology and Prehistory*. 5:35-43.

Gaudet JJ and Melack JM (1981). Major ion chemistry in a tropical African lake basin. *Freshwater Biol. II*, 309-333.

Gleisner H P Thejll (2003). Patterns of tropospheric response to solar variability, *Geophys. Res. Lett*. 30(13), 1711, doi:10.1029/2003GL017129.

Goerner A, Jolie E, Gloaguen R (2009). Non-climatic growth of a saline Lake Beseka, Main Ethiopian Rift. *Journal of Arid Environments.* 73:287-295.

Haigh JD, Blackburn M, Day R (2005). The response tropospheric circulation to perturbations in lower stratospheric temperature. *J. Clim.* 18:3672-3691.

Haigh JD(2011). Climate variability and the influence of the sun. *Science* 294, 2109-2111.

Hancock GR, Martinez C, Evans KG, Moliere DR (2006). A comparison of SRTM and high-resolution digital elevation models and their use in catchment geomorphology and hydrology:Australian examples. *Earth Surf Processes* 31:1394-1412.

Hastenrath S and Kutzbach JE (1983). Paleoclimatic estimates from water and energy budgets of East African Lakes. *Quaternary Research* 19:141-53.

Hillaire-Marcel C, Carro O, Casanova J (1986). ^{14}C and Th/U Dating of Pleistocene and Holocene Stromatolites from East African Paleolakes, *Quaternary Research,* 25:312-329.

Hastenrath S, Nicklis A, Greischar L (1993). Atmospheric-hydrospheric mechanisms of climate anomalies in the western equatorial Indian Ocean. *J. Geophys. Res.* 98:20219–20235.

http://iri.columbia.edu/climate/ (March 2011).

http://www.cpc.ncep.noaa.gov/data/indices/nino34.mth.ascii.txt (March 2011).

http://www.cpc.ncep.noaa.gov/products/fews/rfe.shtml (March 2011).

http://www.jamstec.go.jp/frsgc/research/d1/iod/ (March 2011).

Hurtrez JE, Sol C, Lucazeau F (1999). Effect of Drainage area on Hypsometry from an analysis of small-scale drainage basins in the Siwalik hills (Central Nepal). *Earth Surf Process* 24:799-808.

Indeje M, Semazzi FHM, Ogallo L J (2000). ENSO signals in East African rainfall seasons. *InternationalJ. Clim* 20:19-46.

Ininda J, Desalegne B, Befekadu A (1987). The characteristics of rainfall in Ethiopia and its relationship to El Nino–Southern Oscillation. In *Proceedings of the First Technical Conference on Meteorology Research in Eastern and Southern Africa*, Kenya Meteorology Department, Nairobi, 6–9 January 1987:133-135.

IPCC (2007) Climate change 2007: The physical science basis. Contribution of Working Group I to the fourth assessment report of the Intergovernmental Panel for Climate change.

Izumo T (2008). The Role of the Western Arabian Sea Upwelling in Indian Monsoon Rainfall Variability. *J. Clim* 21:5603-5623.

Johansson H, Brolin AA, Håkanson L (2007). New Approaches to modeling of Lake basin morphometry. Environ Model Assess 12:213-228.

Johnson AI (1967). Specific yield - compilation of specific yields for various materials. U.S. Geological Survey Water Supply Paper 1662-D. 74 pp.

Johnson TC (1996). Sedimentary processes and signals of past climatic change in the large lakes of the East African Rift Valley In:Johnson, T.C., Odada, E.O. (Eds.), The Limnology, Climatology and Paleoclimatology of the East African Lakes. Gordon and Breach, Amsterdam, p. 367 412.

Johnson TC and Malala (2009). Lake Turkana and Its Link to the Nile in The Nile: Origin, Environments, Limnology and Human Use. *The Nile: Monographiae Biologicae*, 89:287-304.

Junginger A and Trauth MH (sub). Solar Variations and Holocene East African Climate.

Kane RP (1995). Quasi-biennial and quasi-triennial oscillations in the summer monsoon rainfall of the meteorological subdivisions of India. *Mon. Wea. Rev*., 123**:** 1178-1184.

Kauahikaua J (1993). Geophysical characteristics of the hydrothermal systems of Kilauea volcano, Hawaii. Geothermics 22:271-299.

Kebede S, Travi Y, Asrat A, Alemayehu T, Ayenew T, Tessem Z (2008). Groundwater origin and flow along selected transects in Ethiopian rift volcanic aquifers. *J. of Hydrol*. 16:55-73.

Knight Piesold & Partners (1992). Ewaso Ngiro (south) Multipurpose project. Environmental impact assessment, Stage III Reports. Socio-economics, ecology and land use, fisheries, flamingo and construction impact. Tour du Vala, Humberside International, ADEC, Trump, Knight Piesold & Partners, Kent.

Kodera K (2004). Solar influence on the Indian Ocean Monsoon through dynamical processes. *Geophys. Res. Lett.* 31, L24209, doi:1029/2004GL020928.

Kodera K, Coughlin K, Arakawa O (2007). Possible modulation of the connection between the Pacific and Indian Ocean variability by the solar cycle. *Geophys. Res. Lett.* 34, L03710, doi: 10.1029/2006GL027827.

Kodera K and Kuroda Y (2002). Dynamical response to the solar cycle. *J. Geophys. Res.* 107 (D24), 4749, doi:10.1029/2002JD002224.

Kutzbach JE, and Guetter JP (1980). On the design of Paleoenvironmental Data Networks for Estimating Large-Scale Patterns of Climate *Quaternary Research* 14:169-187.

Kutzbach JE, Street-Perrott FA (1985.) Milankovitch forcing of fluctuations in the level of tropical lakes from 18 to 0 kyr BP. *Nature* 317:130–134.

Legesse D, Gasse F, Radakovitch O, Vallet-Coulomb C, Bonnefille R, Verschuren D, Gibert E, Barker P (2002). Environmental changes in a tropical lake (Lake Abiyata, Ethiopia) during recent centuries. *Palaeogeogr Palaeoclimatol Palaeoecol* 187:233-258.

Lenat, JF, Fitterman DV, Jackson DB, Labazuy P (2000). Geo-electrical structure of the central zone of Piton de la Fournaise Volcano (Réunion), *Bull. Volcanol.,* 62:75–89.

Le Turdu C, Tiercelin JJ, Gibert E, Travi Y, Lezzar KE, Richert JP, Massault M, Gasse F, Bonnefille R, Decobert M, Gensous B, Jeudy V, Tamrat E, Mohammed MU, Martens K, Atnafu B, Chernet T, Williamson D, Taieb M (1999). The Ziway-Shala basin system, Main Ethiopian Rift:influence of volcanism, tectonism, and climate forcing on basin formation and sedimentation. *Palaeogeogr Palaeoclimatol Palaeoecol* 150:135-177

Levin NE, Zipser EJ, Cerling TE (2009). Isotopic composition of waters from Ethiopia and Kenya: Insights into moisture sources for eastern Africa. *J. Geophys. Res.* 114, D23306, doi: 10.1029/2009JD012166.

Lockwood M and Fröhlich C (2007). Recent oppositely directed trends in solar climate forcings and the global mean surface air temperature. *Proc. R. Soc.* 463, 2447-2460.

Luo JJ, Behera SK, Masumoto Y, Sakuma H Yamagata, T (2008). Successful prediction of the consecutive IOD in 2006 and 2007. *Geophys. Res. Lett.* 35, L14S02.

Makin MJ, Kingham TJ, Waddams AE, Birchall CJ, Eavis BW (1976). Prospects for irrigation development around lake Ziway, Ethiopia. Land Res. Study. Division, Ministry of Overseas Development, 26. Tolworth, UK, 270 pp.

Mason SJ, and PD Tyson (1992). The Modulation of Sea Surface Temperature and Rainfall Associations Over Southern Africa With Solar Activity and the Quasi-Biennial Oscillation, *J. Geophys. Res*., 97(D5), 5847–5856, doi:10.1029/91JD02189.

Manning AH, and Solomon DK (2005). An integrated environmental tracer approach to characterizing groundwater circulation in a mountain block, *Water Resour. Res*., 41, W12412, doi: 10.1029/2005WR004178.

Manzella A, Volpi G, Zaja A, Meju M (2004). Combined TEM- MT investigation of shallow-depth resistivity structure of Mt Somma-Vesuvius. *Journal of Volcanology and Geothermal Research,* 131:19-32.

Marchitto TM, Muscheler R, Ortiz JD, Carriquiry JD, van Geen A (2010). Dynamical Response of the Tropical Pacific Ocean to Solar Forcing During the Early Holocene. *Science* 330:1378-1381.

Mazor E and Nativ R (1992). Hydraulic calculation of groundwater flow velocity and age:Examination of the basic premises. *J. Hydrol*. 138:211-222.

McAnelly RL and Cotton WR (1989). The precipitation life cycle of mesoscale convective complexes over the central United States. *Mon. Wea. Rev*. 117:784–808.

McCann DL (1974). Hydrologic investigation of the Rift Valley catchments. Unpublished. U.N. Geothermal project report.

Mccall GJH (1957). Geology and groundwater in the Nakuru area. Ministry of works (Hydraulic Branch) Technical report 3.

Maitima JM (1991). Vegetation response to climatic change in Central Rift Valley, Kenya. *Quat Res* 35:234–245.

McNeill JD (1990). Use of electromagnetic methods for groundwater studies. In:Ward SH (ed) Geotechnical and environmental geophysics, vol 1. Review and Tutorial, Society of Exploration Geophysicists Investigations, no 5:107-112.

Meehl GA, Arblaster JM, Matthes K, Sassi F van Loon H (2009). Amplifying the pacific climate system response to a small 11-year solar cycle forcing, *Science* 325, 1114-1118.

Meehl GA, Arblaster JM, Loschnigg J (2003). Coupled ocean–atmosphere dynamical processes in the tropical Indian and Pacific Oceans and the TBO. *J. Clim,* 16**,** 2138-2158.

Meehl GA and Arblaster JM (2002). The tropospheric biennial oscillation and Asian–Australian monsoon rainfall. *J. ate* 15**:** 722–744.

Medina-Elizalde and Lea DW (2005). The Mid-Pleistocene Transition in the Tropical Pacific. *Science* 310:1009-1012.

Mehta V and Lau KM (1997). Influence of solar irradiance on the Indian monsoon–ENSO: Relation at decadal–multidecadal time scales. *Geophys. Res. Lett.* 24:159–162.

Meisner B and P Arkin (1987). Spatial and annual variations in the diurnal cycle of large-scale tropical convective cloudiness and precipitation. *Mon. Wea. Rev.*, 115:2009 –2032.

Meyers G A, McIntosh P C, Pigot L, Pook M J (2007). The years of El Nino, La Nina, and interactions with the tropical Indian Ocean. *J. Clim*.. 20:2872– 2880.

Muchemi, G. Geothermal (1998.): Exploration in the Kenya Rift. Paper Submitted in the Geothermal Training Program, 20th Anniversary workshop Oct. 1998. United Nations University.

Montgomery DR, Balco G, Willett SD (2001). Climate, tectonics and the morphology of the Andes. *Geology* 29:579-582.

Moy CM, Seltzer GO, Rodbell DT, Anderson DM (2002). Variability of El Niño/Southern Oscillation activity at millennial timescales during the Holocene epoch. *Nature* 420:162-165.

Narasimha R and Bhattacharyya S (2010). A wavelet cross-spectral analysis of solar-ENSO-rainfall connections in the Indian monsoons. *Appl. Comput. Harmon. Anal.* 28:285-295.

Neff U, Burns S J, Mangini A, Mudelsee M, Fleitmann D, Matter A (2001). Strong coherence between solar variability and the monsoon in Oman between 9 and 6 kyr ago. *Nature* 411:290-293.

Nicholson SE (1996). A review of dynamics and climate variability in Eastern Africa. In:Johnson TJ, Odada EO (eds), The Limnology, Climatology and Paleoclimatology of the Eastern African lakes. Gordon and Breach, Amsterdam, p. 25-56.

Nicholson SE and Entekhabi D (1987). Rainfall variability in equatorial and southern Africa: Relationships with sea surface temperatures along the southwestern coast of Africa. *J. ate Appl. Meteor.* 26**:** 561–578.

Nicholson S and Yin X (2004). Mesoscale Patterns of Rainfall, Cloudiness and Evaporation over the Great Lakes of East Africa. *The East African Great Lakes: Limnology, Palaeolimnology and Biodiversity Advances in Global Change Research*, 12:93-119.

Nilsson, E (1931). Quaternary Glaciations and Pluvial lakes in British East Africa. *Geografiska Annaler.* 13:249-349.

Nyenzi BS, Kiangi PMR, Rao NNP (1981). Evaporation values in East Africa. *Arch Met Geoph Biokl* Ser B 29:35-55.

Nylor WI (1972). Geology of the Eburru and Olkaria geothermal prospects. Unpublish UNDP/EAPL Geothermal exploration project report.

Odada EO, Olago DO, Bugenyi F, Kulindwa K, Karimumuryango J, West K, Ntiba M, Wandiga S, Aloo-Obudho P, Achola P (2003). Environmental assessment of the East African Rift Valley lakes. *Aquat Sci* 65:254-271.

Ojiambo BS (1992). Hydrologic, hydrogeochemical and environmental isotopes study of possible interactions between Olkaria geotherma, shallow subsurface and Lake Naivasha waters, Central rift valley, Kenya. Msc thesis, University of Nevada, Reno.

Ojiambo BS and Lyons WB (1996). Residence times and major ions in Lake Naivasha, Kenya and their relationship to lake hydrology. In Limnology, climatology and Paleoclimatology of the East African lakes. Ed T.C. Johnson and E. O. Odada, 267-278. Amsterdam:Gordon and Breach Publ.

Ojiambo BS, Poreda RJ, Lyons WB (2001). Groundwater/ surface water interactions in Lake Naivasha, Kenya, using δ^{18} O, δD, and $^{3}H/^{3}He$ Age dating. *Groundwater* 39:526-533.

Oki T and K Musiake (1994). Seasonal change of the diurnal cycle of precipitation over Japan and Malaysia. *J. Appl. Meteor.* 33:1445–1463.

Okoola R (1999). A diagnostic study of the Eastern African monsoon circulation during the northern hemisphere spring season. *Int. J. atol.* 19**:**143–168.

Olago DO (1995). Late Quaternary lake sediments of Mount Kenya, Kenya. DPhil thesis, University of Oxford.

Olago DO (2001). Vegetation changes over palaeo-time scales in Africa. *Clim Res* 17:105-121.

Olago D, Opere A Barongo J (2009). Holocene palaeohydrology, groundwater and climate change in the lake basins of the Central Kenya Rift. Hydrological sciences. Special Issue. Groundwater and Climate in Africa. 54, 4.

Olago DO, Street-Perrott FA, Perrott RA, Ivanovich M, Harkness DD, Odada EO (2000). Long-term temporal characteristics of paleomonsoon dynamics in equatorial Africa. *Global and Planetary Change* 26, 159-171.

Olaka LA, Odada, EO, Trauth MH, Olago DO (2010). The sensitivity of East African rift lakes to climate fluctuations. *J Paleolimno*l 44, 629-644.

O'Leary DW, Friedman JD, Pohn HA (1976). Lineaments, linear, lineation – some proposed new standards for old terms. *Geol Soc Am Bul*l 87:1463–1469.

Owen RB, Renaut RW, Hover VC, Ashley GM, Muasya AM (2004). Swamps, Springs and diatoms:Wetlands of the semi-arid Bogoria-Baringo Rift, Kenya. *Hydrobiologia* 518:59-78.

Paltineanu C, Mihailescu IF, Seceleanu I, Dragota C, Vasenciuc F (2007). Using aridity indices to describe some climate and soil features in Eastern Europe:a Romanian case study. *Theor Appl Climatol* 90:263-274.

Partridge TC, Demenocal PB, Lorentz SA, Paiker MJ, Vogel JC (1997). Orbital forcing of climate over South Africa a 200 000-year record from the Pretoria Saltpan. *Quaternary Science Reviews* 16:1125-1133

Philander SG, and Fedorov AV (2003). Role of tropics in changing the response to Milankovich forcing some three million years ago. *Paleoceanography,* 18(2), 1045, doi:10.1029/2002PA000837.

Pienitz R and Lotter AF (2009). Editorial:Advances in Paleolimnology. PAGES news vol. 17:92.

Pike RJ, Wilson SE (1971). Elevation–relief ratio, hypsometric integral and geomorphic area–altitude analysis. *Geol Soc Amer Bull* 82:1079-1084.

Riaroh D and Okoth W (1994). The geothermal fields of the Kenya Rift. *Tetonophysics* 236:117-130.

Richardson J L and Dussinger RA (1986). Paleolimnology of Mid-elevation lakes in the Kenyan Rift Valley, *Hydrobiologia* 143:167-174.

Richardson JL, Richardson AE (1972). History of an African Rift lake and its climatic implications. *Ecolo Monogr* 42:499–535.

Ring U, Hilde L, Schwartz L, Bromage TG, Sanaane C (2005). Kinematic and sedimentological evolution of the Manyara Rift in northern Tanzania, *East Afr Geol Mag* 142:355-368.

Rodriguez E, Morris C, Belz E (2006). A global assessment of the SRTM performance. Photogramm Eng Rem S 72:237-247.

Rowntree KM (1989). Rainfall characteristics, rainfall reliability, and the definition of drought:Baringo District, Kenya. *S Afr Geog J* 71:74-80.

Roxy M, Gualdi S, Drbohlav HL, Navarra A (2010). Seasonality in the relationship between El Nino and Indian Ocean dipole. *ate Dynamics*, DOI: 10.1007/s00382-010-0876-1.

Russel JM and Johnson TC (2007). Little Ice Age drought in equatorial Africa: Intertropical Convergence Zone migrations and El Niño–Southern Oscillation variability. *Geology*, 35, 21–24.

Saji NH, Xie SP, Yamagata T (2006). Tropical Indian Ocean Variability in the IPCC Twentieth-Century ate Simulations. *Journal of ate* 19: 4397-4416.

Saji NH, Goswami BN, Vinayachandran PN, Yamagata T (1999). A dipole mode in the Indian Ocean. *Nature* 401: 360-363.

Sanford WE and Wood WW (1991). Brine evolution and mineral Deposition in Hydrologically open evaporite basins. *American Journal of science* 291:687-710.

Schefuß E, Schouten S, Schneider RR (2005). Climatic Controls on the Central African Hydrology during the past 20,000 years. *Nature,* 437:1003-1006.

Scholz CA, Moore TC, Hutchinson DR, Golmshtok AJ, Klitgord KD, Kurotchkin AG (1998). Comparative sequence stratigraphy of low-latitude versus high-latitude lacustrine rift basins:seismic data examples from the east African and Baikal rifts. *Palaeogeography Palaeoclimatology Palaeoecology* 140:401-420.

Semazzi HFM, Burns B, Lin NH, Schemm JE (1996). A GCM study of the teleconnections between the continental ate of Africa and global sea-surface temperature anomalies. *J* 9:2480–2497.

Sepulchre P, Ramstein G, Fluteau F, Schuster M, Tiercelin J, Brunet M (2006). Tectonic uplift and eastern Africa aridification. *Science* 313:1419-1423.

Sherwood SC and Wahrlich R (1999). Observed evolution of tropical deep convective events and their environment. *Mon. Wea. Rev*. 127:1777–1795.

Singer A and Stoffers P (1980). Clay mineral diagenesis in two East African lake sediments. *Clay Miner* 15:291-307.

Singh KP (1968). Some factors affecting baseflow. *Water Resources Research* 4:985-999.

Skinner L (2008). Facing future climate change:is the past relevant? Phil. *Trans. R. Soc.* 366:4627-4645.

Smol JP (1992). Paleolimnology: an important tool for effective ecosystem management. *J. EcosystemHealth,* 1:49–58.

Soreghan MJ, Scholz CA, Wells JT (1999). Coarse-grained, deep-water sedimentation along a border fault margin of Lake Malawi, Africa; seismic stratigraphic analysis. *Journal of Sedimentary Research* 69:832-846.

Spiegel C, Kohn BP, Belton DX, Gleadow AJW (2007). Morphotectonic Evolution of the Central Kenya rift flanks:Implications for late Cenozoic environmental change in East Africa. *Geology* 35:427-430.

Spigel RH and Coulter GW (1996). Comparison of hydrology and physical limnology of the East African Great Lakes:Tanganyika, Malawi, Victoria, Kivu and Turkana (with reference to some North American Great Lakes). In:Johnson TC, Odada EO (eds) The Limnology, Climatology and Paleoclimatology of East African Lakes:Gordon and Breach, Toronto, p 103-139.

Strecker MR, Blisniuk PM, Eisbacher GH (1990). Rotation of extension direction in the central Kenya Rift. *Geology* 18:299-302.

Street FA (1980). The relative importance of climate and local hydrogeological factors in influencing lake-level fluctuations. *Palaeoecol Afr* 12:137-158.

Street FA and Grove AT (1976). Environmental and climatic implications of Late Quaternary lake level fluctuations in Africa. *Nature* 261. 385-390.

Street-Perrott FA, Harrison SP (1985). In: Hecht AD (ed), Paleoclimate Analysis and Modeling. Wiley, New York, 291-340.

Sturchio NC, Dunkley PN, Smith M (1993). Climate-driven variations in the geothermal activity in the northern Kenya rift valley. *Nature* 362:233-234.

Stute M, Clement AC, Lohmann G (2001). Global climate models: past, present, and future. *Proceedings of the National Academy of Sciences* 98:10529–10530.

Tarits C, Renaut RW, Tiercelin J, Le Hérissé A, Cotten J, Cabon J (2006). Geochemical evidence of hydrothermal recharge in Lake Baringo, central Kenya Rift Valley. *Hydrol Proces*s 20:2027-2055.

Telford RJ, Lamb HF, Mohammed MU (1999). Diatom-derived palaeoconductivity estimates for Lake Awassa, Ethiopia. *J Paleolimnology* 21:409-421.

Thompson AD and Dodson R (1963). Geology of the Naivasha Area. Geological Survey of Kenya, Nairobi, Kenya. Report 55.

Thomson MC, Doblas-Reyes FJ, Mason SJ, Hagedorn R, Connor SJ, Phindela T, Morse AP, Palmer TN (2006). Malaria early warnings based on seasonal climate forecasts from multi-model ensembles. *Nature* 439:576-579 (2 doi:10.1038/nature04503.

Tiercelin JJ (1990). Rift-sedimentation:responses to climate, tectonism and volcanism. Examples of the East African Rift. *J Afr Earth Sci* 10:283-305.

Tiercelin JJ, Lezzar KE (2002). A 300 Million years history of rift lakes in central and east Africa:an updated broad view. In Odada EO and Olago DO (eds) The East African great Lakes:Limnology, Paleolimnology and Biodiversity. Kluwer Academic Publishers. Dordrecht, p. 3-62.

Todd DK (1980). Groundwater Hydrogeology, Wiley, New York, 535 p.

Trauth MH, Maslin MA, Deino A, Strecker MR (2005). Late Cenozoic moisture history of East Africa. *Science* 309:2051-2053.

Trauth M H, Maslin M A, Deino AL, Strecker MR, Bergner AGN, Dühnforth M (2007). High- and low-latitude forcing of Plio-Pleistocene East African climate and human evolution. *J Hum Evol* 53:475-486.

Trauth MH, Maslin MA, Deino A, Junginger A, Odada E, Olago D, Olaka L, Strecker MR, Tiedemann R (2010). Human Evolution and Migration in a Variable Environment:The Amplifier Lakes of East Africa. *Quaternary Science Reviews*. 29:2981-2988.

Tsakiris G, Vangelis H (2005). Establishing a drought index incorporating evapotranspiration. *Eur Wat* 9/10:3-11.

Tweed S, Leblanc M, Cartwright I (2010) Remote sensing and hydrochemistry of lakes-groundwater interaction. Unpub communication.

UNFPA (2010). The state of the worlds population 2010. From conflicts and Crisis to Renewal: Generations of change.

van Loon H and Meehl GA (2008). The response in the Pacific to the sun's decadal peaks and contrasts to cold events in the Southern Oscillation, Journal of Atmospheric and Solar-Terrestrial Physics, 70; 1046-1055, DOI: 10.1016/j.jastp.2008.01.009.

van Loon H, Meehl GA, Arblaster JM (2004). A decadal solar effect in the tropics in July–August. *J. Atmos. Sol. Terr. Phys.* 66, 1767–1778.

van Loon H and Labitzke K (1994). The 10–12 year atmospheric oscillation. *Meteorol. Z*. 3, 259–266.

Verschuren D (1999). Sedimentation controls on the preservation and time resolution of climate proxy records from shallow fluctuating lakes. *Quaternary Science Reviews* 18:821-837.

Verschuren D, Laird KR and Cumming B (2000). Rainfall and drought in equatorial East Africa during the past 1,100 years. *Nature* 403, 410-14.

Verschuren D, Tibby J, Sabbe K, Roberts N (2000). Effects of depth, salinity and substrate on the invertebrate community of a tropical fluctuating lake. *Ecology* 81:164-182.

Verschuren D and Russel J (2009). Paleolimnology of African lakes: Beyond the exploration phase. PAGES news 3 October 2009. 17:112-114.

Vincent CE, Davies TD, Primblecombe P, Beresford AKC (1989). Lake levels and glaciers:indicators of the changing rainfall in the mountains of East Africa. In:Mahaney, W.C. (Ed.), Quaternary and Environmental Research on East African Mountains. York University, North York, Canada, p. 199-216.

Wallace JM (1975). Diurnal variations in precipitation and thunderstorm frequency over the conterminous United States. *Mon. Wea. Rev.* 103:406–419.

Wang B and Fan Z, (1998). Choice of South Asian Summer Monsoon Indices. *Bulletin of the American Meteorological Society*. 80: 629-638.

Wang YJ, Cheng H, Edwards RL, He Y, Kong X, An Z, Wu J, Kelly MJ, Dykoski AC, Li X (2005). The Holocene Asian Monsoon: Links to Solar Changes and North Atlantic Climate. *Science* 308, 854-857.

Washbourn C (1967). Lake levels and Quaternary climates in the eastern Rift Valley of Kenya. *Nature* 216:672–673.

Washbourn-Kamau C (1970). Late Quaternary chronology of the Nakuru-Elmenteita Basin, Kenya. *Nature* 226:253–254.

Washbourn-Kamau C (1971). Late Quaternary lakes in the Nakuru-Elmenteita Basin, Kenya. *Geograph J* 137:522–535.

Washbourn-Kamau CK (1975). Late Quaternary shorelines of Lake Naivasha, Kenya. Azania X:77–92.

Wolfenden E, Ebinger C, Yirgu G, Deino A, Ayalew D (2004). Evolution of the northern Main Ethiopian rift:birth of a triple junction *Earth and Planetary Science Letters* 224:213-228.

Yang G and Slingo J (2001). The Diurnal Cycle in the Tropics. *Mon. Wea. Rev.*, 129, 784–801.

Yin Z and Brook GA (1992). The topographic Approach to Locating High-Yield Wells in Crystalline Rocks:Does it work? *Ground Water* 30, 96-102.

Zachos JC, Flower BP, Paul H (1997). Orbitally paced climate oscillations across the Oligocene/ Miocene Boundary, *Nature* 388, 567-571.

Zachos J, Pagani M, Sloan L, Thomas E, Billups K (2001). Trends, Rhythms, and Aberrations in Global Climate 65 Ma to Present. *Science.* 292:686-693.

APPENDIX

APPENDIX 1

ENVIRONMENTAL VARIABILITY IN LAKE NAIVASHA, KENYA, OVER THE LAST TWO CENTURIES

Abstract

Lake Naivasha, Kenya, is one of a number of freshwater lakes in the East African Rift System. Since the beginning of the 20th century, it has experienced greater anthropogenic influence as a result of increasingly intensive farming of coffee, tea, flowers, and other horticultural crops within its catchment. The water-level history of Lake Naivasha over the past 200 years was derived from a combination of instrumental records and sediment data. In this study, we analysed diatoms in a lake sediment core to infer past lacustrine conductivity and total phosphorus concentrations. We also measured total nitrogen and carbon concentrations in the sediments. Core chronology was established by ^{210}Pb dating and covered a ~186-year history of natural (climatic) and human-induced environmental changes. Three stratigraphic zones in the core were identified using diatom assemblages. There was a change from littoral/epiphytic diatoms such as Gomphonema gracile and Cymbella muelleri, which occurred during a prolonged dry period from ca. 1820 to 1896 AD, through a transition period, to the present planktonic Aulacoseira sp. that favors nutrient-rich waters. This marked change in the diatom assemblage was caused by climate change, and later a strong anthropogenic overprint on the lake system. Increases in sediment accumulation rates since 1928, from 0.01 g cm^{-2} y^{-1} to 0.08 g cm^{-2} y^{-1} correlate with an increase in diatom-inferred total phosphorus concentrations since the beginning of the 20th century. The increase in phosphorus accumulation suggests increasing eutrophication of freshwater Lake Naivasha. This study identified two major periods in the lake's history: 1) the period from 1820 to 1950 AD, during which the lake was affected mainly by natural climate variations, and 2) the period since 1950, during which the effects of anthropogenic activity overprinted those of natural climate variation.

A1.1 Introduction

Lake sediments are frequently analysed to make paleoenvironmental inferences regarding changes in lake hydrology and surrounding ecosystems. These environmental changes can be caused by climatic fluctuations, by geomorphological and geological processes within the catchment area, and by human activities. The most recent climate records in lake-sediment archives are frequently overprinted by a local anthropogenic signal, confounding interpretation of environmental changes that were due to solely natural processes (Hausmann et al., 2002; Lotter and Birks 1997). Lake sediments may also fail to reflect past climate changes accurately in cases where non-climatic factors such as geomorphic and hydrologic setting influence the system (Fritz 2008). In the Naivasha basin, the last 100 years have been characterized by intense anthropogenic influence within the catchment, such as the damming of input rivers and the farming of coffee, tea and flowers around the lake (Verschuren 1996).

Diatoms in lake sediments are frequently used as bioindicators to infer ecological changes that have occurred within a lake and its surrounding catchment (Osborne 2000). This is possible because diatoms are remarkably sensitive to variations in water nutrient content, conductivity and pH. Past lake-water chemistry can be inferred from diatom valves in a sediment core, using transfer functions (Gasse et al., 1995). Such transfer functions have been developed from regional-scale studies in Africa (Gasse et al., 1995) and from combined, worldwide datasets (European Diatom Database Initiative, EDDI, http://craticula.ncl.ac.uk/Eddi/jsp/).

Lake Naivasha was listed as a Ramsar site in 1995 (www.ramsar.org) and its one-million-year history has been investigated over various timescales. Studies of its most recent history indicate the increasing importance of human influences, in addition to natural factors, on ecosystem changes (Verschuren et al., 2000; Trauth et al., 2003, 2005). The human population in the town of Naivasha and the area around the lake has increased 50-fold over the past three decades, to ~120,000 (Edeghonghon Jimoh et al., 2007). Consequently the aquatic health of the lake has become increasingly important for the people who depend on it. It is particularly important to protect the lake against increasing eutrophication (Hubble and Harper 2001). Anthropogenic influence since the beginning of the 20th century is reported to have caused major changes in nutrient input, plankton composition and macrophyte abundance (Ballot et al., 2009; Hubble and Harper 2001). Published data on the floral shift, however, cover only the period between 1929 and 2005 AD, and because data collection was relatively patchy, the data do not provide a clear picture of the timing of species changes (Ballot 2009; Hubble and Harper 2001).

This study refines the temporal resolution of the environmental record of Lake Naivasha, using a continuous and well dated sediment record from the lake, covering about the last 200 years. The record reveals substantial changes in sedimentation rate and diatom assemblages, which were caused by human activities rather than by climate-driven processes.

A1.2 Study site

At 1,889 m a.s.l., Lake Naivasha (0°55'S 36°20'E) is the highest closed-basin lake in the East African Rift System (Figure A.1). The modern lake covers an area of about 180 km^2 and has a water volume of ~0.85 km^3 (Bergner et al., 2003), a catchment area of 3,400 km^2 and an average depth in 1983 of 8 m (Verschuren 1999). Crescent Island Crater (CIC) is a partially-submerged crater in the eastern part of the lake that represents the area of greatest water depth, 16 m in 1983 (Verschuren 2001). At low water levels, the crater becomes increasingly isolated from the main lake, and as a result, becomes chemically distinct (Hubble and Harper 2001).

The regional climate of this equatorial lake basin is influenced by the seasonal migration of the Intertropical Convergence Zone (ITCZ), causing a strongly bimodal annual cycle, with rains in March/April and October/November (Nicholson 1996). The area receives additional rainfall from the "Congo air boundary," with westerly to south-westerly airflow during August and September, the so-called September rains (Nicholson 1996). Average rainfall in the vicinity of the lake is ~650 mm yr^{-1}, whereas the Aberdare Range in the eastern part of the catchment receives up to 2,400 mm yr^{-1}. Interannual variations in precipitation are linked to E-W adjustments in the zonal Walker circulation associated with the Indian Ocean Dipole and the El Niño/Southern Oscillation (Saji et al., 1999; Moy et al., 2002). There is considerable variation in rainfall, temperature and vegetation throughout the catchment area as a result of large differences in altitude.

Lake Naivasha is the second-largest freshwater lake in Kenya. It has a pH of ~8.1 (Åse 1987), which makes it unique in the semi-arid climate zone of the eastern arm of the Rift Valley, where other lakes are both alkaline and saline. Because potential evapotranspiration in the lake area is about 1,900 mm yr^{-1} (Clarke et al., 1990), the relatively low pH is attributed to high freshwater inflow from the Malewa and

the Gilgil Rivers, which enter from the north. These two rivers drain the high-elevation Kinangop Plateau, and the Aberdare Range to the north and north-east, which receive high amounts of precipitation (Bergner et al., 2003). It is estimated that about 15% of the river input leaves the lake by underground seepage through porous volcanic material (Bergner et al., 2003). An understanding of this subsurface outflow process is fundamental to explaining the hydrochemical budget and solute export from the lake (Gaudet and Melack 1981; Ojiambo and Lyons 1996).

A major threat to Lake Naivasha is sediment pollution caused by human activities. The most important impacts are clearance of natural vegetation for agriculture, especially horticulture, and removal of the fringing papyrus swamps along the main inflow rivers, the Malewa and Gilgil, as these swamps buffer the lake from excess sediment input (Melack 1976; Harper et al., 1995). Consequences of sediment pollution are a reduction in water transparency and changes in the input and recycling of nutrients (Golterman et al., 1977). Additional factors that influence the health of the lake are the growing human population's activities in the upper catchment, which require increasing water abstraction from the lake and catchment (Jimho 2007). Since the 1920s, several exotic invasive species have been introduced into the lake, resulting in changes to the structure and dynamics of the food web. Despite these recent anthropogenic impacts, Lake Naivasha is still considered to be reasonably healthy (Hubble and Harper 2001).

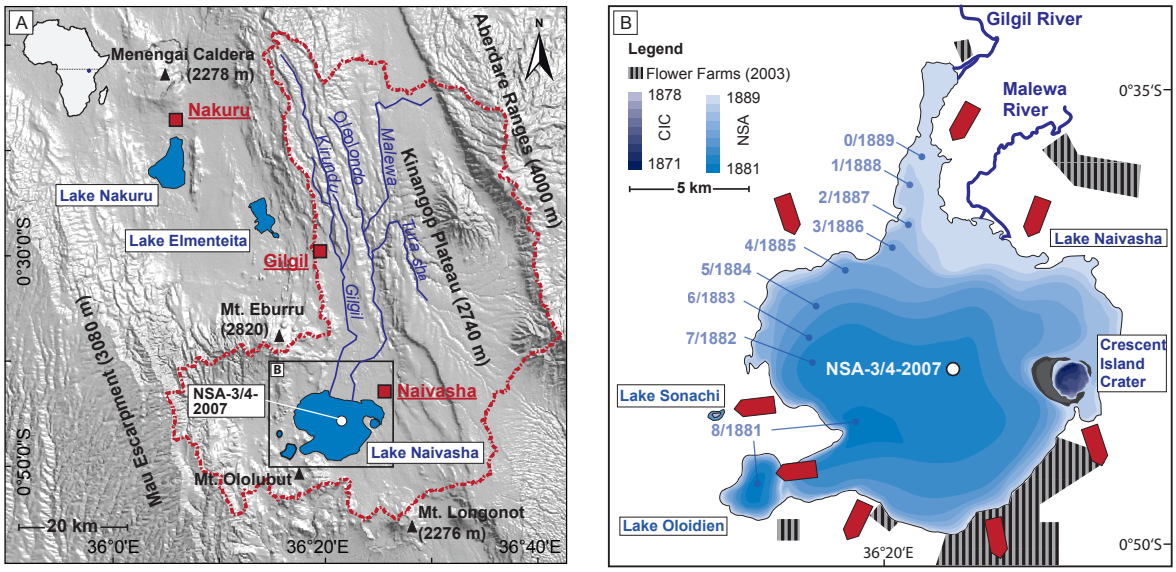

Figure A1.1 (A) Location map for Lake Naivasha within the highest basin of the Kenyan Rift System, together with the catchment area and sites discussed in the text. (B) Bathymetry of the Lake Naivasha main lake, and its satellite basins Crescent Island Crater and Lake Oloidien (1983), and Lake Sonachi (1990) (modified from Åse et al., 1986; Hickley et al., 2004; Verschuren 1999). Coring locality shown as white circle; arrows show the direction of groundwater flow, taken from Gaudet and Melack (1981).

A1.3 Material and Methods

A1.3.1 Core sampling

Parallel sediment cores (NSA-3 and NSA-4) were collected from the centre of Lake Naivasha (0°45'47.30"S, 36°21'58.31"E) in August 2007 with a KC Kajak sediment core sampler (KC-Denmark A/S) (Figure A1.1). A transparent coring tube was used and the core was extruded in the field. The core lengths (37.8 cm for NSA-3 and 35.4 cm for NSA-4) were limited by our inability to penetrate deeper into the compacted sediment (Figure A1.2).. Both cores were sampled at 2.1-cm intervals and samples were

stored in the dark in Whirl-Pak® plastic bags. Once in the laboratory, samples were kept in the dark at 10°C. Samples from the NSA-4 core were used for ^{210}Pb dating, while the NSA-3 samples were analysed for sediment type, organic content, and diatoms.

A1. 3.2 Chronology (^{210}Pb)

Oven-dried subsamples from the Lake Naivasha NSA-4 sediment core were analysed for ^{210}Pb, ^{226}Ra and ^{137}Cs by direct gamma assay in the Liverpool University Environmental Radioactivity Laboratory using Ortec HPGe GWL series well-type, coaxial, low-background intrinsic germanium detectors (Appleby et al., 1986). ^{210}Pb was determined via its gamma emissions at 46.5 keV, and ^{226}Ra by the 295 keV and 352 keV γ-rays emitted by its daughter radionuclide ^{214}Pb following 3 weeks of storage in sealed containers to allow radioactive equilibration. ^{137}Cs was measured by its emissions at 662 keV. The absolute efficiencies of the detectors were determined using calibrated sources and sediment samples of known activity. Corrections were made for the effect of self-absorption of low energy γ-rays within the sample (Appleby et al., 1992).

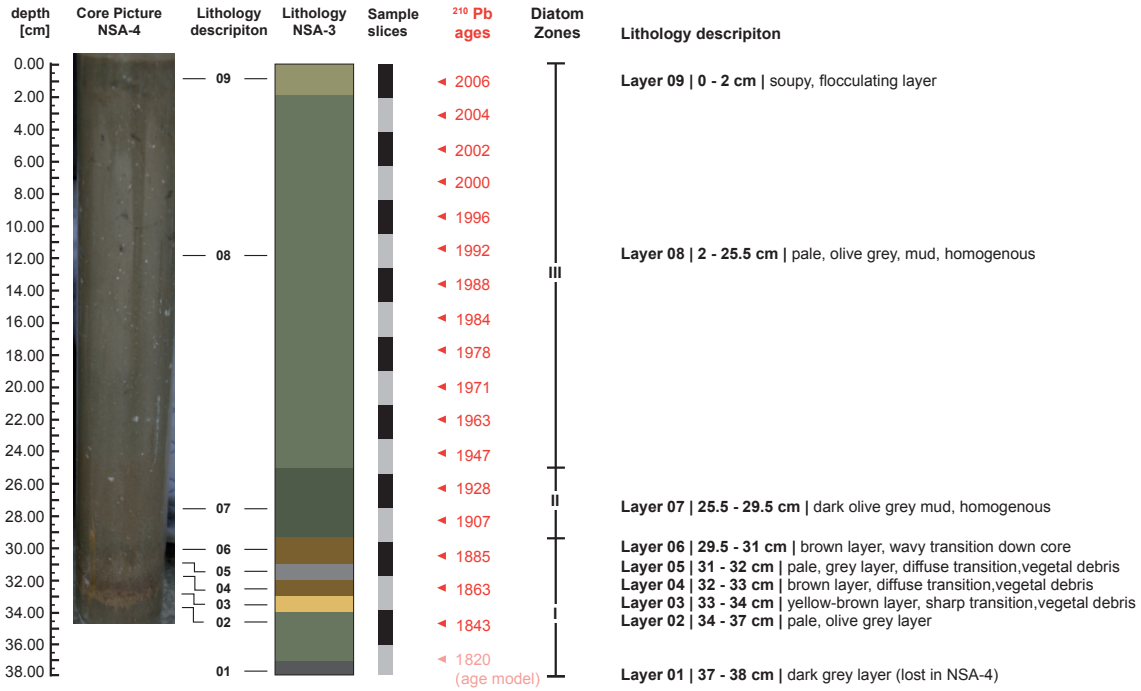

Figure A1.2 Lithology, chronology, sampling slices and diatom-based zonation of NSA-3/4. Sediment chronology in years AD, based on seventeen ^{210}Pb dates from NSA-4.

A1.3.3 Sedimentology and Geochemistry

Total carbon (TC) and total nitrogen (TN) were analysed concurrently by IR spectroscopy and heat conductivity detection after burning weighed aliquots in an oxygen gas flow at 1,350°C, using a LECO CHN-2000 Elemental Analyzer. The TOC was determined after release of CO_2 in carbonates by reaction with hot 4% and 25% HCl, followed by analysis with the LECO CHN-2000 system. Total inorganic carbon (TIC) was obtained by subtracting TOC from TC. Mass accumulation rates (MARs) of sediment components were calculated from the bulk sediment accumulation rate (SAR) * %M/100, where %M is the percent mass of TIC, TOC or TN.

Prior to sedimentological analysis, mineral assemblages in samples from NSA-3 were determined by X-ray diffraction (XRD) analysis of powdered bulk samples, without further treatment, using a Siemens D5000 diffractometer. In addition, sediment samples NSA-3-1 to NSA-3-18 were examined with an optical microscope to semi-quantitatively cross-check the mineral content as well as the abundance of sponge spicules, macrophyte fossils, and other constituents.

A1.3.4 Diatom counts and Transfer Functions

Between 0.25 and 0.35 g of sample material was processed for 90 minutes in 15-ml Falcon tubes containing 4 ml of 30% H_2O_2, which were placed in a water bath at 80°C. This was done to remove organic matter. After adding 10 µl of 2N HCl, sample tubes were filled with VE water and incubated overnight at 10°C. The supernatant was then discarded and samples were washed with VE water before being centrifuged at 3,000 rpm for 4 minutes. This washing step was repeated four times, after which 1:4 and 1:10 solutions were prepared and samples were settled on coverslips and dried overnight before being mounted on glass slides using Naphrax™. Diatom species identification was carried out using a Leica DM 4000B optical microscope at 1,000x magnification. A total of 300 to 500 valves were counted per slide. The diatom species were determined following Hustedt (1949), Gasse (1986) and Krammer and Lange-Bertalot (1986, 1988, 1991a, b). Diatom percentages were zoned using stratigraphically constrained cluster analyses with ZONE, an unpublished software tool provided by S. Juggins, University of Newcastle.

Major changes in the diatom assemblages over the last two centuries were determined by a detrended correspondence analysis (DCA) with CANOCO 4.5 software (ter Braak and Šmilauer 2002). The DCA also provided information about whether the species distribution was uniform or Gaussian with a single mode. The data were log-transformed in to stabilize the variance and rare species were down-weighted. A gradient length of 1.8 indicated a uniform species distribution. The main trends in diatom variations down-core were subsequently analysed using a principal component analysis (PCA) of the log-transformed species percentages.

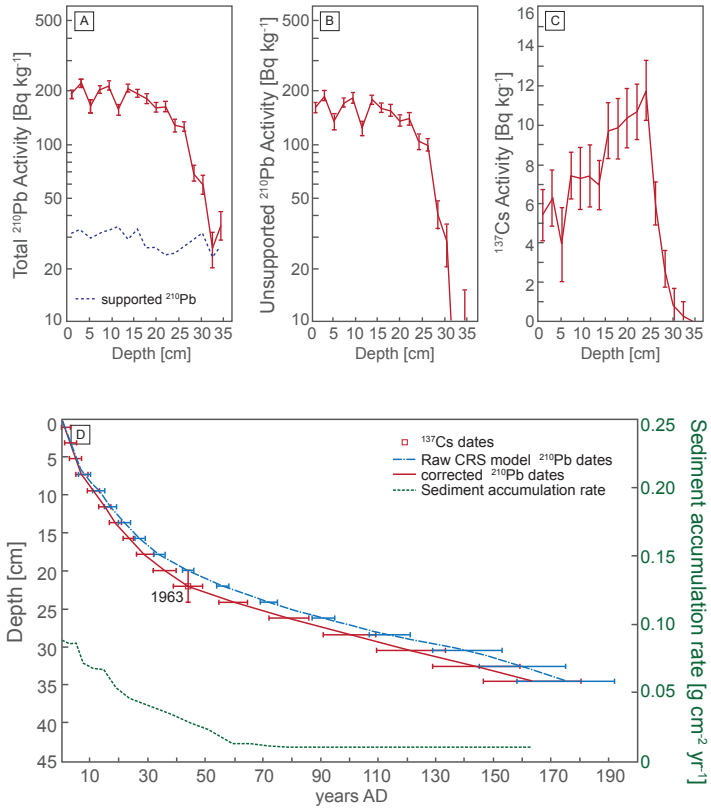

Figure A1.3 Radiometric chronology of Lake Naivasha sediment core NSA-4. Fallout radionuclides in the NSA-4 Lake Naivasha sediment core, showing (A) total and supported ^{210}Pb, (B) unsupported ^{210}Pb, (C) ^{137}Cs concentrations versus depth. (D) The raw CRS model ^{210}Pb dates and the 1963 depth determined from the ^{137}Cs record, together with the corrected ^{210}Pb dates and sedimentation rates calculated using the ^{137}Cs date as a reference point

Table A1.1
Fallout radionuclide concentrations in the Lake Naivasha core NSA-4-2007

		^{210}Pb			
Depth		Total	Unsupported	Supported	^{137}Cs
[cm]	[g cm^{-2}]	[Bq kg^{-1}]	[Bq kg^{-1}]	[Bq kg^{-1}]	[Bq kg^{-1}]
1.05	0.10	193.4 ± 10.8	161.9 ± 11.0	31.5 ± 2.1	5.4 ± 1.3
3.15	0.28	222.8 ± 11.9	189.9 ± 12.2	32.8 ± 2.5	6.3 ± 1.4
5.25	0.43	165.6 ± 14.2	135.8 ± 14.5	29.8 ± 3.0	3.9 ± 1.9
7.35	0.62	205.7 ± 9.8	173.9 ± 9.9	31.8 ± 1.7	7.4 ± 1.2
9.45	0.89	216.4 ± 12.9	183.7 ± 13.1	32.6 ± 2.2	7.3 ± 1.6
11.55	1.16	158.2 ± 11.2	123.9 ± 11.5	34.3 ± 2.7	7.4 ± 1.6
13.65	1.39	209.2 ± 10.4	180.2 ± 10.6	29.0 ± 2.0	7.0 ± 1.3
15.75	1.62	195.4 ± 9.7	162.3 ± 9.8	33.1 ± 1.7	9.7 ± 1.4
17.85	1.87	182.9 ± 12.0	156.6 ± 12.2	26.3 ± 2.3	9.8 ± 1.5
19.95	2.13	163.3 ± 9.6	137.2 ± 9.7	26.1 ± 1.8	10.4 ± 1.5
22.05	2.41	164.5 ± 10.9	140.6 ± 11.1	23.9 ± 2.1	10.7 ± 1.4
24.15	2.66	128.8 ± 10.7	104.6 ± 10.9	24.2 ± 2.2	11.8 ± 1.5
26.25	2.88	126.8 ± 7.7	99.9 ± 7.8	26.8 ± 1.5	6.0 ± 1.1
28.45	3.09	69.3 ± 7.1	40.6 ± 7.3	28.7 ± 1.5	2.7 ± 0.9
30.45	3.31	59.9 ± 7.4	27.9 ± 7.6	32.0 ± 1.6	0.9 ± 0.8
32.55	3.54	26.1 ± 6.0	3.2 ± 6.2	22.9 ± 1.3	0.3 ± 0.7
34.50	3.74	35.3 ± 6.6	8.4 ± 6.7	27.0 ± 1.3	0.0 ± 0.0

Salinity, as represented by conductivity (log10 µS cm^{-1}), was reconstructed using the East African Salinity dataset included in the European Diatom Database (EDDI, http://craticula.ncl.ac.uk/Eddi/jsp/index.jsp). This dataset includes 579 diatom species identified from 187 samples which came from 98

sites between latitudes 19°N and 14°S and longitudes 27°N and 43°E. The sites range from Afro-alpine bogs at altitudes of up to 4,000 m to hypersaline lakes below sea level. The conductivity in these lakes ranges from 40 to 50,000 µS cm^{-1} and the pH from 5 to 10.9. In this study, results were back-transformed into µS cm^{-1} and classified according to the ecological habitats of the species:planktonic, planktonic/littoral, littoral and littoral/epiphytic diatoms. The total phosphorus (TP) was reconstructed using the EDDI combined TP dataset, including 347 samples from various European lakes. Finally, the results were back-transformed to total phosphorus values in µg l^{-1}.

Diatom-based inference models based on weighted averaging with inverse deshrinking (WAinv) were used for the reconstruction of conductivity and TP, as this gives an overall lower root mean-squared error (RMSE) of prediction (Birks at al. 1990). We used modern analog technique (MAT) analysis to test how well fossil diatom assemblages were represented in the dataset. This analysis evaluates the sample of the dataset for the closest analogues of floristic match by means of a similarity index. An index value above 100-150 indicates a poor floristic similarity to any of the samples from the underlying dataset, while values below this threshold indicate a high similarity. The MAT analysis indicates whether or not the analysed samples are similar to those of the underlying datasets, thus providing a measurement of the validity of the reconstructed environmental features.

A1.4 Results

A1.4.1 Chronology (^{210}Pb)

Total ^{210}Pb activity reached equilibrium with ^{226}Ra activity at a depth of about 33 cm (Tab. A1.1, Figure A1.3a). Unsupported ^{210}Pb (Tab. A1.1, Figure 3.3b) declined irregularly with depth. Concentrations in the top 15 cm were relatively constant, fluctuating around a mean value of 164 Bq kg^{-1}. Below 15 cm, there was a slow decline down to a depth of 22 cm, at which point there was a relatively abrupt change to a much steeper gradient. Concentrations below 30 cm were close to or below the detection limit. ^{137}Cs concentrations had a well defined peak between 20 and 25 cm depth, probably recording the 1963 fallout maximum from atmospheric testing of nuclear weapons (Tab. A1.1, Figure A1.3c). Raw ^{210}Pb dates calculated using the CRS dating model (Appleby and Oldfield 1978) place 1963 at a depth of 20 cm, in relatively good agreement with the depth determined from the ^{137}Cs record (Tab. A1.1, Figure A1.3d). The mean, post-1963 SAR calculated from the ^{137}Cs stratigraphic date is 0.055 g cm^{-2} y^{-1}, compared to the mean pre-1963 value calculated from the gradient of the ^{210}Pb profile of 0.010 g cm^{-2} y^{-1}. Corrected ^{210}Pb dates were calculated by applying the CRS model in a piecewise way using the ^{137}Cs date as a reference level (Appleby 2001). Results suggest that the relatively slow SAR persisted until the middle of the 20th century, but increased significantly thereafter (Tab. A1.2, Figure A1.3). The mean SAR value during the past 10 years was 0.080 g cm^{-2} y^{-1}. Using the corrected ^{210}Pb chronology, the extrapolated age for the base of the NSA-3-18 core is 1820 AD, assuming a SAR of 0.01 g cm^{-2} y^{-1} at the maximum core depth.

A1.4.2 Lithology and Geochemistry

Sediments of the core from the centre of Lake Naivasha consist of 37.8 cm of organic mud that shows layers of different colors in the lower part of the core (Figure A1.2). Macroscopic observation is not supported by the XRD results. The large amount of organic matter in the sediment, including diatoms, overwhelms any mineralogical signal. Therefore, XRD is inapplicable for sediment investigations of the NSA-3 core.

Diatom composition and geochemistry of the NSA-3 core, together with their paleo-environmental interpretations, are summarized in Figures A1.4, A1.6 and A1.7. TOC accumulation rates vary between 1.2 mg cm^{-2} y^{-1} and 6.2 mg cm^{-2} y^{-1}, with rates increasing towards the top of the core. The generally low

TN accumulation rates show a similar trend, varying between 0.1 mg cm^{-2} y^{-1} and 0.8 mg cm^{-2} y^{-1}. TOC/TN ratios range between 4 and 9 and tend to increase slightly down-core. The accumulation of organic (TOC, TN) and inorganic (TIC) matter is almost constant throughout the period between 1843 and 1947 AD. After 1947, TOC, TC and TN accumulation rates increase regularly, all reaching a maximum in the uppermost sample, except for the TN rate, which decreases slightly in 2006. TIC accumulation rates fluctuate at the beginning of the 1970s, but show an overall increasing trend. Since MARs are a direct function of the bulk sedimentation accumulation rate, all MAR values increase significantly after 1947 AD (Tab. A1.2, Figure A1.6). TOC/TN ratios vary between 8 and 9 in the period between 1843 and 1990 AD, but then show a decreasing trend until 2004, dropping to a value of 4 before again increasing slightly towards 2006. The quantity of fine-grained minerals is constant throughout the sediment core, whereas the numbers of macrophyte fossils and sponge spicules increase sharply down-core from sample NSA-3-15 to sample NSA-3-18.

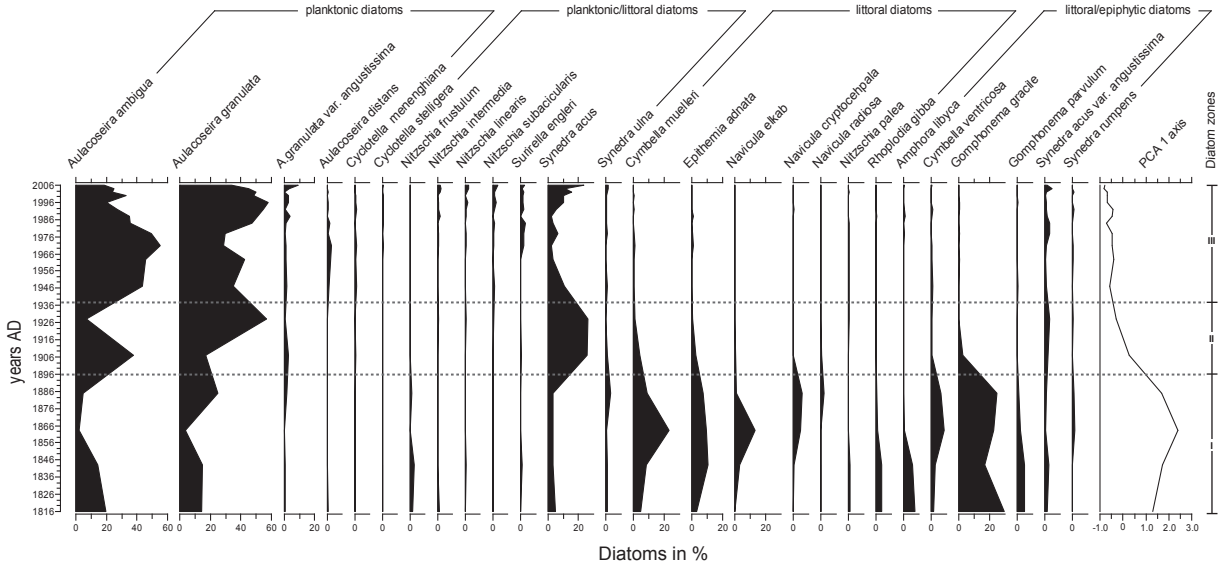

Figure A1.4 Summary of the diatom assemblages from Lake Naivasha core NSA-3, PC1 scores, and diatom-based zonation.

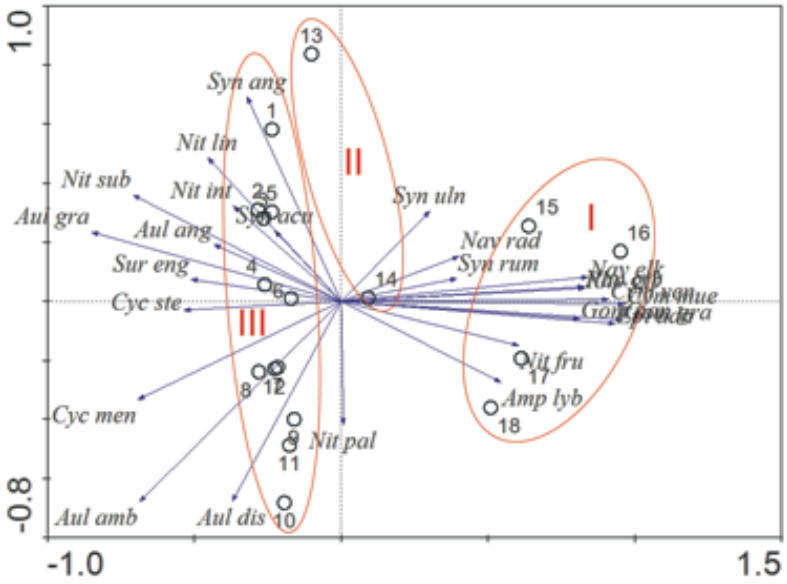

Figure A1.5 PCA biplot of species and sample data. Arrows represent species and circles represent samples. Ellipses indicate the diatom-inferred zones

Table A1.2
^{210}Pb chronolgy of the Lake Naivasha core NSA-4-2007

Depth	Chronology				Sedimentation Rate		
[cm]	[g cm^{-2}]	AD	years	error	[g cm^{-2} y^{-1}]	[cm^{-2} y^{-1}]	± [%]
0.00	0.00	2007	0	± 0	-	-	-
1.05	0.10	2006	1	± 2	0.089	1.01	8.0
3.15	0.28	2004	3	± 2	0.086	1.09	7.8
5.25	0.43	2002	5	± 2	0.086	1.05	11.6
7.35	0.62	2000	7	± 2	0.073	0.67	7.5
9.45	0.89	1996	11	± 2	0.068	0.53	8.9
11.55	1.16	1992	15	± 2	0.066	0.56	11.0
13.65	1.39	1988	19	± 2	0.054	0.50	8.7
15.75	1.62	1984	23	± 2	0.046	0.41	9.5
17.85	1.87	1978	29	± 3	0.042	0.34	11.6
19.95	2.13	1971	36	± 4	0.036	0.31	12.5
22.05	2.41	1963	44	± 5	0.029	0.18	15.2
24.15	2.66	1947	60	± 5	0.013	0.12	13.6
26.25	2.88	1928	79	± 7	0.010	0.11	13.6
28.45	3.09	1907	100	± 9	0.010	0.10	13.6
30.45	3.31	1885	122	± 12	0.010	0.09	13.6
32.55	3.54	1863	144	± 15	0.010	0.10	13.6
34.50	3.74	1843	164	± 17	0.010	0.10	13.6

Table A1.3
Stratigraphical zonation inferred by diatoms their dominant and subdominant diatom taxa.

Zone	Core depth [cm]	Age [year AD]	Dominant taxa	Subominant taxa
III	0 - 25.14	2006 - 1938	*Aulacoseira ambigua, Aulacoseira granulata*	*Synedra acus* sp.
II	25.14 - 29.45	1938 - 1896	*Aulacoseira granulata, Synedra acus* sp.	*Aulacoseira ambigua, Cymbella muelleri, Gomphonema gracile*
I	29.45 - 37.8	1896 - 1820	*Gomphonema gracile, Cymbella muelleri*	*Epithemia adnata, Aulacoseira granulata, Aulacoseira ambigua*

Table A1.4
Performance of the conductivity and TP models used for paleolimnological reconstructions.

Gradient	Method	r^2	RMSE	r_{jack}^2	RMSEP
Conductivity	WAinv	0.86	0.32	0.78	0.41
TP	WAinv	0.71	0.30	0.63	0.33

WAinv, weighted averaging with inverse deshrinking; RMSE, root mean squared error of prediction; RMSEP, jackknifed RMSE; r^2, jackknifed coefficient of determination.

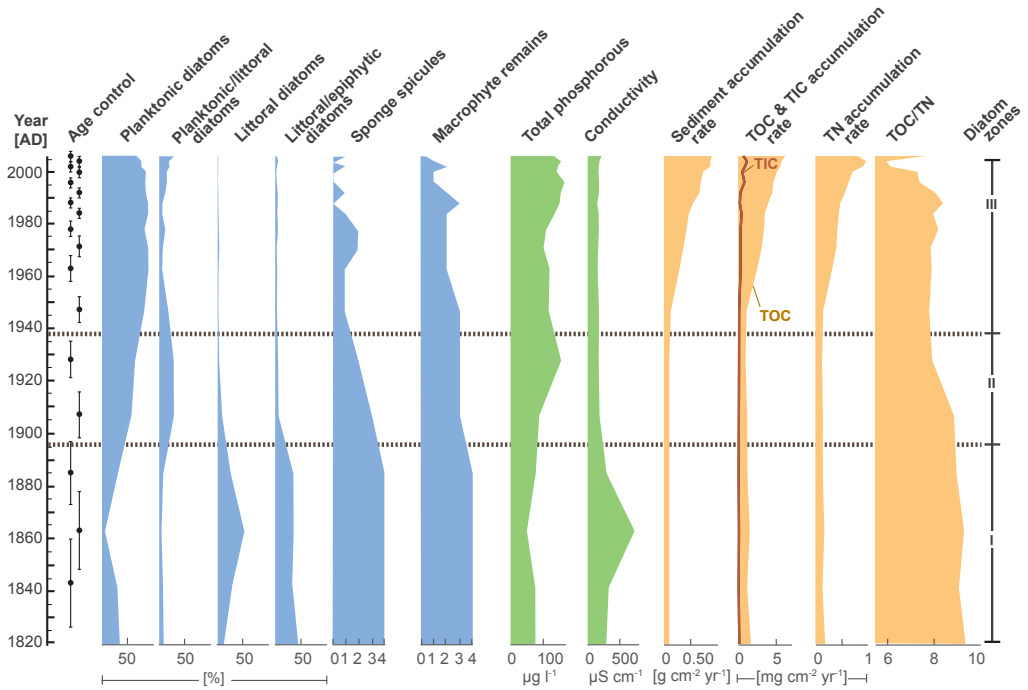

Figure A1.6 Down-core variations in diatom habitat preferences, diatom-based zonation, diatom-inferred conductivity and total phosphorous (TP) values, sediment accumulation rates (SAR) and mass accumulation rates for geochemical variables (TN-total nitrogen, TOC-total organic carbon, TIC-total inorganic carbon and the TOC/TN ratio) based on the age model. Age control is provided with error bars

A1.4.3 Diatom assemblages

Thirty-nine species were identified in the core, but only those whose abundances >0.5% were plotted in Figure A1.4. The species were grouped into four ecological types:planktonic, planktonic/littoral, littoral, and littoral/epiphytic, following Gasse (1986) and Gasse et al., (1995). Valve preservation was generally good throughout the core. Three diatom assemblage zones were identified in the core (Tab. A1.3, Tab. A1.4, Figure A1.4).

Zone I, between 38.7 and 29.5 cm, corresponds to the time interval between ca. 1820 and 1896 AD (samples NSA-3-18 to NSA-3-15). The diatom assemblage of this zone is dominated by the littoral/epiphytic and littoral diatoms Gomphonema gracile Ehrenberg (up to 26%), Epithemia adnata Kützing (up to 11%), Cymbella muelleri Hustedt (up to 22%), and Navicula elkab Müller (up to 18%). Abundances of planktonic species, such as Aulacoseira ambigua (Grunow) Simonsen and A. granulata (Ehrenberg) Simonsen, as well as the planktonic/littoral species Synedra acus Kützing, vary between 5% and 20%. In sample NSA-3-16 (33.6-31.5 cm, ca. 1863 AD), each of these planktonic species reaches a maximum abundance of only 5%, whereas Cymbella muelleri and Navicula elkab reach their maximum relative abundances within this zone, and reach similar abundances in samples NSA-3-18 to NSA-3-16. Aulacoseira sp. dominates in samples from NSA-3-16 to the top of the core. When A. ambigua is scarce, A. granulata is abundant, and vice versa.

Zone II ranges from 29.4 to 25.2 cm, corresponding to the time interval between ca. 1896 and 1938 AD (samples NSA-3-14 to NSA-3-13), and is transitional between Zones I and III. Within this zone, the planktonic/littoral Synedra acus is dominant, with a mean abundance of 23%. The planktonic species A. ambigua and A. granulata increase rapidly to peak abundances of 38% and 57%, respectively. The littoral and littoral/epiphytic species of flora decline and reach their minima around 1930 AD, shortly before the start of Zone III.

Zone III is the core interval between 25.1 and 0 cm, corresponding to the time interval between ca. 1938 and 2007 AD (samples NSA-3-12 to NSA-3-1). The diatom assemblage within this zone is characterized by A. ambigua, A. granulata and Syndra acus. The uppermost sample shows very high numbers of Synedra acus, however, with less frequent A. ambigua and A. granulata. The abundance of macrophytes and sponge spicules decreases within this zone, and they are almost absent between 1998 and 2004 AD (samples NSA-3-7 to NSA-3-2).

A1.4.4 Statistical analysis and environmental reconstruction

The PCA of the data matrix of samples and the diatom percentages show that the first two principle components (PC) account for 72% of the total variance (PC1 63%, PC2, 9%). The PC1 scores are plotted in stratigraphic order, together with the distribution of diatom species (Figure A1.4). Species and samples from the underlying dataset are plotted on the PC1 axis, with the inferred diatom zones marked in red ellipses (Figure A1.5). The grouping of samples in this plot suggests that PC1 serves as an indicator for the ratio of planktonic diatom species (negative PC1 scores) to epiphytic/littoral diatom species (positive PC1 scores). Moving up-core, the PC1 scores change from -0.8 to 2.4 with the change from littoral/epiphytic to planktonic assemblages in transitional Zone II.

The modern analogue technique (MAT) analysis for the conductivity dataset indicates a good floristic match by comparing species composition of the analysed samples with those of the underlying samples in the dataset. All identified species are included in the East African salinity dataset. Because the East African conductivity dataset contains several samples from Lake Naivasha, it shows good agreement with the analysed samples. Samples NSA-3-18 to NSA-3-15 (ca. 1816 to 1885 AD), and in particular sample NSA-3-16 (ca. 1863 AD), perform relatively poorly because they show a high abundance of littoral and littoral/epiphytic species, which may not typically occur in any of the dataset samples. Sample NSA-3-16 has the highest similarity to a mud sample from Lake Kamuru in Uganda. Most of the analysed samples, however, correlate best with either a sediment sample from Lake Rugwero in Rwanda or a core-top sample from Lake Naivasha (Crescent Island Crater site). All three modern analogue samples are from freshwater lakes.

Results of the conductivity and TP reconstructions are shown in Figure A1.6. Reconstructions indicate the highest conductivity values in Zone I, about 731 µS cm^{-1} in sample NSA-3-16 - ca. 1863 AD, driven mainly by the occurrence of littoral species Cymbella muelleri and Navicula elkab. In particular, N. elkab favors highly saline (~13 mS cm^{-1}) and alkaline (~pH 9) waters (Gasse 1986). Apart from this sample, Zone I is characterized by an average reconstructed conductivity of 300 µS cm^{-1}. Conductivity values for Zones II and III are almost identical, generally varying between 150 and 185 µS cm^{-1}. The uppermost core sample (Zone III) shows a slightly higher conductivity value (215 µS cm^{-1}).

The TP dataset includes only 34 of the 39 diatom species identified in our study. The MAT analyses for TP reconstructions were therefore of poorer quality than the conductivity reconstructions. Uppermost sample and samples NSA-3-18 to NSA-3-15 have the least similarity to the dataset samples, which relates to the fact that Navicula elkab and Cymbella muelleri are completely absent from the dataset. The diatom-inferred TP reconstruction yields lowest values in Zone I, including a minimum of 49 µg l^{-1} in sample NSA-3-16. Moderate TP values of ca. 80 µg l^{-1} are indicated for Zone II. After ~1938, the reconstructed TP values increase briefly to 155 µg l^{-1} and then decline to 100 µg l^{-1} at around 1970 AD. The reconstructed TP values subsequently increase to a maximum of 164 µg l^{-1} in 1996 (sample NSA-3-5) before once again decreasing slightly to 132 µg l^{-1} at present.

A1.5 Discussion

The radiometric chronology of the Naivasha core is thought to be quite reliable for the time between 1907 and 2007 AD, showing a low, ±2-5 yr error range. The raw ^{210}Pb dates place 1963 at a depth of 20 cm, which is in relatively good agreement with the depth determined from ^{137}Cs.
The ^{137}Cs peak appears to preclude mixing as a cause of the irregular ^{210}Pb record. Before 1907 AD, errors on dates are greater, from ±9 years (sample NSA-3-14) to ±17 years (sample NSA-3-17). This section of the core also displays an apparent decrease in sedimentation rate, which must be interpreted with caution.
Sedimentation rates and geochemical data, together with the environmental reconstructions of conductivity and total phosphorus, conform with the three diatom assemblage zones (Figure A1.7). Zone I covers the time from 1820 to the end of the 19th century and was influenced mainly by natural climate variations, in particular by long periods of drought. Zone II represents a transition zone characterized by a shift from primarily climate-driven influences to a period when human increasingly altered the environment of Lake Naivasha. In Zone III, which covers the period from 1938 to 2007 AD, natural conditions in the lake are overprinted by anthropogenic influences, which are mainly reflected by high sedimentation rates and a rapid shift in the diatom assemblage.

A1.5.1 Zone I (ca. 1820 to 1896 AD):

"Natural climatic variations – minor human activity"

Relatively low and constant bulk sediment accumulation rate (0.01 g cm^{-2} y^{-1}) and mass accumulation rates for TN (0.2 mg cm^{-2} y^{-1}) and TOC (2 mg cm^{-2} y^{-1}) indicate low sediment input from the catchment into Lake Naivasha during this period. The influence of human activity was minor because nomadic tribes only made sporadic use of the lake and its surroundings for water supply and food. The diatom-inferred TP values are relatively low, but increase slightly from 50 µg 1^{-1} to 88 µg 1^{-1} between 1863 and the end of Zone I. According to the classification scheme for warm-water tropical lakes, TP values serve as an indication of the shift from mesotrophic to eutrophic conditions (Salas and Martino 1991). A growing predominance of littoral and/or epiphytic diatom assemblages is indicative of rising conductivity values ranging between 290 µS cm^{-1} and 731 µS cm^{-1}, suggesting low water level in the lake, presumably caused by a drier climate. Low TN values and TOC/TN ratios ~9 reflect organic matter contributions from epiphytic and/or benthic diatoms and abundant aquatic macrophytes, both indicative of low water levels related to drier conditions (Meyers 2003). This interpretation is consistent with the large numbers of sponge spicules in the sediments, and the historically documented Laparanat-Mahlathule drought that caused low lake stands between 1760 and 1840 (Verschuren et al., 2000). Reconstructed lake levels for the Crescent Island Crater (CIC) indicate two major lowstands during this period (Verschuren et al., 2000), whereas East African rainfall anomalies reconstructed by Nicholson (2001) indicate a prolonged dry period with rare events of pronounced rainfall. Zone I contains only one peak in inferred conductivity around 1863±15 AD, during the identified long dry period. This may have been a consequence of erosion and dissolution of salts formed during the long drought that occurred before 1840 AD, and perhaps lasted even longer, as suggested by the records of Verschuren (2000) and Nicholson (2001). Lake Naivasha is particularly sensitive to such declines in lake stage in that a small drop in lake level exposes a large area of lake bottom due to the shallow slope of the littoral area, particularly along the north shore. Declining lake level caused by a dry climate may have desiccated lake sediments where evaporites accumulated (LNROA 1993, Gaudet 1979). Thus, conductivity rises, rather than falls, with the onset of rains, as dissolved ions increase in the system with greater precipitation (Figure A1.4). A rise in water level dissolved accumulated salts in the previously exposed sediments, which led to a brief increase in conductivity, with a peak of 731 µS cm^{-1} about 1863±15 AD (sample NSA-3-16). Thereafter, the Naivasha basin was persistently filled with water and the lake displayed lower conductivity. Considering the age error on sample NSA-3-16, it is not possible to identify

exactly which precipitation event led to this early conductivity peak. It could have been the short wet period around 1850 AD (Verschuren 2000), alternatively 1860 or 1870 AD, years for which Nicholson (2001) inferred enhanced rainfall events.

Another explanation for the single conductivity peak is that lake level had decreased considerably after a long drought, which led to higher conductivity values in the Lake. Because sample NSA-3-16 represents ~20 years of lake history, and thus the average conductivity during that time, it is very difficult to infer the short-term environmental changes that occurred during that period, though there may have been high variability. It is difficult to compare our diatom record from the main basin of Lake Naivasha with lake level changes in the Crescent Island Crater. Although the basins are hydrologically connected from time to time, their bathymetries differ, and consequently, they may display differences in sedimentation patterns and sensitivity to climate changes.

In general, high conductivity is indicated by the presence of two littoral species, Cymbella muelleri and Navicula elkab, and the littoral/epiphytic species Gomphonema gracile, which is very sensitive to pollution in modern lakes (Kelly et al., 2005). All three species favor water with moderate to high ionic strength, from 1,000 to 30,000 µS cm^{-1} (Gasse 1986). The conductivity values decrease up-core from ~1863 until the beginning of the 20th century, and remain constant at ~170 µS cm^{-1} thereafter. This change in water chemistry corresponds to a decrease in littoral and epiphytic diatom frequencies. After a generally dry period from 1820 to 1882 (Nicholson 2001) during which Lake Naivasha was nearly desiccated and its groundwater reservoirs emptied, a wetter period occurred from 1883 to 1894 (Nicholson 1995).

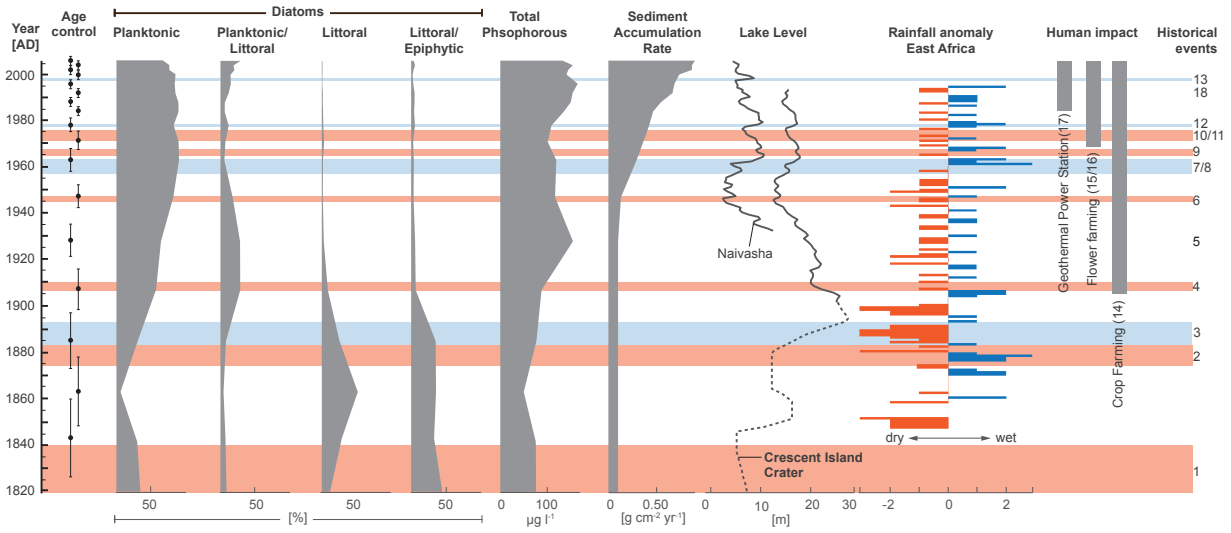

Explanation historical events & human impact

1 1760 - 1840 Laparanat drought (equatorial drought as part of the Little Ice Age); Lake Naivasha fell dry (a, b)
2 1870s - early 1880 nearly desiccation of Lake Naivasha and Lake Sonachi (c)
3 1883 - 1894 major transgression of Lake Naivasha following a decade of above-average rainfall (a)
4 1906 - 1910 low stand Lake Sonachi (d)
5 1928 Subukia Earthquake
6 1946 historical low stand Lake Naivasha (d)
7 1956 - 1958 wet period (e)
8 1961 - 1963 wet period (e, f, g)
9 1964 - 1967 drought
10 1972 - 1973 drought (d)
11 1975 - 1976 drought (d)
12 1977 - 1978 wet period (d)
13 1997 - 1998 El Nino - wet period
14 1904 - 1918 intensive coffee farming Aberdare Ranges
15 1969 begin flower farming
16 1982 intensive flower farming
17 1984 start Kengen thermal power station
18 ~1990 liberalization of fertilizers in Kenya (h)

Figure A1.7 Compilation of diatom assemblage variations, sediment accumulation rate (SAR), total phosphorus (TP) and historical records of environmental and land use data. Water levels for the main Lake Naivasha (NSA) are instrument-based while those for the Crescent Island Crater Lake (CIC) are a combination of instrumental (solid line) and sediment proxy (dashed line) (Åse et al., 1986; Verschuren et al., 2000). Rainfall anomaly for Eastern Africa (EA):data combined from rainfall proxy indicators for the 19th century and instrumental data for the 20th century, from Nicholson (2001). References to historical events:a - Nicholson 1995; b – Verschuren 2001; c – Sikes 1936; d – Verschuren 1999; e – Nicholson 1988; f - Vincent et al., 1979; g - Gaudet and Melack 1981; h – Ariga and Jayne 2006; blue bars indicate historical highstands of CIC/NSA or Lake Sonachi; red bars indicate historical lowstands of CIC, NSA or Lake Sonachi. Age control is provided with error bars.

A1.5.2 Zone II (ca. 1896 to 1938 AD):

"Transition zone - increased human activity"

From about 1883 to 1894 AD, Naivasha experienced a wetter period, indicated by a lake level highstand in the Crescent Island Crater (Verschuren et al., 2000), although sedimentation rates during that time were still low (0.01 g cm^{-2} y^{-1}). An increase in commercial farming of tea and coffee in the early 20th century had no discernible effect on sedimentation rate in the lake. Such large catchments are known to store sediments in sinks within the basins for many years before they transported to the lake. Nutrients, however, reach the lake much more quickly, as they are transported rapidly in dissolved form after rainfall events (Phillips 2003). This may explain the rapid increase in total phosphorus from around 1900 AD. Since the 1930s, the diatom-inferred TP values have exceeded 111 µg 1^{-1}, indicating progressive eutrophication of the lake (Salas and Martino 1991). The arrival of the British colonists at the end of the 19th century and the intensive tea and coffee farming that followed coincide with nutrient enrichment of Lake Naivasha. Nutrient input favored planktonic species A. ambigua and A. granulata, both of which increased in abundance within this zone and maintain high abundance in Zone III. A slight decline in TOC/TN ratios towards values ~8 indicative of planktonic diatoms parallels the rising TP values (Meyers 2003). This implies a direct link to increased nutrient input in the lake from intensive coffee, tea and pyrethrum farming in the highland areas of the catchment.

Following this wet episode of the late 19th century, climate became drier beginning around 1910 AD, as indicated by a shift to a negative water balance (Nicholson 2001). Nevertheless, the large aquifers that filled during the wet period continued to provide groundwater to the lake, contributing to the low salinity in Lake Naivasha.

A1.5.3 Zone III (ca. 1938 to 2007 AD):

"Human activity overprints natural climatic variation"

At the beginning of Zone III, the sediment accumulation rate increased to a maximum of 0.08 g m^{-2} y^{-1}. The most likely reason for this higher sediment accumulation rate was human activity within the catchment. Conversion of natural sediment traps such as papyrus swamps to horticulture and intensively farmed landscapes in the upper catchment fostered soil erosion and consequent sediment delivery to the lake. Anomalously high rainfall between 1962 and 1964 and a relatively wet period that continued through 1990 AD contributed to further degradation of the loose upper soil layers. The Ba/Ca ratios of marine corals off the East African coast (Fleitmann et al., 2007) support our interpretation of increasing erosion within Zone III since the year 1908±5 AD due to human activities in the Kenyan Highlands.

Eutrophication in Zone III was caused by an increased supply of phosphorus and nitrogen to the lake (Osborne 2000). The steady rise of Aulacoseira sp., which prefers nutrient-rich waters, coincides with a reduction in species that are more sensitive to pollution, such as Gomphonema gracile, and indicates the continuing eutrophication of Lake Naivasha. The diatom-inferred total phosphorus values show a positive trend since ca. 1963, increasing to 165 µg l^{-1} in 1996. This trend in TP is probably attributable to the increasing numbers of Aulacoseira within Zone III. Aulacoseira species occur commonly in eutrophic European and American lakes (Kilham et al., 1986; Karst et al., 1998; Anderson et al., 1990), and this genus is therefore regarded as an indicator of eutrophic conditions. Ballot et al., (2009) found TP values between 70 and 200 µg 1^{-1} in Lake Naivasha from 2001 to 2005, and noted that the eutrophication of the lake was reflected by changes in the phytoplankton community, including a decrease in species richness. Modern Lake Naivasha is dominated by Cyanocatena planktonica (Cyanobacteria), Pediastrum simplex (Chlorophyceae) and A. granulata.

Along with rising SARs, TOC and TN accumulation rates rise between 1947 and 2007 AD. The TOC/TN ratios are fairly stable around 8 until 1990 AD. According to Meyers (2003), TOC/TN values between 4

and 8 reflect an abundance of nitrogen-rich proteinaceous organic matter source such as phytoplankton. Diatoms account for a large proportion of the algae in Lake Naivasha, and TOC/TN values around 9 drop even lower towards the top of the core. This may have been due to TN enrichment. An increase in TN could be attributed to the use of fertilizers in Kenya after 1990, when the fertilizer market was liberalized in the early 1990s (Ariga and Jayne 2006).

Total nitrogen and phosphorus are minor contributors to the conductivity of lake waters, as is silicate. These constituents, however, are important in biological cycles. They are often the drivers of productivity in continental waters and are incorporated into living organisms. Because of their contribution to the ionic strength of waters, is not surprising that diatom-inferred conductivity remained relatively constant (~170 µS cm^{-1}) during the eutrophication process.

The growing human population and intensive flower farming on the southern shore of the lake brought fertilizers into the lake and further promoted eutrophication. Despite inputs of sediments and nutrients, as well as dam construction and removal of water in the catchment areas, and water consumption by the Olkaria geothermal power station, Lake Naivasha remains a freshwater system. Even the documented lowstand of Lake Naivasha between 1944 and 1955 (~5 m lowering) did not increase the conductivity, according to the diatom flora. The hydrological balance of the lake is highly dependent on groundwater flow, which may explain the lack of a conductivity response to arid intervals (Telford and Lamb 1999; Ayenew et al., 2007). A recent study on Lake Beseka in the Ethiopian Rift Valley suggests a close relationship between tectonic activity and expansion of the lake due to enhanced groundwater discharge (Goerner et al., 2008). This model may also apply to Lake Naivasha, which is also situated within a highly tectonically active region.

A1.6 Summary and Conclusions

In summary, this study has shown that over the last ~200 years, Lake Naivasha's water chemistry and biology have been influenced by natural climatic variations and anthropogenic activities. Lake Naivasha's water level responded to natural rainfall variations, as occurred in the period between 1820 and 1882 AD, when long dry periods led to low water levels and/or complete desiccation (Verschuren et al., 2000). The enduring Laparanat drought (1760-1840 AD) caused slightly saline conditions in the lake and favored the abundance of saline-tolerant diatoms such as Navicula elkab and Cymbella muelleri. In the generally wetter period from 1883 to 1894 AD, the lake received more freshwater from the catchment and groundwater reservoirs, which helped maintain the freshwater nature of the lake. These freshwater conditions favor diatoms such as Synedra sp. and Aulacoseira sp. that prefer waters with low conductivity. After 1900 AD, shorter wet and dry periods alternated and the lake level fluctuated in response to these variations. This is documented by instrumental lake level data since 1932 and by both proxy and instrumental rainfall data since 1850 (Nicholson 2001). The sediment accumulation rate increased from 1947 to 2007 AD, due to higher rates of soil erosion from cultivated areas within the lake catchment, rather than as a consequence of intensive rainfall. Higher erosion rates caused greater inputs of nutrients and pollutants to the lake. Nutrient-rich waters favored eutrophic diatoms such as Aulacoseira sp. and led to displacement of pollution-sensitive diatom species such as Gomphonema gracile.

Since the middle of the 20th century, intense anthropogenic activity around Lake Naivasha has led to cultural eutrophication, which has overprinted the influence of natural climate variation on the lake. Several previous studies have suggested that human activity, in particular agriculture, is the main reason for higher sediment fluxes into lakes (Mannion 1995; Bookman et al., 2010). In addition to inputs of soil and nutrients, transport of fertilizers, pesticides, and other pollutants resulting from intensive land use, has far-reaching implications for the future of Lake Naivasha and numerous other lakes (Plater 2006). This study demonstrated that Lake Naivasha is highly sensitive to changes in catchment

activities. It will therefore be important to monitor conditions in the lake that are influenced by anthropogenic activities, to be able to manage the lake wisely. The human population around the lake, as well as numerous other species, depend on the health of Lake Naivasha.

Acknowledgements

This project was carried out through the Graduate School's GRK 1364 research program on ‘Shaping Earth’s Surface in a Variable Environment’, funded by the German Research Foundation (DFG). We are grateful to the Government of Kenya (Research Permits MOST13/001/30C 59/10, 59/18 and 59/22) and the University of Nairobi for the research permits and their support. We also thank Yannick Garcin and Laura Epp for the field support that they provided. We are grateful to Antje Musiol for the TC and TN measurements, and to Peter Appleby from the University of Liverpool for the ^{210}Pb dating. We would also like to thank Ulrike Herzschuh, Andreas Bergner and all of the graduate school members and participants for inspiring discussions. We also thank Ed Manning for professional proofreading of the manuscript.

References

Anderson NJ, Rippey B, Stevenson AC (1990) Change to a diatom assemblage in a eutrophic lake following point source nutrient re-direction:a paleolimnological approach. *Freshwat Biol* 23:205-217.

Appleby PG, Nolan PJ, Gifford DW, Godfrey MJ, Oldfield F, Anderson NJ, Battarbee RW (1986) ^{210}Pb dating by low background gamma counting. *Hydrobiologia* 141:21-27.

Appleby PG, Oldfield F (1978) The calculation of ^{210}Pb dates assuming a constant rate of supply of unsupported ^{210}Pb to the sediment. *Catena* 5:1-8.

Appleby PG, Richardson N, Nolan PJ (1992) Self-absorption corrections for well-type germanium detectors. Nucl Inst Methods B 71:228-233.

Appleby PG (2001) Chronostratigraphic techniques in recent sediments, in Tracking Environmental Change Using Lake Sediments. In:Last WM, Smol JP (eds) Volume 1:Basin Analysis, Coring, and Chronological Techniques. Kluwer Academic:171-203.

Ariga J, Jayne TS (2006) Can the market deliver? Lessons from Kenya's rising use of fertilizer following liberalization. Policy brief, Tegemeo Institute for Agricultural Development and Policy 7:1-4.

Åse LE (1987) A note on the water budget of lake Naivasha, Kenya. *Geografiska Annaler* 69A:3-4.

Ayenew T, Becht R, Lieshout van A, Gebreegziabher Y, Legesse D, Onyando J (2007) Hydrodynamics of topographically closed lakes in the Ethio-Kenyan Rift:The case of lakes Awassa and Naivasha. *Journal of Spatial Hydrology* 7:1.

Ballot A, Kotut K, Novelo E, Krienitz L (2009) Changes of phytoplankton communities in Lakes Naivasha and Oloidien, examples of degradation and salinization of lakes in the Kenyan Rift Valley. *Hydrobiologia* 632:359–363.

Bergner AGN, Trauth MH, Bookhagen B (2003) Paleoprecipitation estimates for the Lake Naivasha basin (Kenya) during the last 175 k.y. using a lake-balance model. *Global Planetary Change* 36:117-136.

Birks HJB, Line JM, Juggins S, Stevenson AC, and ter Braak CJF (1990) Diatoms and pH reconstruction. Philosophical Transactions of the Royal Society of London, B 327:263–278.

Bookman R, Driscoll CT, Effler SW, Engstrom DR (2010) Anthropogenic impacts recorded in recent sediments from Otisco Lake, New York, USA. *J Paleolimnol* 43:449–462.

Clarke MCG, Woodhall DG, Allen D, Darling G (1990) Geological, volcanological and hydrogeological controls on the occurrence of geothermal activity in the area surrounding Lake Naivasha, Kenya. Ministry of Energy 1-138.

Edeghonghon Jimoh H, Vogler C, Waters, JJJ (2007) Perceived and real sources of pollution in Lake Naivasha. http://www.pdf-searcher.com/Perceived-and-real-sources-of-pollution-in-Lake-Naivasha.html, 01.12.2010.

EDDI, http://craticula.ncl.ac.uk/Eddi/jsp/, 12.09.2009.

Fleitmann D, Dunbar RB, McCulloch M, Mudelsee M, Vuille M, McCanahan TR, Cole JE, Eggins S (2007) East African soil erosion recorded in a 300 year old coral colony from Kenya. *Geophys Res Lett* 34, L04401 doi:10.1029/2006GL028525.

Fritz SC (2008) Deciphering climatic history from lake sediments. *J Paleolimnol* 39:5-16.

Gasse F (1986) East African diatoms - Taxonomy, ecological distribution. Bibliotheca diatomologica 11. Cramer, Stuttgart, 202 p.

Gasse F, Juggins S, Ben Khelifa L (1995) Diatom-based transfer functions for inferring hydrochemical characteristics of African palaeolakes. *Palaeogeography, Palaeoclimatol,ogy Palaeoecology* 117:31–54.

Gaudet JJ, Melack JM (1981) Major ion chemistry in a tropical African lake basin. *Freshw Biol* 11:309-333.

Goerner A, Jolie E, Gloaguen R (2008) Non-climatic growth of the saline Lake Beseka, Main Ethiopian Rift. *J Arid Environ* 73, 3:287-295.

Golterman HL (1977) Sediments as a source of phosphate for algal growth. In:Golterman HL (ed), Interactions between sediments and fresh water. Proceedings of an International Symposium held at Amsterdam, 6-10 September 1976. The Hague, Dr W Junk Publishers, Wageningen, PUDOC p 286–293.

Harper DM, Adams C, Mavuti K (1995) The aquatic plant communities of the Lake Naivasha wetland, Kenya:pattern, dynamics, and conservation. *Wetlands Ecol Manag* 3:111-123.

Hausmann S, Lotter AF, van Leeuven FN, Ohlendorf C, Lemcke G, Grönlund E, Sturm M (2002) Interactions of climate and land use documented in the varved sediments of Seebergsee in the Swiss Alps. *Holocene* 12:279–289.

Hubble DS and Harper DM (2001) What defines a healthy lake? Evidence from Lake Naivasha, Kenya, A*quat Ecosyst Health* 4:243-250.

Hustedt F (1949) Süßwasserdiatomeen aus dem Albert-Nationalpark in Belgisch Kongo, In:Damas H (ed), Exploration du Parc National Albert (1935-1936). Hayez, Bruxelles.

Karst TL, Smol JP (1998) Tracking the cultural eutrophication history of Collins Lake (Southeastern Ontario, Canada) using paleolimnological techniques. *Lake and Reservoir Manag* 14:456-465.

Kelly MG, Bennion H, Cox EJ, Goldsmith B, Jamieson J, Juggins S, Mann DG , Telford JR (2005) Common freshwater diatoms of Britain and Ireland:an interactive key. Environment Agency, Bristol.

Kilham P, Kilham SS, Hecky RE (1986) Hypothesized resource relationships among African planktonic diatoms. *Limnol Oceanogr* 31:1169:1181.

Krammer K, Lange-Bertalot H (1986–1991) Süβwasserflora von Mitteleuropa, vols. 2/1–2/4. Gustav Fischer Verlag, Stuttgart.

LNROA - Lake Naivasha Riparian Owners Association (1993) A three-phase environmental impact study of recent developments around Lake Naivasha. Phase I, An assessment of current information on the lake, relevant to a management plan, and recommendations for phase II of the study. LNROA, Naivasha, 109p.

Lotter AF and Birks HJB (1997) The separation of the influence of nutrients and climate on the varve time-series of Baldeggersee, Switzerland. *Aquat Sci* 59:362–375.

Mannion AM (1995) Agriculture and environmental change:temporal and spatial dimensions. Wiley, Chichester.

Melack JM (1976) Limnology and Dynamics of Phytoplankton in Equatorial African Lakes. Ph.D Thesis, Duke University, USA.

Meyers PA (2003) Applications of organic geochemistry to paleolimnological reconstructions:a summary of examples from the Laurentian Great Lakes, Org *Geochem* 34:261. 289.

Moy, CM, Seltzer, GO, Rodbell, DT, and Anderson, DM, 2002, Variability of El Niño/Southern Oscillation activity at millennial timescales during the Holocene epoch: *Nature*, 420:162–165.

Nicholson SE, Kim J, Hoopingarner J (1988) Atlas of African rainfall and its interannual variability. Florida State University.

Nicholson SE (1995) Environmental change within the historical period. In:Goudie AS, Adams WM, Orme A (eds), The physical geography of Africa. Oxford Univ. Press, p 60–75.

Nicholson SE (1996) A review of dynamics and climate variability in Eastern Africa. In:Johnson TC, Odada EO (eds), The Limnology, Climatology and Paleoclimatology of the East African Lakes. Gordon and Breach, Amsterdam, p 25–56, 63–75.

Nicholson SE (2001) Climatic and environmental change in Africa during the last two centuries. *Clim Res* 17:123–144.

Ojiambo BS and Lyons WB (1996) Residence times and major ions in Lake Naivasha, Kenya, and their relationships to lake hydrology. In:Johnson TC, Odada EO (eds), The Limnology, Climatology and Paleoclimatology of the East African Lakes. Gordon and Breach, Amsterdam, p 267–278.

Osborne PL (2000) Tropical Ecosystems and Ecological Concepts. University Press, Cambridge p 177–182.

Paaijmans, KP, Read AF and Thomas MB (2009). Understanding the link between malaria risk and climate, *PNAS 18,. 106:13844-13849* doi:10.1073/pnas.0903423106 Phillips J (2003) Alluvial storage and the long-term stability of sediment yields. *Basin Res* 15:153–163.

Plater AJ, Boyle JF, Meyers C, Turner SD, Stroud RW (2006) Climate and human impact on lowland lake sedimentation in Central Coastal California:the record from c. 650 AD to the present. *Reg Environ Change* 6:71–85.

www.ramsar.org, 29.11.2010

Salas HJ, Martino P (1991) A simplified phosphorus trophic state model for warm-water tropical lakes. *Water Res* 25:341-350.

Saji NH, Goswami BN, Vinayachandran PN, Yamagata T (1999) A dipole mode in the tropical Indian Ocean. *Nature* 401:360–363.

Sikes HL (1935) Notes on the hydrology of Lake Naivasha. Journal of East Africa and Uganda Natural History Society 13:74-89.

Telford RJ, Lamb HF (1999) Groundwater-mediated response to Holocene climatic change recorded by the diatom stratigraphy of an Ethiopian crater lake. Q*uat Res* 52:63-75.

ter Braak CJF, Šmilauer P (2002) CANOCO references manual and user's guide to Canoco for Windows:software for Canonical Community Ordination version 4.5. Microcomputer Power, Ithica, NY.

Trauth MH, Deino AL, Bergner AGN, Strecker MR (2003) East African climate change and orbital forcing during the last 175 kyr BP. *Earth Planet Sc Lett* 206:297-313.

Trauth MH, Maslin MA, Deino A, Strecker MR (2005) Late Cenozoic moisture history of East Africa. *Science* 309:2051-2053.

Trauth MH, Maslin MA, Deino A, Junginger A, Lesoloyia M, Odada EO, Olago DO, Olaka LA, Strecker MR, Tiedemann R (2010) Human evolution in a variable environment:The amplifier lakes of Eastern Africa. *Quaternary Sci Rev* 29:2981-2988.

Vincent CE, Davies TD, Beresford AKC (1979) Recent changes in the level of Lake Naivasha, Kenya, as an indicator of equatorial Westerlies over East Africa. *Clim Change* 2:175-189.

Verschuren D (1996) recent and late Holocene paleolimnology of lakes Naivasha and Sonachi, Kenya. Ph.D Thesis, University of Minnesota, USA.

Verschuren D (1999) Influence of depth and mixing regime on sedimentation in a small, fluctuating tropical soda lake. *Limnol Oceanogr* 44:1103-1113.

Verschuren D, Laird KR, Cumming BF (2000) Rainfall and drought in equatorial east Africa during the past 1,100 years. *Nature* 403:410-414.

Verschuren D (2001) Reconstructing fluctuations of a shallow East African lake during the past 1800 yrs from sediment stratigraphy in a submerged crater basin, *J Paleolimno*l 25:297-311.

SUPPLEMENTARY MATERIAL

1. **Figure S1** Rainfall distribution for each season between 1996-2010 in East Africa, based on ten day satellite Rainfall Estimates (RFE) from FEWSNET. The seasons are classified as MAM (March, April, May), JAS (July. August, September) ON (October, November) DJF (December January February)shaded grey area represents the solar flux for the period. The East African Country boundaries are outlined.

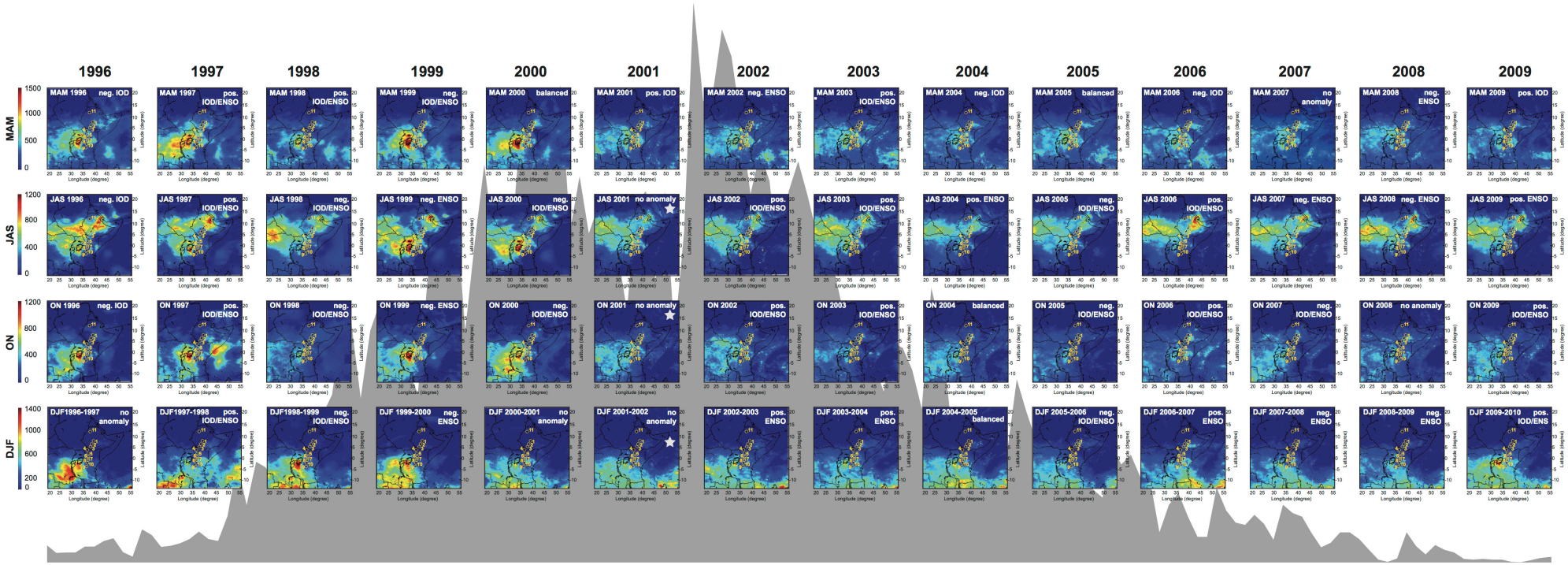
1996
1997
1998
1999
2000
2001
2002
2003
2004
2005
2006
2007
2008
2009
MAM
JAS
ON
DJF
MAM 1996 neg. IOD
MAM 1997 pos. IOD/ENSO
MAM 1998 pos. IOD/ENSO
MAM 1999 neg. IOD/ENSO
MAM 2000 balanced
MAM 2001 pos. IOD
MAM 2002 neg. ENSO
MAM 2003 pos. IOD/ENSO
MAM 2004 neg. IOD
MAM 2005 balanced
MAM 2006 neg. IOD
MAM 2007 no anomaly
MAM 2008 neg. ENSO
MAM 2009 pos. IOD
JAS 1996 neg. IOD
JAS 1997 pos. IOD/ENSO
JAS 1998 neg. IOD/ENSO
JAS 1999 neg. ENSO
JAS 2000 neg. IOD/ENSO
JAS 2001 no anomaly
JAS 2002 pos. IOD/ENSO
JAS 2003 pos. IOD/ENSO
JAS 2004 pos. ENSO
JAS 2005 neg. IOD/ENSO
JAS 2006 pos. IOD/ENSO
JAS 2007 neg. ENSO
JAS 2008 neg. ENSO
JAS 2009 pos. ENSO
ON 1996 neg. IOD
ON 1997 pos. IOD/ENSO
ON 1998 neg. IOD/ENSO
ON 1999 neg. ENSO
ON 2000 neg. IOD/ENSO
ON 2001 no anomaly
ON 2002 pos. IOD/ENSO
ON 2003 pos. IOD/ENSO
ON 2004 balanced
ON 2005 neg. IOD/ENSO
ON 2006 pos. IOD/ENSO
ON 2007 neg. IOD/ENSO
ON 2008 no anomaly
ON 2009 pos. IOD/ENSO
DJF1996-1997 no anomaly
DJF1997-1998 pos. IOD/ENSO
DJF1998-1999 neg. IOD/ENSO
DJF 1999-2000 neg. ENSO
DJF 2000-2001 no anomaly
DJF 2001-2002 no anomaly
DJF 2002-2003 pos. ENSO
DJF 2003-2004 pos. ENSO
DJF 2004-2005 balanced
DJF 2005-2006 neg. IOD/ENSO
DJF 2006-2007 pos. ENSO
DJF 2007-2008 neg. ENSO
DJF 2008-2009 neg. ENSO
DJF 2009-2010 pos. IOD/ENS
Longitude (degree)
Latitude (degree)